2012

Forebrain Noradrenergic Alterations and Anxiety After Myocardial Infarction

Jaimee Glasgow
Loyola University Chicago

LOYOLA UNIVERSITY CHICAGO

FOREBRAIN NORADRENERGIC ALTERATIONS AND ANXIETY AFTER MYOCARDIAL INFARCTION

A DISSERTATION SUBMITTED TO

THE FACULTY OF THE GRADUATE SCHOOL

IN CANDIDACY FOR THE DEGREE OF

DOCTOR OF PHILOSOPHY

PROGRAM IN CELL BIOLOGY, NEUROBIOLOGY, AND ANATOMY

BY

JAIMEE ELIZABETH GLASGOW

CHICAGO, ILLINOIS

AUGUST 2012

ACKNOWLEDGEMENTS

First and foremost, I would like to thank my advisor, Karie Scrogin, for her boundless knowledge and patience. Throughout my training, she has encouraged and challenged me to grow as a scientist, and in all areas of my life. I would also like to thank the other members of my dissertation committee, Dr. EJ Neafsey, Dr. Kuei Tseng, Dr. George Battaglia, Dr. Wendy Kartje, and Dr. Thackery Gray, for their time and thoughtful input throughout my studies. Finally, I would like to thank my friends and family for their contribution to this research through their unconditional love and support. I would especially like to thank my mother, Peggy Glasgow, for her unwavering encouragement until her final days.

TABLE OF CONTENTS

LIST OF TABLES

LIST OF FIGURES

LIST OF ABBREVIATIONS

α_2AR	Alpha2-adrenergic receptor
AP	Arterial pressure
AV	Atrioventricular
ACE	Angiotensin-converting enzyme
ACTH	Adrenocorticotropic hormone
AVP	Arginine vasopressin
βAR	Beta-adrenergic receptor
β_1AR	Beta1-adrenergic receptor
β_2AR	Beta2-adrenergic receptor
BLAc	Basolateral complex of the amygdala
BLA	Basolateral nucleus of the amygdala
cAMP	Cyclic adenosine monophosphate
CAL	Coronary artery ligation
CeA	Central nucleus of the amgydala
CeL	Central amygdala: lateral division
CeM	Central amygdala: medial division
Cg	Anterior cingulate cortex
CN	Central nervous system
CO	Cytochrome oxidase

CS	Conditioned stimulus
DPM	Decays per minute
ECG	Electrocardiogram
EPM	Elevated plus maze
FO	Fractional occupancy
FS	Fractional shortening
Gαi	G inhibitory protein
Gαs	G stimulatory protein
GABA	Gamma-aminobutyric acid
GPCR	G protein-coupled receptor
HPA	Hypothalamic-pituitary-adrenal
HPLC	High-performance liquid chromatography
HR	Heart rate
ICM	Intercalated cell masses
^{125}ICYP	125-Iodocyanopindolol
IL	Infralimbic cortex
Ins	Insular cortex
LVDD	Left ventricular diastolic diameter
M	Motor cortex
MAP	Mean arterial pressure
OF	Orbitofrontal cortex
PKA	Protein kinase A

PrL	Prelimbic cortex
LAD	Left anterior descending coronary artery
LC	Locus coeruleus
LV	Left ventricle
MI	Myocardial infarction
mPFC	Medial prefrontal cortex
NE	Norepinephrine
OD	Optical density
PAG	Periaqueductal gray
PFC	Prefrontal cortex
PNS	Parasympathetic nervous system
PTSD	Post-traumatic stress disorder
PVC	Preventricular contraction
PVN	Paraventricular nucleus of the hypothalamus
RVLM	Rostral ventrolateral medulla
SA	Sinoatrial
SCD	Sudden cardiac death
SM	Somatosensory cortex
SNS	Sympathetic nervous system
US	Unconditioned stimulus
VF	Ventricular fibrillation
VT	Ventricular tachycardia

CHAPTER 1

INTRODUCTION

Significance

Depression and anxiety are common comorbidities found with coronary artery disease (Frasure-Smith and Lesperance, 2003; Gander and von Kanel, 2006; Shemesh et al., 2006). Thirty to 45% of patients who suffer a myocardial infarction (MI) go on to develop anxiety disorders and/or depression, while the normal population demonstrates an incidence of approximately 5% (Frasure-Smith and Lesperance, 2003; Wiedemar et al., 2008; Friedmann et al., 2006). The development of mood and anxiety disorders following MI is a major risk factor for cardiovascular morbidity and mortality (de Jonge et al., 2006; Moser et al., 2007b; Huffman et al., 2008). About 50% of deaths in post-MI patients are caused by sudden cardiac death (SCD), i.e., unpredictable death due to cardiac arrhythmias (Zipes and Wellens, 1998), and the risk of SCD is even greater in post-MI patients with depression or anxiety (Friedmann et al., 2006; Frasure-Smith and Lesperance, 2008; Barefoot et al., 1996). Furthermore, SCD is often precipitated by emotional stressors (Vlastelica, 2008).

Together, these data suggest that the ischemic event itself, or the subsequent biochemical sequelae, produce specific changes in the central nervous system (CNS) that influence emotional reactivity and lower the threshold

for arrhythmia activation (Watkins et al., 2006; Grippo et al., 2004). Despite extensive documentation of the association between anxiety and cardiovascular-related death (Albert et al., 2005), little is known about the CNS mechanisms that give rise to anxiety after MI.

Appropriate emotional responding to stimuli requires the coordination of brainstem, cortical, and subcortical brain regions, and perturbations in the activation of, or communication among, these structures is thought to underlie the development of anxiety and mood disorders. The locus coeruleus (LC) of the dorsal pons is activated in response to stress or novelty and provides widespread noradrenergic input to the forebrain, including the medial prefrontal cortex (Aston-Jones and Bloom, 1981; Florin-Lechner et al., 1996). The medial prefrontal cortex (mPFC) is responsible for so-called executive function, including the evaluation of the salience of stimuli and determination of appropriate behavioral responses. The mPFC suppresses inappropriate emotional and autonomic responses to stress by inhibiting the output of the amygdala, a collection of subcortical nuclei that coordinate emotional and autonomic responses to stress (Aston-Jones and Bloom, 1981; Quirk et al., 2003). Patients suffering from depression and anxiety have exaggerated responses to stress and have difficulty in classifying cues as threatening or safe. Aberrant functioning of the mPFC and amygdala circuitry is thought to underlie these aberrant responses and contribute to the development of depression and anxiety (Britton et al., 2011).

Determining the specific brain circuits and neurotransmitter systems that are perturbed after MI will allow for the development of more targeted therapies to treat this vulnerable subset of patients.

Main hypothesis

The studies reported in this dissertation were designed to test the overall hypothesis that alterations in noradrenergic transmission in the forebrain contribute to the development of anxiety disorders and arrhythmia susceptibility after myocardial infarction. The following specific aims were designed to help address this hypothesis.

Specific Aim 1: To determine if metabolic activity is elevated in the amygdala and reduced in the medial prefrontal cortex of rats after myocardial infarction and whether locus coeruleus stimulation exaggerates changes in metabolic activity in these regions.

Rationale: Little is known about the central nervous system mechanisms underlying anxiety after MI. However, the majority of depressed and anxious MI patients die of sudden cardiac death. Evidence suggests that cortical and subcortical forebrain regions contribute to sympathetic activation and arrhythmia generation (Carpeggiani et al., 1992; Skinner and Reed, 1981; Ter Horst, 1999).

The amygdala is a cluster of subcortical nuclei that coordinate behavioral and autonomic responses to stressful or emotional stimuli. The amygdala is

necessary for forming associations between stressors and environmental cues, and hyperactivity of the amygdala has been implicated in anxiety disorders, including post-traumatic stress disorder (Koenigs and Grafman, 2009). The amygdala also may facilitate arrhythmia generation, as cryogenic blockade of the amygdala delays or prevents ventricular fibrillation (VF) during reversible myocardial ischemia in conscious, psychologically stressed pigs (Carpeggiani et al., 1992), suggesting that hyperactivation of the amygdala may be arrhythmogenic.

The prefrontal cortex (PFC) consists of several distinct regions that regulate “higher order” processes including working memory and planning (Ramos et al., 2005), but are also involved in modulating autonomic responses to acute stress and learned fear (Frysztak and Neafsey, 1994). Brain imaging studies of heart failure patients demonstrate abnormalities in the prefrontal cortex (Woo et al., 2009). Cryogenic blockade of the prefrontal cortex delays or prevents ventricular fibrillation during myocardial ischemia in pigs (Skinner and Reed, 1981), implicating the PFC as a potential modulator of heart rhythms.

Both the amygdala and mPFC are modulated by noradrenergic input. The locus coeruleus (LC) is the primary source of norepinephrine (NE) to the forebrain, and the LC is activated by salient and noxious stimuli, resulting in the release of NE in multiple regions of the forebrain, hindbrain, and spinal cord (Florin-Lechner et al., 1996; Chen and Sara, 2007; Van Bockstaele et al., 1989; Proudfit and Clark, 1991). Myocardial infarction increases long-term neuronal

activation in the LC, as indicated by increased levels of Fra, a marker of chronic neuronal activation, and increased activity of hexokinase, an enzyme necessary for glucose metabolism (Patel et al., 1993; Vahid-Ansari and Leenen, 1998). In addition, human heart failure patients exhibit elevated NE turnover in the subcortical forebrain (Aggarwal et al., 2002).

Norepinephrine acting on beta-adrenergic receptors (βARs) in the central nervous system is thought to contribute to arrhythmia generation. Intracerebroventricular administration of the βAR antagonist, propranolol, delays the development of VF induced by coronary ischemia in pigs (Parker et al., 1990). Similarly, chronic intracerebroventricular administration of the β_1AR antagonist, metoprolol, was shown to attenuate left ventricular remodeling in rats subjected to MI (Gourine et al., 2008). These results suggest that β_1ARs in the brain contribute to the sympathetic activation after MI.

In previous studies in our laboratory, rats subjected to MI exhibited paradoxical anxiety-like behavior (increased open arm activity and head-first jumps) in the elevated plus maze (Henze et al., 2008). Therefore, the goal of this study was to identify brain regions that might be involved in anxiogenic responses in heart failure and determine if they are more responsive to activation of noradrenergic input.

Experimental Objectives:

A) To determine if rats display altered basal and locus coeruleus-modulated metabolic activity in the prefrontal cortex and amygdala after myocardial infarction, using cytochrome oxidase histochemistry after locus coeruleus stimulation

B) To determine if rats subjected to myocardial infarction display enhanced arrhythmia susceptibility in response to acute stress-like norepinephrine release, using electrocardiogram (ECG) analysis during locus coeruleus stimulation

C) To determine if myocardial infarction in rats leads to increased anxiety as measured by the open field test

Specific Aim 2: To determine if MI results in alterations of β_1AR density and G protein coupling in the amygdala and PFC.

Rationale: Many βAR antagonists, including propranolol, are lipophilic and can thus cross the blood-brain barrier, and their actions in the brain may contribute to their therapeutic cardiovascular effects. βARs in the CNS have been implicated in arrhythmia generation (Parker et al., 1990) and left ventricular remodeling after MI (Gourine et al., 2008). However, the localization of these changes in βAR receptor number and/or function is currently unknown.

Noradrenergic signaling through βARs in the CNS is thought to play a role in the encoding and maintenance of fear-related memories, with dysregulation of these pathways leading to exaggerated emotional responses to fear-associated stimuli. Activation of β_1ARs in the amygdala is thought to contribute to the formation and maintenance of fear-related memory. For example, infusion of propranolol into the lateral nucleus of the amygdala (LA) of rats during reconsolidation of fear conditioning reduces freezing in response to a fear-associated cue (Debiec and LeDoux, 2006). However, the localization and the βAR subtypes that may mediate exaggerated stress responses after MI is unknown.

Agonists of G protein-coupled receptors (GPCRs) must bind to receptors coupled to their heterotrimeric G protein in order to mediate their effects. Additionally, the affinitity of an agonist is higher for a coupled than an uncoupled receptor. In most cases, βARs are coupled to $G\alpha_s$, the activation of which leads to adenylyl cyclase activation, and thus formation of the second messenger, cyclic AMP (cAMP). Increases in cAMP lead to subsequent increases in cell excitability and synaptic strength through, among other mechanisms, activation of gene transcription by phosphorylation of transcription factors by protein kinase A (Pedarzani and Storm, 1993). Thus, both the number and the coupling state of receptors βARs determine the response to NE release as a result of LC activation.

Currently, it is unknown how MI affects the density and G protein coupling of βARs in brain regions that may contribute to post-MI anxiety. Therefore, this study sought to assess changes in βAR density and functional coupling in the amygdala and PFC in response to MI using autoradiography.

Experimental Objectives:

A) To determine if MI results in decreased β_1AR density in the PFC, but increased β_1AR density in the amygdala, using receptor autoradiography

B) To determine if MI results in changes in G protein coupling of β_1ARs in the amygdala and PFC, using autoradiographic analysis of agonist inhibition of labeled antagonist binding

Specific Aim 3: To determine if rats subjected to myocardial infarction have deficits in the acquisition and retention of conditioned fear extinction

Rationale: In our studies in Specific Aim 1, we found increased baseline metabolic activity in the infralimbic (IL) mPFC in rats subjected to MI. In response to LC stimulation, we found a decrease in metabolic activity in the IL cortex in MI rats, while sham-operated rats tended to show increased activity in the IL mPFC with LC stimulation. In our studies in Specific Aim 2, we found a decrease in β_1ARs in the IL. Noradrenergic signaling through IL βARs has been shown to contribute to the extinction of conditioned fear responses in rats

(Mueller et al., 2008). Humans suffering from depression and anxiety tend to have persistent and exaggerated fear responses and have difficulty discriminating between safety and danger cues (Britton et al., 2011). These exaggerated and persistent emotional responses can increase sympathetic drive. Especially for post-MI patients, increased sympathetic drive can lead to arrhythmia generation and increased risk for SCD. Therefore, this study sought to assess the effect of MI on the extinction of conditioned behavioral and cardiovascular fear responses.

Experimental Objectives:

To determine if rats subjected to myocardial infarction display deficits in the acquisition and recall of extinction of conditioned fear, determined by freezing, blood pressure, and heart rate responses to presentation of tones previously paired with footshock.

CHAPTER 2

REVIEW OF RELATED LITERATURE

Anxiety and Depression after MI and in Heart Failure

Coronary artery disease is a leading cause of hospitalizations and death in the US and other industrialized nations, and often leads to myocardial infarction (MI) and subsequent heart failure (Heidenreich et al., 2011). Depression and anxiety are common comorbidities found with CAD (Frasure-Smith and Lesperance, 2003; Gander and von Kanel, 2006; Shemesh et al., 2006). Thirty to 45% of patients who suffer an MI go on to develop anxiety disorders and/or depression, while the entire United States population demonstrates an incidence of approximately 5% (Frasure-Smith and Lesperance, 2003; Wiedemar et al., 2008; Friedmann et al., 2006).

The development of mood and anxiety disorders following MI is a major risk factor for cardiovascular morbidity and mortality (de Jonge et al., 2006; Moser et al., 2007b; Huffman et al., 2008). In fact, the development of depression and anxiety after an ischemic event is a better predictor of mortality than is a diagnosis of depression and anxiety prior to MI (Dickens et al., 2008; Frasure-Smith et al., 1993). One study also found post-MI anxiety to be an independent risk factor for cardiovascular complications, even more so than depression (Huffman et al., 2008). Patients who experience an acute MI and

subsequently develop anxiety during their hospital stay tend to have more in-hospital cardiovascular complications, including reinfarction and ventricular fibrillation (Moser et al., 2007a).

About 50% of deaths in post-MI patients are caused by sudden cardiac death (SCD), i.e., unpredictable death due to cardiac arrhythmias (Zipes and Wellens, 1998). Recent evidence indicates that death in post-MI patients with depression and anxiety is most often caused by SCD, and depressed post-MI patients have a 69% increased risk for SCD compared to non-depressed post-MI patients (Friedmann et al., 2006; Frasure-Smith and Lesperance, 2008; Barefoot et al., 1996). Furthermore, SCD is often precipitated by emotional stressors (Vlastelica, 2008). Patients with depression and anxiety often have exaggerated emotional responses to stressors and have difficulty discriminating between safety and danger cues (Britton et al., 2011).

Together, these data suggest that the ischemic event itself, or the subsequent biochemical sequelae, produce specific changes in the central nervous system that influence emotional reactivity and lower the threshold for arrhythmia activation (Watkins et al., 2006; Grippo et al., 2004). Despite extensive documentation of the association between anxiety and cardiovascular-related death (Albert et al., 2005), little is known about the central nervous system mechanisms that give rise to anxiety after MI.

Assessments of Depression and Anxiety

Classical conditioning has been used in animal models and humans to study the neural substrates of aberrant stress responses and the development of anxiety disorders. In classical conditioning, subjects develop conditioned responses to a previously neutral stimulus by the pairing of this stimulus with a salient (aversive or appetitive) stimulus. Thus, the neutral conditioned stimulus (CS) comes to elicit the same response as the salient unconditioned stimulus (US). After repeated presentations of the CS without the US, responses to the CS normally abate. However, this extinction process is often delayed or absent in anxiety disorders, including post-traumatic stress disorder (Garakani et al., 2006). In post-traumatic stress disorder (PTSD), the neutral cues associated with the trauma (the US) continue to elicit intense fear responses long after the trauma. Exaggerated emotional responses to neutral stimuli or mild stressors are common in both depression and anxiety, as is a deficit in the ability to classify stimuli as threatening or safe (Britton et al., 2011).

In rodents, exposure to an auditory CS previously paired with an aversive stimulus, such as footshock, elicits well-characterized conditioned emotional responses, including freezing, in which the animal ceases movements except those necessary for respiration. Lesion studies have demonstrated that the midbrain periaqueductual gray (PAG), under control of the central nucleus of the amygdala (CeA), is necessary for this response. Exposure to fear-associated stimuli also elicts profound cardiovascular responses in rats. Exposure to an

auditory CS evokes an increase in arterial pressure, and lesion studies have shown that the lateral hypothalamus, also under control of the CeA, is necessary for this response (LeDoux et al., 1988).

The blood pressure and heart rate responses to CS presentation in rats are multiphasic. Presentation of a tone previously paired with footshock has been shown to first elicit a brief and sudden increase in blood pressure in restrained rats. The increase in blood pressure is accompanied by a transient burst in sympathetic nerve activity. This transient initial pressor response (termed the C_1 response) is followed by a smaller, sustained pressor response (the C_2 response). Minor decreases in heart rate accompany the two pressor responses. A dramatic increase in total peripheral resistance accompanies the C_1 pressor response, while increased cardiac output primarily mediates the C_2 response (Randall et al., 1994). In restrained rats, presentation of a stimulus that is explicity unpaired with shock during training, i.e., a CS- tone, elicits a different hemodynamic response than a tone paired with shock (i.e., a CS+). The CS- does evoke a C_1 pressor response, but of a slightly smaller magnitude than the CS+. The CS- does not, however, elicit a C_2 pressor response, and so may provide a means to determine whether an animal is able to discriminate between the stimuli. (El-Wazir et al., 2005).

Presentation of a CS alone (without shock) leads to decreased emotional and autonomic responding to the CS upon subsequent exposures (i.e., extinction). However, extinguished fear responses can spontaneously recover

over time {{639 Quirk 2002}}, indicating that the extinction of learned fear does not erase the original CS-US association. Rather, extinction is a form of new learning that inhibits the conditioned response. Because deficits in fear extinction in rodents model the perseveration of stress responses in anxiety disorders including PTSD and phobias, understanding the neural pathways governing the process of fear extinction is important for developing new therapies for these patients.

In addition to classical fear conditioning, other methods of assessing anxiety-like behavior in rodents include the elevated plus maze (EPM), open field test, and social interaction test. Rather than creating associations between neutral stimuli and either aversive or appetitive stimuli (as in classical conditioning), these tests examine the inhibition of non-defensive behaviors (such as exploration) during exposure to novel and potentially dangerous stimuli. In the EPM, animals are allowed to explore an elevated apparatus with 2 opposing arms with high walls (closed arms), and 2 arms with no walls (open arms). In the traditional interpretation of this test, the time spent and number of entries in open arms is negatively correlated with anxiety behavior, as anxiolytic drugs (benzodiazepines) increase the open arm exploration, but anxiogenic drugs (including yohimbine and methamphetamine) decrease open arm exploration (Pellow et al., 1985). However, some studies suggest that increased open arm activity can represent severe anxiety-like behavior. Rats subjected to severe stress during puberty (Pohl et al., 2007) or amygdala kindling (Kalynchuk

et al., 1997; Buckman et al., 2009) display increased open arm activity, as do mice during opiate withdrawal (Buckman et al., 2009). Previous studies in our laboratory have shown increased EPM open arm activity in MI rats compared to sham-ligated rats (Henze et al., 2008). In this study, some MI rats also jumped head-first off the apparatus, suggestive of escape-seeking behavior as is seen during panic.

A similar test for anxiety-like behavior is the open field test. In this test, rats explore a round or square box, and their activity and time spent in the periphery (near the walls) of the apparatus indicates anxiety-like behavior. Additionally, the rat's latency to begin exploring indicates a neophobic response. This test is sometimes also known as "hole-board" since it often includes holes which subjects may explore with their snouts, with nose pokes used as an index of exploratory behavior (File and Wardill, 1975a; File and Wardill, 1975b). Chronic mild stress has been shown to decrease central square activity (Hu et al., 2010), and anxiolytic drugs, including propranolol, decrease peripheral activity of in this test (Angrini et al., 1998). Another test of anxiety-like activity is the social interaction test, in which a rat is placed in a novel arena with an unfamiliar rat, and the amount of interactions with the new rat (e.g. grooming, following) is negatively correlated with anxiety-like behavior (File et al., 2004; Wongwitdecha and Marsden, 1996). Stress, including social isolation, decreases the time spent interacting with the new rat in this test (Wongwitdecha and Marsden, 1996).

Several behavioral tests have been employed to measure depression-like behavior in rodents by modeling one or more of the symptoms of major depression in humans. Anhedonia is the loss of the ability to enjoy previously pleasurable activities. A simple test of anhedonia is the sucrose preference, which measures rats' ingestion of a palatable sucrose solution (when presented with the choice of sucrose or water). Rat subjected to chronic mild stress, a rodent model of depression, exhibit decreased sucrose consumption compared to non-stressed controls (Grippo et al., 2003b). Another measure of anhedonia is intracranial self-stimulation. Rats are chronically implanted with stimulating electrodes in the lateral hypothalamus and are then trained to press a lever to receive pulses of pleasurable stimulation. A reduction in lever pressing to receive stimulation (or a higher current level to elicit lever pressing) is considered to be indicative of anhedonia (Edmonds and Gallistel, 1974). Rats subjected to MI have been shown to require a greater current to elicit level pressing for rewarding stimulation than sham-operated rats (Grippo et al., 2003b). The feeling of helplessness is another symptom of major depression. The forced swim test is a rodent test of helplessness. Animals are placed in a tank of water, and the time spent swimming and attempting to escape before becoming immobile is negatively correlated with depression-like behavior. In rats, treatment with antidepressant drugs, but not anxiolytic drugs, decreases immobility in this test (Porsolt et al., 1978).

While these behavioral tests are useful for screening potential therapies or elucidating brain mechanisms of neuropsychiatric disorders, few are valid and practical for investigating the mechanisms of post-MI depression and anxiety, since physiological changes after MI confound some of these tests (particularly tests of depressive-like behavior). For example, neurohumoral activation (particularly angiotensin II) after MI causes fluid retention and changes in thirst and appetite that would affect the rat's behavior in the sucrose preference test, thus confounding it as an assessment of anhedonia. Reduced exercise tolerance after MI would confound the forced swim test, as immobility in MI rats may reflect physical exhaustion rather than helplessness. Many tests of anxiety, including the open field test and extinction of conditioned fear, are less susceptible to these confounds. Anxiety-like behavior in rats following MI has rarely been investigated, and no studies, to our knowledge, have examined the effect of MI on extinction of conditioned fear. Therefore the studies in this dissertation were designed to investigate the effects of MI on anxiety-like behavior.

Neural Control of the Normal and Failing Heart

Normal Cardiac Function

The heart is a complex organ that pumps oxygen-rich blood through the arterial side of the vasculature to maintain the function of every living cell in the body. From the venous side of the vasculature, deoxygenated blood is pumped

through the right side of the heart to the lungs by the pulmonary arteries. This blood is oxygenated in the lungs, and this oxygenated blood then returns to the left atrium, from which it enters the left ventricle via the mitral valve. The contraction of the left ventricle pumps oxygenated blood into the aorta to deliver blood to all areas of the body, including the heart itself, which has a very high oxygen demand (Boulpaep, 2005). The left and right coronary arteries originate just above the aortic valve. The right coronary artery supplies blood to the right ventricle, the interventricular septum, and the diaphragmatic surface of the left ventricle. The left coronary artery divides into the circumflex branch and the left anterior descending branch (LAD). The circumflex branch supplies the lower lateral wall and a portion of the posterior wall of the left ventricle, and the LAD supplies the majority of the left ventricle, the portion of the heart responsible for ejection of oxygenated blood to the periphery (Segal, 2005).

Contraction of the heart is mediated by cardiomyocytes, which contract in concert upon stimulation by membrane depolarization. Cardiomyocytes are specialized cells that have properties of both muscle (i.e. contractility) and neurons (i.e. excitability and conductivity). Action potentials generated in the sinoatrial (SA) node are conducted to the remainder of the heart via the conduction system, which also includes the atrioventricular (AV) node, the bundle of His, the left and right bundle branches, and the Purkinje fibers. Although pacemaker cells in the AV node exhibit spontaneous depolarlization and can initiate contraction of cells, the SA node has the highest rate of spontaneous

depolarization. The transient hyperpolarization of cardiomyocyte membranes that develops after generation of an action potential prevents action potential firing in response to other pacemakers. Thus, the SA node cells override the other pacemakers to set the heart beat. A rhythm that originates in the SA node and is below 100 beats per minute in humans is known as normal sinus rhythm. Action potentials generated in the SA node are propagated through the atria and AV node and travel through the septum via the Bundle of His. The conduction pathway splits into left and right bundle branches to reach the apex of the ventricles. Depolarization of the ventricles begins at the apex and spreads up the outer walls of the ventricle. Cells that are not directly contacted by the conduction system are depolarized by the spread of current through gap junctions situated between myocytes. Contraction of the myocytes is due to increased intracellular calcium that develops immediately following membrane depolarization of the myocardium (Berne and Levy, 2001).

Autonomic Nervous System: Overview

The autonomic nervous system regulates the heart and vasculature in order to allow rapid changes in blood flow that may be required to meet the constantly changing demands of various body tissues, including the heart. The autonomic nervous system consists of two often opposing components: the sympathetic nervous system (SNS) and the parasympathetic nervous system (PNS). The SNS regulates “fight-or-flight” responses, i.e., prepares the body to

respond to emergencies. Stimuli that activate the SNS result in increased cardiac output (i.e. the amount of blood that exits the aorta per unit time, defined as the product of heart heart and stroke volume) and patterned vasoconstriction that mobilizes blood to areas of demand (e.g. the hindlimbs to enable escape from a threat). In contrast, the PNS regulates “rest and digest” functions, and serves to decrease cardiac output in times of low demand. The autonomic nervous system consists of components in the CNS and periphery, and is often called a “two-neuron” system. Autonomic neurons with cell bodies in the central nervous system (i.e., brainstem as well as lower cervical, thoracic and upper lumber spinal segments) project to clusters of neurons (autonomic ganglia) where they release acetylcholine. Acetylcholine in turn, activates nicotinic receptors on peripheral ganglion cells. Ganglionic neurons send unmyelinated postganglionic fibers to their target organs (Richerson, 2005).

The preganglionic cell bodies responsible for sympathetic innervation of the heart are located in the intermediolateral cell column of the lower cervical, thoracic and upper lumbar spinal cord. These neurons receive tonic excitation from the rostral ventrolateral medulla (RVLM) of the brainstem. The RVLM also receives excitatory input from a few forebrain structures including the central nucleus of the amygdala (CeA) and paraventricular nucleus (PVN) of the hypothalamus. Sufficient excitation of preganglionic neurons results in the excitation of neurons in the paravertebral or prevertebral ganglia. Activation of cells in the cervical and stellate ganglia results in the release of norepinephrine

(NE) from post-ganglionic nerve terminals in the SA node and ventricles. Additionally, excitation of preganglionic neurons can activate chromaffin cells of the adrenal medulla (analogous to sympathetic ganglion cells), resulting in the release of epinephrine and NE into the systemic circulation. The NE and epinephrine act in the heart and systemic circulation to mediate their effects through α- and β-adrenergic receptors (βARs). Sympathetic activation of the heart results in increased contractility and heart rate (thereby increasing cardiac output) via βARs (signaling through $G\alpha_s$ to increase cAMP). Sympathetic activation of the vasculature results in vasoconstriction via α_1-adrenergic receptors, signaling through $G\alpha_q$ to increase intracellular calcium (Richerson, 2005).

The PNS mediates many of its effects in the periphery through the vagus nerve (cranial nerve X). In contrast to the sympathetic ganglia, parasympathetic ganglia are located close to or within effector organs. Post-ganglionic fibers of the PNS release acetylcholine, which mediates its effects through muscarinic receptors. Parasympathetic drive to the heart primarily decreases heart rate and has a mild effect on contractility via M_2 receptors expressed both on atrial cardiomyocytes and on pacemaker cells in the SA and AV nodes (Vandecasteele et al., 1999). Acetylcholine acting through M_2 receptors (coupled to Gαi) can also inhibit NE release from sympathetic nerve terminals, further reducing heart rate and contractility (Trendelenburg et al., 2005).

Myocardial Infarction and Heart Failure

Heart Failure is the inability of the heart to sufficiently pump oxygenated blood to meet the demands of peripheral tissues. Heart failure often results from myocardial infarction (MI), which is caused by stenosis or blockage of one or more coronary arteries. This lack of blood flow to the heart results in necrosis and subsequent scar formation in the ventricular tissue (Pfeffer and Braunwald, 1990). The subsequent decrease in viable contractile myocardium causes a decrease in cardiac output. However, the loss of cardiac output alone does not define heart failure. Rather, heart failure is a constellation of symptoms that develop that develop as a result of compensatory responses that attempt to regain normal cardiac output after MI.

These compensatory mechanisms include increased sympathetic drive (to increase heart rate and contractility) and release of vasoactive hormones (to increase peripheral resistance and blood volume). However, over time, this increased sympathetic drive and volume overload initiates changes in the remaining viable ventricular tissue that further reduce contractility, thereby further decreasing cardiac output. These changes in the size, shape, and function of the ventricle are known as remodeling. Remodeling can include thinning of the remaining ventricular tissue (due to volume overload) or compensatory hypertrophy (Pfeffer and Braunwald, 1990). In addition to morphological remodeling, the heart also undergoes electrical and neural remodeling after MI that lead to aberrant conduction and arrhythmia susceptibility(Chen et al., 2001).

In the explanted hearts of human heart transplant recipients, increased sympathetic nerve fibers (identified with immunohistochemistry) are found on the border between the viable and infarcted tissue, and this increased sympathetic innervation is correlated with patient history of ventricular arrhythmia (Cao et al., 2000b). Furthermore, neural remodeling induced by injecting nerve growth factor into the stellate ganglion increases the incidence of ventricular tachycardia (VT), VF, and sudden cardiac death in dogs previously subjected to MI (Cao et al., 2000a).(Cao et al., 2000b)

Autonomic Nervous System in MI and Heart Failure

In response to myocardial infarction, sympathetic drive to the heart increases, as demonstrated by an immediate and persisting elevation in plasma norepinephrine spillover from the heart (Hasking et al., 1986). This increase in sympathetic drive is also evident in measurements of muscle sympathetic nerve activity, and this increase is a predictor of mortality (Barretto et al., 2009). The increase in sympathetic drive is accompanied by a withdrawal of parasympathetic drive to the heart (Dunlap et al., 2003). Increased sympathetic activation after MI is associated with increased oxygen demand (Ohte et al., 2002) and arrhythmia susceptibility (Wen et al., 2010). Increased stimulation by NE and epinephrine also leads to a desensitization of cardiac βARs (Kompa et al., 1999) by agonist-induced internalization and subsequent degradation, thus decreasing the ability of the heart to respond to further sympathetic stimulation.

The Endocrine System in MI and Heart Failure

Following MI, the release of vasoactive hormones is a compensatory mechanism that attempts to restore normal cardiac output. One of the principal neurohumoral mechanisms is the the renin-angiotensin-aldosterone system. When renin is released from the juxtaglomerular apparatus of the kidney, it cleaves circulating angiotensinogen to release angiotensin I. Angiotensin converting enzyme (ACE) then cleaves angiotensin I to create angiotensin II. Angiotensin II increases blood pressure and blood volume through multiple mechanisms. Angiotensin II increases blood pressure directly through vasoconstriction (via $G_{\alpha q}$) and also acts directly on the kidney's proximal tubules to increase sodium resorption. In the adrenal cortex, angiotensin II induces the release of aldosterone, which further facilitates fluid retention. This inhibition of diuresis by activation of the renin-angiotensin-aldosterone system contributes to the increased blood volume, and often leads to the tissue edema that is characteristic of congestive heart failure. Patients with congestive heart failure have increased levels of angiotensin II, aldosterone, and epinephrine, and these increases in vasoactive hormones are positively correlated with increased mortality (Swedberg et al., 1990). Treatment with an ACE inhibitor has been shown to reduce mortality in CHF patients
(CONSENSUS trial study group. 1987).

Angiotensin II further acts in the brain to increase blood pressure and blood volume by stimulating the release of arginine vasopressin (AVP) from the posterior pituitary. Like angiotensin II, AVP increases blood pressure directly by vasoconstriction, as well as by acting in the kidneys to increase fluid retention. Angiotensin II also stimulates the hypothalamic-pituitary-adrenal (HPA) axis, resulting in the release of adrenocorticotropic hormone (ACTH) from the pituitary, which elicits the release of glucocorticoids from the adrenal cortex (Krause et al., 2011). Although these stress hormones do not directly modulate blood pressure or blood volume, glucocorticoids have been implicated in the development of atherosclerosis, a major contributor to coronary artery disease (Fantidis, 2010). Angiotensin II further acts in the hypothalamus to reduce appetite by decreasing orexin and neuropeptide Y, two neuropeptides that regulate appetite (Yoshida et al., 2012; Sukhanov et al., 2011). Angiotensin II is also produced locally in the brain. In rats subjected to MI, central blockade of angiotensin II receptors was shown to decrease renal sympathetic nerve activity, suggesting that local angiotenin II contributes to increased sympathetic drive after MI. Similarly, rats lacking brain angiotensin II were shown to have attenuated left ventricular dysfunction after MI compared to wild-type rats subjected to MI (Wang et al., 2004).

Arrhythmia Generation After MI

The ischemia associated with an MI, as well as the sympathetic activation that follows MI, can lead to arrhythmia generation. Arrhythmias can be detected and analyzed through electrocardiogram (ECG) tracings, which display differences in potential between various electrical poles during the cardiac cycle. The normal cardiac cycle consists of 3 major complexes of waves. In lead II formation, the P wave is a relatively small positive deflection that represents atrial depolarization. Next is a large deflection known as the QRS complex, which results from ventricular depolarization. Finally, the T wave is a small positive deflection resulting from ventricular repolarization. Arrhythmias can result from dysfunction in impulse initiation or impulse conduction, and they are evident on ECG recordings in changes in the orientation, amplitude, and timing of these wave complexes (Lederer, 2005).

Common arrhythmias after MI include premature ventricular contractions (PVCs). In contrast to normal beats, which are iniated in the SA node, PVCs are beats initiated by ectopic ventricular pacemakers, which can develop as a result of disruption of normal conduction pathways by scar tissue. A PVC will be generated if this ectopic focus can depolarize the ventricles before the normal sinus stimulus arrives. Enhanced sympathetic drive can lead to aberrant action potential generation during diastole, which can generate PVCs.

Because ventricular-initated contraction is not associated with atrial depolarization, ECG tracings of PVCs lack P waves. Although occasional PVCs

are normal in healthy subjects, the prevalence of PVCs is greatly increased in myocardial ischemia. The alternation of normal beats with PVCs is known as bigeminy, and a series of 4 or more PVCs is known as ventricular tachycardia (VT). Both bigeminy and VT are common after MI (Engelen et al., 2003), and sustained VT can lead to sudden cardiac death. A lack of unified electrical activity in the ventricles is known as ventricular fibrillation (VF), in which the heart quivers and twitches without contracting. Sustained VF also leads to sudden cardiac death.

Susceptibility to arrhythmia is also evident in animal models of MI. Rats subjected to MI by coronary artery ligation develop VT or VF in response to electrical stimulation of the heart. Additionally, cardiomyocytes from rats subjected to MI display heterogeneity of the timecourse of repolarization and longer action potentials compared to those obtained from normal rats (Qin et al., 1996). In a perfused heart model, prior coronary artery ligation results in enhanced ventricular arrhythmia generation in response to sympathetic nerve stimultion, and βAR blockade prevents this effect, providing further evidence for sympathetic activation as a trigger for ventricular arrhythmia generation (Du et al., 1999).

Emotional Stressors, Sympathetic Activation, and Arrhythmia

It is estimated that 20 to 40% of sudden cardiac deaths are precipitated by acute emotional stressors (Vlastelica, 2008; Ziegelstein, 2007). During panic

attacks, patients exhibit large sympathetic bursts and increased risk of coronary artery spasm (Esler et al., 2004). Emotional stress itself, even without prior cardiac dysfunction, can result in left ventricular dysfunction and induce cardiac arrhythmias. Stress-induced cardiomyopathy is thought to be mediated by excess sympathetic activation, as these patient with stress-induced cardiomyopathy exhibit elevated levels of catecholamines and their metabolites (Wittstein et al., 2005). Rats exposed to chronic mild stress, a rodent model of depression, exhibit increased vulnerability to ventricular arrhythmias in response to intravenous infusion of the arrhythmogenic drug, aconitine (Grippo et al., 2004).

Mental stress and strong emotion have an established connection with ventricular arrhythmias (Brodsky et al., 1987). Mental stress tasks have been shown to destabilize and prolong induced VT in patients with implantable cardioverters (Wittstein et al., 2005). In a study of patients with cardioverters who kept a diary of mood states, anger was shown to frequently precede ventricular tachycardia or fibrillation requiring shock (Lampert et al., 2002). Furthermore, inducing anger in patients with implantable cardioverters has been shown to induce T-wave alternans (alternating changes in T-wave shapes or amplitudes), and those patients who develop T-wave alternans are more susceptible to future cardiac arrhythmias (Lampert et al., 2009). Even in healthy subjects, mental stress tasks have been shown to induce myocardial ischemia and a concomitant rise in plasma epinephrine and NE levels, implicating

sympathetic activation (Becker et al., 1996). In response to a mental stress test, CAD patients display a greater myocardial ischemia than healthy subjects (Krantz et al., 1991).

Cortical and Subcortical Control of Heart Rhythms

Much evidence implicates increased sympathetic activity in arrhythmia generation. Though the brainstem is the primary locus of sympathetic control, various forebrain regions are also involved in sympathetic control and arrhythmia generation. In the rat amygdala, activation of $GABA_A$ receptors with muscimol reduces the tachycardic response to restraint stress and reverses the accompanying increase in the sympatho-vagal ratio of autonomic input to the heart (Salome et al., 2007). Similarly, in psychologically stressed pigs, cryoblockade of the amygdala results in delay or prevention of ischemia-induced VT or VF (Carpeggiani et al., 1992). Cryoblockade of the PFC in psychologically stressed pigs yielded the same protection from arrhythmia generation (Skinner and Reed, 1981), implicating both the amygdala and PFC in arrhythmogenesis.

Studies of human heart failure patients also provide evidence for forebrain control of cardiac function. Human heart failure patients display an increase in forebrain subcortical NE turnover compared to age-matched controls, determined by measurement of NE and its metabolites in internal jugular venous blood samples (after scans to determine distribution of cerebral venous drainage in individual subjects). This increase in forebrain subcortical NE was positively

correlated with elevated whole-body NE spillover (Aggarwal et al., 2002). Additionally, acute blockade of CNS βARs has been shown to delay the development of ischemia-induced VT or VF in pigs (Parker et al., 1990), and chronic CNS β_1AR has been shown to attenuate left ventricular remodeling in rats subjected to MI (Gourine et al., 2008).

Central Nervous System Pathways Mediating Stress Responses

Amygdala

The amygdala is a group of subcortical nuclei deep to the ventrolateral temporal lobe that coordinate behavioral and autonomic responses to stress. While the necessity of the amygdala in encoding, maintaining, and expressing learned fear is well established, the intra-amygdala circuits governing these processes are complex and less well understood. The lateral nucleus of the amygdala (LA) is necessary for classical auditory fear conditioning because it is a site of convergence for nociciptive stimuli (the US) and auditory stimuli (the CS). The LA receives auditory signals from both the thalamus via the subcortical path and the auditory association cortex via the cortical path (Romanski et al., 1993). Just ventral to the LA is the basolateral nucleus, which receives contextual input from the hippocampal formation (Pitkanen et al., 1997). The basolateral nucleus of the amygdala (BLA nucleus) has been shown to play a critical role in the acquisition of learned fear, and is also thought to be necessary for fear memory storage.

Because of their close proximity, many studies have coupled these two nuclei, and together they are often referred to as the basolateral complex. Lesions of the BLA complex (including the lateral nucleus and basolateral nucleus) prior to both contextual and auditory-cued fear conditioning were shown to result in deficits in conditioned freezing. In contrast, lesions of the hippocampus impair conditioned responses only to contextual conditioning (Phillips and LeDoux, 1992). The BLA nucleus is necessary for storage of fear memory across the lifetime, as lesions of the BLA induced 24 hours after fear conditioning result in deficits in conditioned responses even 16 months after auditory fear conditioning (Gale et al., 2004).

Although primarily associated with acquisition and maintenance of fear memory, the BLA may also be involved in fear extinction. In a recent study, transient inactivation of the BLA just prior to extinction of auditory fear conditioning was shown to induce deficits in both fear expression and extinction (Sierra-Mercado et al., 2011). However, these results conflict with previous studies which found that BLA lesions induced after fear conditioning produce deficits in fear expression but have no effect on fear extinction (Anglada-Figueroa and Quirk, 2005).

Central Nucleus

The central nucleus of the amygdala, specifically the medial division (CeM), mediates autonomic, neuroendocrine, and behavioral responses to

conditioned fear via projections to the hypothalamus, including the PVN, lateral hypothalamus, and the brainstem including the nucleus of the solitary tract and the dorsal motor nucleus of the vagus (Wallace et al., 1992). Lesion studies have demonstrated that different projections of the CeM mediate the autonomic and behavioral components of conditioned fear; the lateral hypothalamus is necessary for conditioned arterial pressure responses, and the midbrain periaqueductal gray (PAG) is necessary for conditioned freezing (LeDoux et al., 1988). The central amygdala has been shown to be necessary for neuroendocrine responses to conditioned fear, as lesion of the central amygdala inhibits both renin and corticosterone production in response to conditioned stress (Van de Kar et al., 1991).

Intercalated Cell Masses

The intercalated cell masses (ICM) are clusters of GABA-ergic cells located between the basolateral and central nuclei of the amygdala and provide feed-forward inhibition to CeM neurons (Royer et al., 1999). Although many investigators have proposed a role for ICM neurons in regulation of conditioned fear, selective lesion or stimulation of these neurons *in vivo* is difficult because these clusters are very small and diffuse. However, the fact that ICM neurons express mu-opioid receptors has allowed for selective lesioning of these cells with a mu-opoid receptor antibody conjugated to the neurotoxin, saporin. Selective lesion of ICM neurons after extinction of auditory fear conditioning

leads to impaired recall of extinction compared to sham-lesioned rats (Likhtik et al., 2008).

Intra-Amygdala Circuitry in Conditioned Fear

Although it is well established that the LA is necessary for encoding, and the the CeM is necessary for the expression of conditioned fear, the sites of intra-amygdala relay of these signals is debatable because the LA does not project directly to the CeM. However, the LA can influence CeM output indirectly via the basolateral nucleus and the ICM (Pitkanen et al., 1997). In an electrophysiological study using amygdala slices from naïve rats and rats subjected to fear conditioning and extinction, previous fear conditioning and extinction was associated with increased BLA-evoked synaptic inhibition in CeM output neurons. Also in this study, ICM neurons in extinguished rats exhibited increased spiking probability in response to BLA stimulation, suggesting that increased excitation of ICM neurons by the BLA contributes to decreased CeM output following extinction (Amano et al., 2010).

The inconsistent results of studies investigating the effect of BLA inactivation on fear conditioning and extinction may be due to the influence of the basomedial nucleus of the amygdala, which is located ventral and medial to the BLA. The BLA and basomedial nucleus have common structural connections, including afferent input from the LA and projections to the CeM (Pitkanen et al., 1997). Both nuclei exhibit increased Fos immunoreactivity in

response to an acute stressor (Bhatnagar and Dallman, 1998). Unit recordings during auditory fear conditioning have shown that the BLA and the basomedial nucleus both respond with increased firing to tones that predict footshock. However, activity of basomedial neurons continue to fire after the end of the tone while BLA neurons fire only during the tone. In the same study, combined inactivation of the BLA and basomedial (but not activation of either nucleus alone) resulted in reduced conditioned freezing, suggesting that both regions are involved in fear expression, but neither is suffient to generate a response alone (Amano et al., 2011).

Prefrontal Cortex: Anatomy and Regulation of Stress Responses

Medial Prefrontal Cortex: Anatomy and Role in Stress Responses

The prefrontal cortex (PFC) is responsible for “executive functions” including working memory, planning responses to relevant stimuli, and emotional regulation. Accordingly, PFC dysfunction or lesion results in distractability, deficits in sensory gating and impulse control (Yamaguchi and Knight, 1990; Wilkins et al., 1987; Rubia et al., 2003). In the rat, the major divisions of the medial PFC (mPFC) are designated as the infralimbic (IL), prelimbic (PrL), and anterior cingulate (Cg) cortices. Although these divisions have dissociable anatomical connections and functional roles, they have several common projections, and often work in concert and have also been shown to have a homogeneity in tonic and phasic signaling (Mattinson et al., 2011).

The divisions of the medial mPFC can be differentiated from one another by their distinct cytoarchiture. The IL cortex is characterized by an indistinct border between cortical layers II and III. Dorsal to the IL is the PrL cortex, which contains a clear border between layers II and III. The anterior cingulate (Cg) cortex can be distinguisted by a thinning of layer I compared to both the PrL cortex on its ventral border and the primary motor context on its dorsal border (Krettek and Price, 1977).

Anatomical tract-tracing studies have elucidated the efferent, afferent, and local connections of the medial prefrontal cortex. In the IL, efferent projections exit through one of three pathways: the dorsal, lateral, and ventral pathways. The dorsal pathway contains fibers coursing through layer I to the PrL and anterior cingulate cortices. Lateral pathway fibers course through the nucleus accumbens or dorsal striatum to the internal capsule. The ventral pathway is the largest, and it contains fibers traveling to the amygdala especially the basolateral nucleus. The ventral pathway also contains fibers targeting autonomic structures, including the nucleus of the solitary tract, the RVLM, the dorsal motor nucleus of the vagus, and even the intermediolateral nucleus of the spinal cord (Neafsey et al., 1986; Hurley et al., 1991; Gabbott et al., 2005).

The PrL cortex shares some efferent connections with the IL cortex, including a dense projection to the BLA. However, the PrL cortex does not share the IL's projections to brainstem autonomic nuclei, such as the nucleus of the solitary tract (Gabbott et al., 2005). The Cg cortex lies dorsal to the prelimbic

cortex and has many similarities in both structural connectivity and function to the IL and PrL cortices. The Cg cortex projects to the BLA, but this projection is much less dense than that of the IL or PrL (Gabbott et al., 2005).

Although it is well established that the mPFC plays an important role in the responses to learned fear, studies investigating the effect of mPFC lesions have had conflicting results. Emerging evidence suggests that the different subregions of the mPFC have differential, and possibly even opposing, roles in these processes. Transient inactivation of the IL prior to extinction of auditory conditioned fear had no effect on initial fear expression (freezing behavior). However, IL inactivation impaired both the acquisition of extinction and the recall of extinction the following day. In constrast, inactivation of the PrL cortex impaired fear expression, but had no effect on extinction memory (Sierra-Mercado et al., 2011). These results suggest that activation of the PrL is essential for fear expression, but the IL is more important in extinction.

The IL and PrL cortices modulate acute stress responses partly through projections to the PVN of the hypothalamus. Lesions of the mPFC (including the IL, PrL, and Cg cortices) have been shown to result in an increase in ACTH and corticosterone production in response to restraint stress compared to sham-lesioned controls (Diorio et al., 1993). Lesion of the mPFC has also been shown to enhance Fos expression in the PVN induced by air-puff stress (Spencer et al., 2005). In addition to neurosecretory cells that initiate the HPA stress response, the PVN also houses neurons involved in autonomic control, including neurons

that project directly to the preganglionic neurons of the spinal cord (Swanson and Sawchenko, 1980). Few studies have examined the influence of the mPFC on autonomic control through the PVN. Lesion of the IL, but not the PrL cortex, was shown to increase Fos expression in pre-autonomic neurons of the PVN (Radley et al., 2006), suggesting that the intact IL inhibits activation of the PVN, possibly relaying through the bed nucleus of the stria terminalis (Crane et al., 2003).

In addition to its structural connectivity with autonomic brain regions, the mPFC has been shown to be a functional locus of forebrain autonomic control, especially in cardiovascular responses to learned fear. Lesions of the IL and ventral PrL cortices have been shown to eliminate the tachycardic response to a tone previously paired with footshock. As determined with pharmacological blockade, mPFC lesion was shown to dramatically decrease the sympathetic component of the tachycardic response to the conditioned stimulus, with no alteration in the parasympathetic bradycardic component of the heart rate response. In contrast, lesions that included the dorsal PrL and ventral anterior Cg cortices result in an increased tachycardic response to the conditioned stimulus, suggesting that the dorsal mPFC may act to decrease heart rate during stress (Frysztak and Neafsey, 1994).

Although the IL and PrL cortices are more often associated with expression and extinction of conditioned fear, the anterior Cg cortex has also been shown to modulate learned fear. Both transient inactivation and permanent lesion of the anterior Cg cortex have been shown to impair the acquisition and

expression of auditory conditioned fear. These studies suggest that the anterior cingulate may inhibit activation of the BLA during association of the aversive stimuli and auditory cues (Bissiere et al., 2008). Similiarly, in humans, EEG and fMRI studies have demonstrated activation of the anterior Cg cortex during response conflict tests (Fan et al., 2007).

Insular Cortex

Another forebrain region involved in autonomic regulation is the insular (Ins) cortex. The insular cortex is responsible for processing visceral sensory and nociciptive information. Human fMRI studies have shown that the insular cortex is activated in response to autonomic challenges including the cold pressor test (i.e., activating the sympathetic nervous system by submersing the subject's hand in very cold water) and Vasalva strain (Macey et al., 2012). The Ins cortex is located in the lateral prefrontal cortex, just ventral to the somatosensory cortex, and it has reciprocal connections with the IL, PrL, and Cg divisions of the mPFC. Like the mPFC, the Ins cortex has reciprocal connections with the lateral and basolateral nuclei of the amygdala (Gabbott et al., 2005; Jasmin et al., 2004).

The Ins cortex has been shown to modulate cardiovascular responses, as chemical stimulation with D,L-homocycteine (DLH) in the rostral portion of the posterior Ins cortex elicits a pressor response, and DLH in the caudal portion of the posterior Ins cortex elicits a depressor response (Yasui et al., 1991). The

cardiovascular control exerted by the Ins cortex is likely mediated by its heavy projections to the posterior lateral hypothalamus (Tsumori et al., 2006). The Ins cortex may play an accessory role in the acquisition and expression of conditioned fear. Combined lesions of the Ins cortex and the posterior intralaminar nucleus of the thalamus (but not the Ins cortex alone) prior to training prevent the expression of fear-potentiated startle in rats (Shi and Davis, 1999). Post-training lesions of these two regions attenuate the expression of auditory conditioned fear, but not contextually conditioned fear (Brunzell and Kim, 2001).

Orbitofrontal Cortex

The orbitofrontal (OF) cortex is located in the dorsal bank of the rostral rhinal sulcus, medial and ventral to the Ins cortex. Like the IL and PrL cortices, the OF cortex has reciprocal connections with limbic structures including the LA and BLA. The OF also projects to the ventral striatum and receives input from the cortices that govern every sensory modality (Price, 2007). These connections allow the OF cortex to encode both the identity and affective aspects of sensory stimuli, e.g., the rewarding properties of food. Accordingly, neurons in the OF cortex are activated during reward-related processes (Schultz et al., 2000). Lesions of the orbitofrontal cortex have been associated with perseverative responding in reversal learning tasks (i.e., tasks requiring learning the reversal of previously-rewarded stimulus-reward contingencies) in rats

(Chudasama and Robbins, 2003) and non-human primates (Rygula et al., 2010). Among PTSD patients, the hypoactivity typically observed in the PFC includes the OF cortex, suggesting that deficits in this region contribute to the perseveration of negative emotional responses that are a hallmark of PTSD (Shin et al., 2004). This region is also involved in mood regulation, as volume and activity of the OF cortex have also been shown to be reduced in major depression (Drevets, 2007).

Prefrontal Cortex-Amygdala Interactions

The mPFC is responsible for regulating emotional responses to relevant or potentially threatening stimuli, as well as the suppression of inappropriate emotional responses. Accordingly, activation of the mPFC has been shown to inhibit amygdala-mediated stress responses, and stimulation of the mPFC inhibits CeM neurons (Quirk et al., 2003). However the mechanism of this mPFC inhibition of the amygdala is unclear, since the most robust projections of both the IL and PrL cortex to the amygdala are glutamatergic projections to the BLA. This excitation of the BLA, in turn, leads to the excitation of projection sites, including the CeM. Since the mPFC has only a sparse projection to the CeM (McDonald, 1998), the mechanism of inhibition is likely indirect.

Because excitatory projections from the mPFC synapse onto both glutamatergic projection neurons and GABAergic interneurons in the BLA (Smith et al., 2000), it is possible that input from the mPFC could activate BLA

interneurons, and thus inhibit BLA projection neurons. *In vivo* electrophysiological studies have provided support for this theory, given that electrical stimulation of the mPFC inhibits firing in both the BLA (Rosenkranz and Grace, 2001) and the LA (Rosenkranz et al., 2003). However, in contrast to these findings, another study found that spontaneous firing of the IL cortex resulted in increased firing in the BLA, suggesting that the locus of inhibition is downstream of the BLA (Likhtik et al., 2005).

One likely mechanism of mPFC inhibition of the CeM is through the the GABA-ergic neurons of the ICM, which provide inhibition to CeM (Royer et al., 1999). In addition to the BLA, the mPFC has a large projection to the ICM (Pinard et al., 2012; Mcdonald et al., 1996). In fact, disinhibition of the IL cortex with the non-competitive GABA-A antagonist, picrotoxin, elicits a large increase in Fos immunoreactivity in neurons of the ICM (Berretta et al., 2005), supporting the idea that activation of the IL normally inhibits CeM neurons via excitation of neurons of the ICM.

Central Noradrenergic Regulation of Stress Responses and Circulation

Locus Coeruleus

The locus coeruleus (LC) of the dorsal pons provides robust noradrenergic innervation to widespread regions of the forebrain, including the BLA and mPFC (Ader et al., 1980). The activity of LC neurons varies with an animal's state of vigilance. In the unasthetized rat, LC neurons exhibit slow, tonic spontaneous

discharge (~1.75 Hz). In response to novel or salient sensory stimulation, LC neurons exhibit a biphasic response, consisting of an initial burst of impulses (~200 ms) followed by a longer period of reduced activity (~600 ms). Multiple modalities of sensory stimulation evoke this response, including auditory stimulation (tone pips), visual stimulation (flashes), and tactile stimulation (gentle touch or tail pinch). Of these stimuli, noxious tactile stimulation generates the most pronounced electrophysiological reponse as well as the greatest behavioral orienting reponse (Aston-Jones and Bloom, 1981; Abercrombie and Jacobs, 1987), suggesting that LC activation is correlated with the level of stimulus salience.

Activation of the LC results in NE release throughout the forebrain, including the amygdala and prefrontal cortex. Activation of the LC by electrical stimulation results in norepinephrine release in the prefrontal cortex, as measured by microdialysis and high-performance liquid chromatography (HPLC). Slow, tonic stimulation results in small increases in NE release, and phasic stimulation (as observed in arousal) results in larger increases in NE release, with higher frequencies stimulation resulting in greater NE release (Florin-Lechner et al., 1996; Berridge and Abercrombie, 1999). Accordingly, salient stimuli that elicit phasic LC activity, such as exposure to an auditory cue previously paired with footshock, results in NE release in the PFC (Feenstra et al., 2001). In turn, this NE release modulates PFC activity, as stimulation of the

LC induces changes in forebrain EEG frequency and amplitude in a βAR-dependent manner (Berridge and Foote, 1991).

In addition to evidence from electrophysiological and HPLC studies, immunohistochemical studies have shown that several different acute stressors, including noise stress, foot shock, restraint stress, forced swim stress, and exposure to an elevated plus maze, induce c-fos expression in the LC (Abercrombie and Jacobs, 1987; Passerin et al., 2000). Chronic intermittent hypoxia increases c-fos expression in the LC following acute exposure to immobilization stress in rats, demonstrating that chronic exposure to physiological stressors can produce lasting changes in LC reactivity to acute psychological stressors (Ma et al., 2008).

Central Noradrenergic Control of Circulation

The LC plays an important role in cardiovascular regulation as well. Noradrenergic neurons of the LC, among other medullary and pontine catecholaminergic cell groups, have been shown to be activated by both hypoxia exposure and electrical stimulation of the carotid sinus nerve, implicating the LC in chemoreflex and baroreflex responses (Erickson and Millhorn, 1994). Additonally, elevations in blood pressure (induced either pharmacologically or with hypervolemia) have been been shown to increase the release of GABA in the LC (Singewald et al., 1995). This response was later shown to be dependent on intact baroreceptor input (Kouvelas et al., 2006).

The role of the LC in the control of blood pressure has been the subject of debate, as electrical stimulation of the LC generally elicits a pressor effect (Berecek and Mitchum, 1986), while chemical stimulation has been shown to elicit both pressor (Chen and Chai, 2002) and depressor effects (Sved and Felsten, 1987; Murase et al., 1993). Ganglionic blockade has been shown to attenuate pressor responses to LC electrical stimulation, thus providing evidence that LC activation facilitates sympathetic outflow (Berecek and Mitchum, 1986). However, the mechanism of this sympathoexcitation is unclear. Projections of the LC to RVLM are primarily inhibitory (Van Bockstaele et al., 1989), while direct descending projections of LC neurons to the spinal cord have variable effects on sympathetic control (Proudfit and Clark, 1991).

It is possible that the LC mediates autonomic and neuroendocrine responses to stress through the PVN, though indirectly. The PVN's primary noradrenergic input is from the A2 region, while a much smaller contribution from the LC reaches only the parvicellular neuroendocrine portion of the nucleus that projects to spinal cord pre-ganglionic cells (Cunningham and Sawchenko, 1988). However, another brain region, such as the mPFC, that receives input from the LC and projects to the PVN, may serve as an intermediary between these two regions (Radley et al., 2008).

In addition to its role in cardiovascular regulation and responses to stressors, the LC is activated after MI. Heart failure following coronary artery ligation was accompanied by increases in long-term neuronal activation in the

LC, as assessed by hexokinase activity (Patel et al., 1993) and Fra-like immunoreactivity (Leenen, 2007). In another study, coronary artery ligation acutely increased norepinephrine turnover in the LC (Sole et al., 1982). It remains to be determined if central noradrenergic responses to psychological stressors are exaggerated after MI.

Noradrenergic Modulation of Stress Responses

It is well documented that NE is released in response to novel or threatening stimuli, but it is the adrenergic receptors on target cells that determine the functional response to NE. While NE can induce hyperpolarization (and thus inhibition) by binding α_2ARs coupled to $G\alpha_i$, NE can induce activation of target cells by binding βARs coupled to $G\alpha_s$ or α_1-adrenergic receptors coupled to $G\alpha_q$. In unstressed rats, electrophysiological studies have shown norepinephrine to inhibit spontaneous and evoked potentials in the BLA complex (with similar responses in the BLA and LA). This effect has been shown to be mediated by α_2ARs, since both an α_2AR agonist (clonidine) and βAR antagonist (propranolol) administration potentiate the inhibition by NE (Buffalari and Grace, 2007). Following chronic cold stress, however, NE activates BLA neurons by acting on βARs, suggesting a stress-induced shift in receptor ratio (Buffalari and Grace, 2009). *In vitro* electrophysiological studies have demonstrated similar inhibitory effects of NE specifically in the LA, i.e., application of NE inhibited evoked potentials in amygdala slices (Johnson et al., 2011).

Exposure to stressful stimuli may result in changes in β_1AR expression, as rats exposed to acute footshock stress display increased β_1AR immunoreactivity in the BLA. Also, β_1AR blockade in the BLA results in decreased freezing behavior in response to a tone previously paired with footshock (Fu et al., 2008). Transient downregulation of β_1ARs produced by direct injection of short-interfering RNA into the BLA impairs retrieval of auditory fear memory in rats. Fear memory is restored when receptor levels return to normal (Fu et al., 2007). Noradrenergic signaling through βARs in the LA has been shown to be necessary for the retrieval of conditioned fear, as noradrengergic blockade by propranolol after retrieval disrupts memory reconsolidation (Debiec and LeDoux, 2006; Debiec and Ledoux, 2004). These data support the notion that noradrenergic signaling through β_1ARs in the LA and BLA is necessary for fear memory consolidation and retrieval.

Although it is well documented that salient stimuli induce the release of NE in the mPFC (Feenstra et al., 2001), the role of noradrenergic signaling in the mPFC is not well established. The amount of NE released in the mPFC is proportional to the salience of a stimulus, whether it is aversive or appetitive in nature (Ventura et al., 2008). In turn, noradrenergic signaling in the mPFC is essential for assigning the motivational value of high salience stimuli, as lesion of noradrenergic terminals in the mPFC eliminates conditioned place preference or avoidance only to salient appetitive or aversive stimuli (Ventura et al., 2008). NE also modulates attention and working memory processes, as depletion of

norepinephrine in this region (IL, PrL, and Cg) impairs rats' performance in an attentional reaction time task (Milstein et al., 2007). The facilitory effect of NE on attention processes is thought to be mediated through α_2ARs, since systemic treatment with the α_2AR agonist, guanfacine, improves performance in an attentional task requiring the PFC. Conversely, mice with a mutation in the α_{2a}AR exhibit deficits in this task (Franowicz et al., 2002).

Electrophysiological studies have demonstrated that NE inhibits the firing of IL pyramidal neurons in an α_2AR-dependent manner (Wang et al., 2010). While NE signaling through α_2ARs is thought to facilitate working memory, β_1AR activation in the mPFC is thought to impair working memory. This idea is supported by the fact that infusion of the β_1AR antagonist, betaxolol, into the mPFC (dorsal IL and ventral PrL) improves performance in a working memory task (Ramos et al., 2005). It is thought that β_1ARs and β_2ARs may mediate opposing effects in the mPFC, as infusion of the β_2AR agonist, clenbuterol, improves performance in a working memory test in aged rats. This effect is reversed by the β_2AR antagonist, ICI-118,551.

Even fewer studies have examined the role of mPFC noradrenergic signaling in stress responses. Selective lesion of noradrenergic nerve terminals specifically in the PrL cortex has been shown to enhance restraint stress-induced Fos expression in the PrL. This enhancement in PrL activation in the absence of NE was accompanied by a decrease in Fos expression in the PVN. These results suggest that NE released during stress normally inhibits the PrL, and this

inhibition allows for enhanced activation of the HPA stress responses (Radley et al., 2008).

Noradrenergic signaling in the IL contributes to the process of fear extinction. Blockade of noradrenergic signaling through βARs in the IL has been shown to impair retrieval of fear extinction. In rats trained to associate a tone with footshock, blockade of IL βARs with propranolol just prior to extinction training impaired retrieval of extinction memory the following day without affecting freezing behavior during the extinction training session. This effect of βAR blockade was localized to the IL cortex, as propranolol infusion in the PrL and Cg cortices prior to extinction had no effect on freezing behavior. In the same study, NE enhanced the increased spike frequency of IL neurons in response to injected current in a prefrontal cortical slice preparation. Pre-treatment with propranolol or the PKA inhibitor Rf-cAMPs prevented the effect of NE, suggesting that noradrenergic enhancement of extinction memory is dependent on βAR activation, but also subsequent cAMP production and PKA activation (Mueller et al., 2008).

It is currently unknown how changes in noradrenergic signaling in the mPFC or amygdala may contribute to the development of anxiety and depression after. Therefore the studies in this dissertation were designed to investigate the effects of MI on anxiety-like behavior, and to assess noradrenergic changes in stress-associated brain regions that may underlie the development of post-MI anxiety and arrhythmia generation.

CHAPTER 3

NEOPHOBIA, ARRHYTHMIA, AND ALTERED FOREBRAIN METABOLIC ACTIVATION AFTER MYOCARDIAL INFARCTION

Abstract:

Depression and anxiety are commonly comorbid with myocardial infarction (MI). Patients who develop depression or anxiety after an MI have increased cardiovascular morbidity and mortality. Sudden cardiac death is the most common cause of death in MI patients and is often preceded by intense emotional arousal. However, the central nervous system mechanisms that contribute to post-MI anxiety and arrhythmia susceptibility are currently unknown. Therefore, we determined if rats subjected to MI (induced by coronary artery ligation) exhibit anxiety-like behavior. We also assessed MI-induced changes in cytochrome oxidase activity, an index of metabolic activation, in regions governing autonomic and behavioral control. In addition, we assessed cardiac arrhythmia generation, both at baseline and in response to central norepinephrine release (induced by locus coeruleus stimulation). MI rats that developed left ventricular dysfunction 7 weeks after surgery exhibited a longer latency to leave the center square of an open field apparatus compared to sham-ligated rats, indicating a neophobic response. Compared to shams, MI rats exhibited an increase in metabolic activity in the lateral amygdala, but a decrease

in activity in the rostral basolateral amygdaloid complex. The infralimbic, prelimbic, and orbitofrontal cortices of MI rats also displayed increased metabolic activity. However, in response to locus coeruleus stimulation designed to mimic a mild stressor, MI rats exhibited a decrease in metabolic activity in these PFC regions. This effect was most profound in the IL cortex, a region necessary for regulating emotional responses to learned fear. MI rats also displayed an increase in ventricular arrhythmias in response to locus coeruleus stimulation. Together, these results suggest that basal and norepinephrine-induced changes in metabolic activity occur after MI in brain regions important in the development of anxiety.

Introduction:

Depression and anxiety are common comorbidities with myocardial infarction (MI) and subsequent heart failure (Frasure-Smith and Lesperance, 2003; Gander and von Kanel, 2006; Friedmann et al., 2006). These two disorders afflict about 5% of the general population, but 30–45% of MI patients (Friedmann et al., 2006). Patients who develop depression or anxiety after an MI have higher rates of future cardiovascular morbidity and mortality, compared to both MI patients with pre-existing depression or anxiety and MI patients who do not develop these disorders (de Jonge et al., 2006; Huffman et al., 2008; Dickens et al., 2008; Moser et al., 2007a; Moser et al., 2007a). The most common cause of death in post-MI patients is sudden cardiac death due to ventricular arrhythmias (Saxon,

2005), and depressed post-MI patients have an even greater risk for sudden cardiac death (Frasure-Smith and Lesperance, 2008; Barefoot et al., 1996). Furthermore, 20–40% of sudden cardiac deaths are precipitated by acute emotional stressors (Vlastelica, 2008; Ziegelstein, 2007). Together, these studies suggest that MI itself precipitates central nervous system changes that contribute to the development of changes in both emotional responding and arrhythmia susceptibility.

Despite extensive documentation of the association between anxiety and cardiovascular-related death, little is known about the central nervous system mechanisms underlying this phenomenon. Increased sympathetic nervous system activation contributes to emotionally-triggered arrhythmias (Du et al., 1999). There is also evidence of a contribution of cortical and subcortical forebrain regions to sympathetic activation and arrhythmia generation (Carpeggiani et al., 1992; Skinner and Reed, 1981; Ter Horst, 1999).
The LC is the primary source of norepinephrine (NE) to the forebrain, and the LC is activated by salient and noxious stimuli, resulting in the release of NE in multiple regions of the forebrain, hindbrain, and spinal cord (Florin-Lechner et al., 1996; Chen and Sara, 2007; Van Bockstaele et al., 1989; Proudfit and Clark, 1991). The LC also becomes activated in response to cardiovascular stimuli (Erickson and Millhorn, 1994), including MI. Turnover of NE is increased in the LC in response to MI in rats (Sole et al., 1982), and MI also increases Fra-like immunoreactivity and hexokinase activity, indicating long-term neuronal

activation in the LC (Patel et al., 1993; Vahid-Ansari and Leenen, 1998). Human heart failure patients have been shown to have elevated NE turnover in the subcortical forebrain, as determined by left or right internal jugular venous blood sampling (after cerebral venous sinus scanning to determine the pattern of venous drainage in individual subjects). This increase in subcortical NE turnover was positively correlated with elevated whole-body NE turnover, suggesting that noradrenergic signaling in the forebrain contributes, in part, to the elevated sympathetic drive following MI (Aggarwal et al., 2002).

Norepinephrine acting on βARs in the central nervous system is thought to contribute to arrhythmia generation. Central administration of the βAR antagonist, propranolol, was shown to delay the development of VF induced by coronary ischemia in pigs (Parker et al., 1990). Similarly, chronic intracerebroventricular administration of the β_1AR antagonist, metoprolol, was shown to attenuate left ventricular remodeling in rats subjected to MI. In this latter study, acute central administration of metoprolol was shown to decrease heart rate, but this effect was prevented by systemic sympathetic blockade (Gourine et al., 2008). These results suggest that β_1ARs in the brain contribute to the sympathetic activation after MI. Still, it remains unclear which brain regions are involved in this central noradrenergic modulation of cardiac control.

The amygdala is a cluster of subcortical nuclei that coordinate behavioral and autonomic responses to stressful or emotional stimuli. The amygdala is necessary for forming associations between stressors and environmental cues,

and hyperactivity of the amygdala has been implicated in anxiety disorders, including post-traumatic stress disorder (Koenigs and Grafman, 2009). The amygdala also may facilitate arrhythmia generation, as cryogenic blockade of the amygdala delays or prevents ventricular fibrillation (VF) during reversible myocardial ischemia in conscious, psychologically stressed pigs (Carpeggiani et al., 1992). Additionally, inhibition of the amygdala with the $GABA_A$ agonist, muscimol, reduces the tachycardic response to restraint stress and reverses the accompanying increase in sympatho-vagal ratio of autonomic input to the heart (Salome et al., 2007), suggesting that hyperactivation of the amygdala may be arrhythmogenic.

The prefrontal cortex consists of several distinct regions that regulate "higher order" processes including working memory and planning (Ramos et al., 2005), but are also involved in modulating autonomic responses to acute stress and learned fear (Frysztak and Neafsey, 1994). Brain imaging studies of heart failure patients demonstrate abnormalities in the prefrontal cortex (Woo et al., 2009). As in the amygdala, cryogenic blockade of the prefrontal cortex was shown to delay or prevent VF during myocardial ischemia in pigs (Skinner and Reed, 1981), implicating the PFC as a potential modulator of heart rhythms.

The long-term metabolic response to MI in brain regions regulating stress responses is currently unknown. It is also unknown whether stress-associated brain regions have an altered response to stress-induced NE release after MI. Though the association between MI and anxiety in humans is well documented,

little is known about the effect of MI on anxiety-like behavior in rats. In previous studies in our laboratory, rats subjected to MI exhibited paradoxical anxiety-like behavior (increased open arm activity and head-first jumps) in the elevated plus maze (Henze et al., 2008). Therefore, this study sought to further characterize anxiety-like behavior in rats in response to MI, and to determine the effect of MI on basal and NE-modulated metabolic activation in multiple regions of the PFC and amygdala. This study also sought to determine the effect of acute stress-associated LC activation on arrhythmia generation in MI and non-infarcted rats.

Materials and Methods:

Animals

All experiments were performed in accordance with the American Physiological Society Guiding Principles for Research Involving Animals and Human Beings (2002) and were approved by the University's Institutional Animal Care and Use Committee. Pair-housed young adult male Sprague-Dawley rats between 275 and 299 g (Harlan, Indianapolis, IN) were acclimated to the virarium for one week prior to surgery with *ad libitum* access to food and water. Rats were housed at a constant temperature of 22 ± 2℃ with a 12/12 hour li ght/dark cycle. Rats of this strain, sex, age, and weight have been used previously by others and us to assess autonomic and behavioral changes after MI (Henze et al., 2008; Grippo et al., 2003b; Francis et al., 2001a).

Coronary artery ligation

To induce MI, rats were subjected to coronary artery ligation (CAL) as described by others (Pfeifer et al., 2001) and us (Henze et al., 2008) previously, with modifications. Briefly, animals were anesthetized with ketamine/xylazine (100 mg/kg + 10 mg/kg, i.m.). The left anterior thorax (extending the entire length of the sternum from the midline to the left midaxillary line) was shaved and scrubbed with a povidone-iodine solution and 70% ethanol. Rats were intubated and mechanically ventilated (60 breaths per minute, 3 mL tidal volume) with room air supplemented with 100% O_2. In order to monitor heart rate and ECG waveforms throughout the surgery, rats were instrumented with subcutaneous recording electrodes in lead II position. The ECG signal was recorded through a Bioamplifier (ADInstruments) and was sampled at 1000Hz using a Powerlab data acquisition system using Chart for Windows. A skin incision was made 1 cm to the left of the sternum and the skin was separated from the muscle with blunt dissection. The pectoralis major and minor muscles were separated with blunt dissection and retracted to expose the anterior thoracic wall. A left thoracotomy was performed through the 4^{th} intercostal space to expose the anterior surface of the heart. The pericardium was removed with fine forceps, and a 6-0 silk suture was inserted through the apex of the heart to allow manipulation of the heart for the ligation procedure.

The left anterior descending coronary artery was ligated with 6-0 silk suture by passing the suture through a portion of the myocardium between the

trunk of the pulmonary artery and the right atrium (see Figure 1 for schematic). After securing the ligature with a square knot, the chest was left open for 10 minutes in order to monitor heart rate and ECG waveforms to prevent fatal ventricular tachycardia (VT) or fibrillation. If a rat exhibited sustained ventricular tachycardia or fibrillation (more than 10 seconds), the heart was mechanically stimulated with a cotton swab until it regained a normal sinus rhythm. The secondary purpose of this monitoring was to obtain a preliminary assessment of infarct severity, as indicated by tissue blanching and the development of ventricular arrhythmias (PVCs, VT, or VF). If a rat did not exhibit blanching and/or arrhythmias after 10 minutes, a second ligature was applied closer to the base of the heart. Rats subjected to sham ligation underwent thoracotomy and removal of the pericardium but had no sutures inserted through the heart.

After ligation, the loose ends of the sutures were cut, and the thoracotomy was closed around a drainage tube with 3-0 chromic gut suture. Negative pressure (-2 mmHg) was applied through the drainage tube during its removal, while closing the thoracotomy. Muscles and skin were closed with 3-0 silk suture in separate layers. Rats were given lidocaine (10 mg/kg, s.c.) just prior to, and every 2 hours, for 8 hours after ligation to reduce the incidence of arrhythmia. All rats were given buprenorphine (50 µg/kg, s.c.) following arousal from surgery and again 16, 24, 40, and 48 hours later. Rats were singly housed after surgery.

Echocardiography

To assess left ventricular function after MI or sham ligation, rats were anesthetized with ketamine/xylazine (100 mg/kg + 7 mg/kg, i.m.) and subjected to 2D guided, M-mode echocardiography (Acuson Sequoia C256, Siemens AG) to assess left ventricular function 1 and 7 weeks after surgery. Rats were scanned using a transthoracic 2-D Acuson 15L8 Microson High Resolution Transducer from 2 cm depth. The parasternal long axis view was used to guide M-mode measurements, which were made just below the level of the papillary muscles in a minimum of 3 successive cardiac cycles. Measurements included left ventricular end-diastolic diameter (LVDD, a measure of dilatation) and left ventricular fractional shortening (a measure of contraction). Fractional shortening (FS) was calculated from the M-mode images as the percent change in intraventricular diameter from systole to diastole at the level of the left ventricular papillary muscle. Representative M-mode images from MI and sham-ligated rats are shown in Figure 2. All sham-operated rats and those CAL rats with FS less than 25% were included in the study.

Open Field Testing

Seven weeks after CAL or sham ligation, rats were subjected to the open field test to assess anxiety-like and exploratory behavior. Rats were placed in a custom-made apparatus, consisting of a 39 x 39 inch polyurethane-coated open wooden box with 13.8 inch-high walls in a sound- and light-attenuated room

(~100 lux). The box was painted gray, and its floor was delineated with white lines into 25 8 x 8-inch squares. A 1.6-inch hole was located 6.7 inches from each corner. In the 12-minute test, rats were placed into the center square. Throughout the test, behavior was video recorded for subsequent analysis by an observer blind to the experimental conditions. Variables analyzed included the time to initially leave the center square, the number of line crossings in wall squares and center squares (all 4 paws must cross the line), time spent in wall squares and center squares, number of rears, fecal boli, and nose hole pokes.

Locus Coeruleus Stimulation

One week after open field testing, rats were anesthetized with chloral hydrate (400 mg/kg, i.p.) and instrumented with a femoral arterial catheter to enable arterial pressure (AP) measurement and a femoral venous catheter to enable delivery of supplemental chloral hydrate anesthesia (80 mg/kg/hour). Catheters consisted of PE-10 tubing heat fused to PE-50 tubing, filled with heparinzed saline (75 USP units/mL). Rats were also instrumented with subcutaneous ECG electrodes in lead II position to assess arrhythmias. Rats were placed in a Kopf stereotaxic frame and a skin incision was made to expose the skull. The periosteum was scraped away, and burr holes were drilled to allow placement of a stainless steel NE-100 concentric bipolar stimulating electrode (Rhodes Medical Instruments, Summerland, CA) into the right locus coeruleus (0.8 mm caudal to the interaural line, 3 mm dorsal to the interaural line, and 1.3

mm to the right of the midline, with the incisor bar positioned 5.8 mm below the inter-aural line). We chose this stereotaxic approach based on our ability to elicit pressor responses to electrical stimulation and either a pressor or depressor response to injection of the neuroexcitatory agent, DL-homocysteic acid with these coordinates in a pilot study. The response we observed with chemical stimulation deviated from the typical depressor response described in the literature depending on anesthesia (i.e. a depressor response with sodium pentobarbital and a pressor response with chloral hydrate). Current pulses were delivered by Pulsar 6i stimulator (Frederick Haer & Co., Bowdoin, ME) in a pattern shown by others to cause significant norepinephrine release in the prefrontal cortex (Florin-Lechner et al., 1996). Specifically, stimulation consisted of trains of three 0.2 ms pulses with an 83 ms inter-pulse interval (12 Hz) and 700 μA amplitude every second for 20 minutes (see Figure 3 for schematic). To enable comparisons of stimulation-induced changes in cytochrome oxidase activity to unstimulated controls, half the rats in each surgical group were instrumented with an electrode but did not receive stimulation. MI rats were assigned to receive stimulation or no stimulation based on their FS determined 7 weeks post-surgery, such that rats with similar fractional shortening were assigned to different stimulation groups. Sham-ligated rats were randomized to receive stimulation or no stimulation.

Euthanasia and Tissue Processing

Five minutes after the end of stimulation, the electrode was slowly removed and the rat was decapitated. The brain was rapidly removed, cooled in -30^{o}C isopentane, frozen in powdered dry ice, and stored at -80^{o}C. The heart and lungs were also removed and weighed to assess cardiac remodeling and pulmonary edema, respectively. Neurohumoral activation in heart failure can lead to cachexia and/or fluid retention that can make body weight an unreliable index of body size (Sukhanov et al., 2011). Therefore, left tibias were also removed and their length measured with a caliper to obtain an additional index of body size. Heart and lung weights were normalized to both body weight and tibia length. Brains were sectioned at 16 μm on a cryostat (chamber temperature -16℃, object temperature -14℃) and sections from the prefrontal cortex and amygdala were thaw-mounted on superfrost plus slides. After air-drying for 5 minutes, slides were stored at -80℃ until cytochrome oxi dase histochemistry.

Cytochrome Oxidase Histochemistry

The cytochrome oxidase activity (CO) histochemical assay has been shown to provide high resolution assessment of neuronal metabolic activity in response to both chronic and acute interventions. In a previous study investigating the range of CO staining generated by different incubation times, staining reached saturation levels at 120–150 minutes, and a 90-minute incubation yielded a signal in the linear portion of the staining curve with minimal

variability (Tseng et al., 2006). Since CO staining intensity varies among brain regions, we conducted a pilot study to determine the best incubation time for CO activity in the BLA. For this pilot study, specimen slides containing BLA sections from naïve rats were allowed to warm to room temperature and dry for 90 minutes, and then slides were incubated for 30, 60, 90, or 120 minutes at 37^{o} C in 0.1 M phosphate buffer containing 0.5 g/L 3,3'-diaminobenzidine, 0.33 g/L cytochrome c from equine heart, 44 g/L sucrose, and 0.2 g/L catalase (all reagents from Sigma-Aldrich). After incubation, slides were rinsed in room-temperature phosphate buffer (2 x 10 minutes), dehydrated in ethanol, cleared in xylene, and coverslipped with DPX.

Cytochrome oxidase activity was determined by digitizing the stained slides (CoolScan V, Nikon) and determining the relative optical density with Image J software. The relative optical density was determined by subtracting the optical density of the structure of interest (e.g., basolateral amygdala) from nearby white matter background (e.g. optic tract for amygdala sections), and then dividing that value by the maximum optical density value. In a pilot study, 90 minutes yielded relative optical density measurements that fell in the linear portion of the curve, with minimal variability. We chose this time frame to enable us to detect both increases and decreases in activity in the amygdala. Identical staining and image analysis procedures were followed for experimental tissue.

Defining structures for quantification of cytochrome oxidase activity

Regions of interest in the amygdala and prefrontal cortex were delineated according to the rat brain atlases of Paxinos and Watson (Paxinos and Watson, 2004) and Swanson (Swanson, 2003). In the amygdala, cytochrome oxidase activity was measured in the lateral amygdala (LA), basolateral nucleus (BLA nucleus, more caudal sections), basolateral complex (BLA complex, more rostral sections) and the lateral and medial divisions of the central nucleus of the amygdala (CeL, CeM). In the prefrontal cortex, cytochrome oxidase (CO) activity was measured in the infralimbic (IL), prelimbic (PrL), anterior cingulate (Cg), primary and secondary motor (M), somatosensory (SM), insular (Ins), and orbitofrontal (OF) cortices. While amygdala structures are readily delineated by white matter boundaries and differential cellular/staining densities, CO staining appears much more homogeneous in the prefrontal cortex. Therefore, in the PFC, the boundaries of regions of interest were determined by observing cytoarchitectonic boundaries as described previously (Krettek and Price, 1977) in several adjacent or similar Nissl-stained sections. For all regions quantified, a single relative optical density value per rat was determined by averaging the measurements of 3 to 4 sections. Initially, measurements were made on only the side of the brain ipsilateral to the stimulating electrode because the LC projects more heavily to the ipsilateral cortex (Ader et al., 1980). In regions where analysis revealed significant differences between stimulated and unstimulated

groups, CO activity was quantified in the contralateral side of the brain for comparison.

Blood Pressure Analysis

To confirm proper placement of stimulating electrodes based on previously reported pressor responses to LC stimulation (Berecek and Mitchum, 1986; Sved and Felsten, 1987), and to determine the effect of MI on the hemodynamic response to LC stimulation, blood pressure and heart rate responses were averaged over each minute of the experiment (starting 6 minutes before the start of stimulation and ending 4 minutes after the end of stimulation).

Arrhythmia Analysis

Analysis of ECG waveforms was used to determine whether the simulated stressor of LC stimulation increased cardiac arrhythmias. The ECG pattern recognition software, ecg-Auto, from EMKA Technologies, was used to detect and quantify arrhythmic waveforms in ECG recordings. Both normal and aberrant waveforms were identified in each rat and added to a library. Arrhythmias were defined according to the Lambeth conventions (Walker et al., 1988), and included PVCs, bigeminy, and VT. Four or more consecutive PVCs were defined as VT. Comparison with the simultaneous AP recording helped resolve ambiguities in ECG waveforms (e.g. the premature ventricular beat in bigeminy often results in an extra-systole evident in the AP recording. The EMKA

analysis protocol detected the number of times each waveform occurred, and at what time each waveform occurred relative to LC stimulation onset.

Statistical Analysis

For echocardiography data, two-way ANOVA with repeated measures were used to assess differences in fractional shortening and left ventricular diastolic diameter between MI and sham-ligated rats over time. For measures of congestion and remodeling, Student's t-tests were used to assess group differences in the ratios of heart and lung weight to both body weight and tibia length. In the open field test, Student's t-tests were used to assess group differences in all behavioral variables, including time to leave the central square, center and wall square entries, time spent in center and wall squares, and fecal boli. For blood pressure and heart rate during the the LC stimulation experiment, 3-way ANOVA with repeated measures were used to determine the effects of surgical treatment and stimulation over time. For arrhythmia analysis, two-way ANOVA on ranks was used (due to lack of normal distribution of data) to assess the effect of MI and stimulation on percent abnormal beats unique to the stimulation (or mock stimulation) period of the experiment. For cytochrome oxidase activity, two-way ANOVA were used to assess the effects of MI and stimulation. Tukey *post hoc* tests were used for further analysis of main effects and interactions for all ANOVA. For all tests, P values of less than 0.05 were defined as significant.

Results:

Echocardiography Measurements

As shown in Figure 2, fractional shortening was significantly decreased in MI rats relative to sham-ligated rats both 1 and 7 weeks after surgery. In MI rats, but not shams, fractional shortening was significantly decreased at week 7 compared to week 1. Left ventricular diastolic diameter was significantly increased in MI rats compared to shams both 1 week and 7 weeks after surgery. Diastolic diameter was significantly increased for MI rats at week 7 compared to week 1. Sham-ligated rats exhibited a significant but smaller increase in diastolic diameter at week 7 compared to week 1.

Terminal Measurements of Congestion and Remodeling

Eight weeks after surgery, sham-ligated rats weighed an average of 400 ± 6 grams, and MI rats weighed an average of 395 ± 7 grams. Ratios of post-mortem lung and heart wet weight to body weight and tibia length are shown for MI and sham-ligated rats (Figure 4). Student's t-test revealed elevated lung and heart weights in MI rats when normalized to both body weight and tibia length.

Open Field Testing

As shown in Figure 5, MI rats took longer than shams to leave the center square of the apparatus. The number of entries into wall squares did not differ

between MI and sham-ligated rats. No difference in the number of center square entries, wall square entries, or total square entries was observed between MI and sham-ligated rats. The total time spent in each square type, as well as the number of nose pokes, rears, and fecal boli did not differ between MI and sham-ligated rats.

Blood Pressure and Heart Rate Responses to Locus Coeruleus Stimulation

The effect of MI and locus coeruleus stimulation on mean arterial pressure (MAP) and heart rate (HR) over time is shown in Figure 6. Compared to a mean baseline MAP of 63 mmHg in sham-ligated rats and 60 mmHg in MI rats, stimulation resulted in a significant increase in MAP for both MI and sham-ligated rats over the course of the stimulation period. Stimulation did not result in as large an increase in MAP in MI rats compared to shams. Mean arterial pressure in unstimulated sham-ligated rats tended to increase slightly over the course of the recording period (from an average baseline MAP of 56 mmHg), while MAP in unstimulated MI rats tended to decrease slightly over the course of the recording period (from a mean baseline MAP of 72 mmHg). There was no significant effect of stimulation or MI on HR over the course of the recording period. Baseline HR was 320, 331, 416, and 385 beats per minute in sham unstimulated, sham stimulated, MI unstimulated, and MI stimulated rats, respectively, and two-way ANOVA revealed a main effect of surgery on baseline heart rate [$F(1,27) = 14.1$, $P<0.01$] due to increased heart rate in MI rats compared to sham-ligated rats.

Lowering the stimulating electrode into the LC resulted in a decrease in blood pressure in all groups, with no effect on heart rate.

Effect of Locus Coeruleus Stimulation on Arrhythmia Generation

Types of arrhythmias analyzed included bigeminy, characterized by alternation of a normal beat with a PVC (Figure 7 and Figure 8), isolated PVCs, and ventricular tachycardia (Figure 7). Representative sequential ECG waveforms are shown for MI rats subjected to LC stimulation (Figure 9). Stimulated MI rats developed significantly more new arrhythmias (pooling bigeminy, PVCs, and ventricular tachycardia) after the initiation of stimulation compared with unstimulated MI rats or stimulated shams. Similarly, stimulated MI rats developed significantly more isolated PVCs than both unstimulated MI rats and stimulated shams. Analysis revealed increased bigeminy as a result of stimulation in both MI and sham-ligated rats. Analysis did not reveal any effects of MI or stimulation on the amount of VT, though only stimulated MI rats developed this arrhythmia (Figure 10). Two sham-ligated rats developed bigeminy as a result of stimulation. However, these 2 sham-ligated rats both took slightly longer (10.96 and 9.83 minutes) to develop begeminy compared to the the average onset time in stimulated MI rats (9.01 minutes after stimulation start). Sham-ligated rats that underwent mock stimulation did not exhibit any arrhythmias.

Cytochrome Oxidase Histochemistry: Pilot Studies

Results from a pilot study performed to optimize incubation time in cytochrome oxidase histochemistry procedures are shown in Figure 11. In this study, the relative optical density generated from a 90-minute incubation yielded miminal variability and fell in the linear portion of the curve.

Cytochrome Oxidase Histochemistry: Main Experiment

Typical cytochrome oxidase staining is shown in regions outlined in Figure 12. Two-way ANOVA revealed a significant interaction between surgery and stimulation in the IL, PrL, and OF cortices, such that unstimulated MI rats had increased CO activity compared to unstimulated sham-ligated rats, yet in response to stimulation, MI rats exhibited lower CO activity compared to unstimulated MI rats (Figure 13). *Post hoc* comparisons revealed that this effect was most profound in the IL cortex. In the IL of MI rats receiving LC stimulation, CO activity was invariably lower in the side ipsilateral to stimulation (Figure 14). Further analyses revealed no significant main effect or interaction ofsurgery or stimulation in the motor cortex (primary and secondary), somatosensory cortex, insular cortex, BLA, or CeA (Table 1).

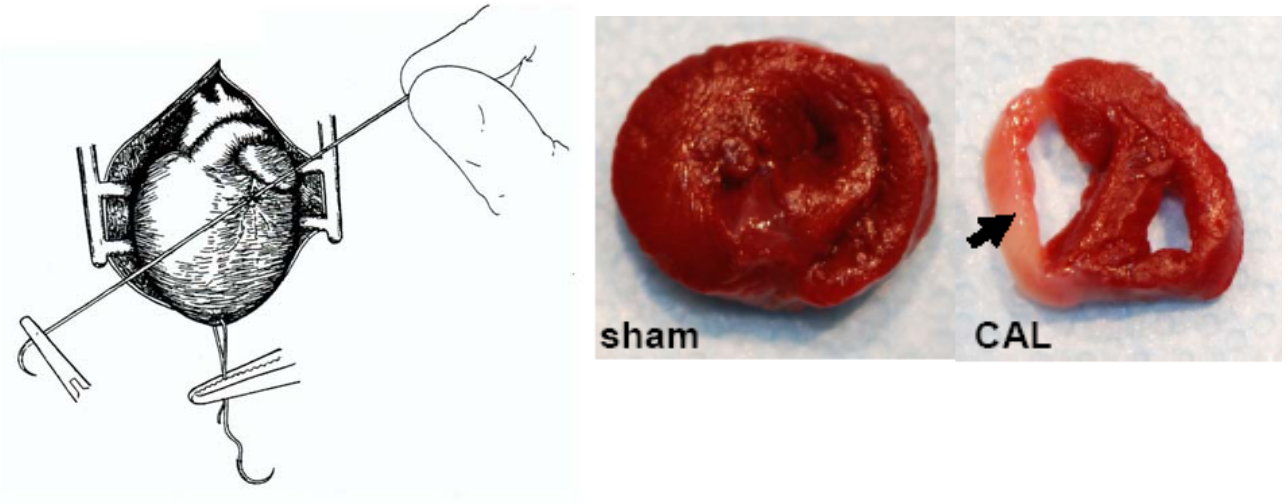

Figure 1. Coronary artery ligation surgery. Schematic of coronary ligation (CAL) surgery (Kilgore), in which silk suture (6-0) is tied around the left anterior descending portion of the left coronary artery and permanently ligated to occlude blood flow to portions of the left ventricle in order to induce MI (A). Cross sections of hearts from rats subjected to sham ligation or CAL 8 weeks prior (B). Note thinning of ventricular tissue, increased chamber size, and scar (indicated by arrow) in CAL heart. Image reproduced from http://www.lonkilgore.com/illustrations.html.

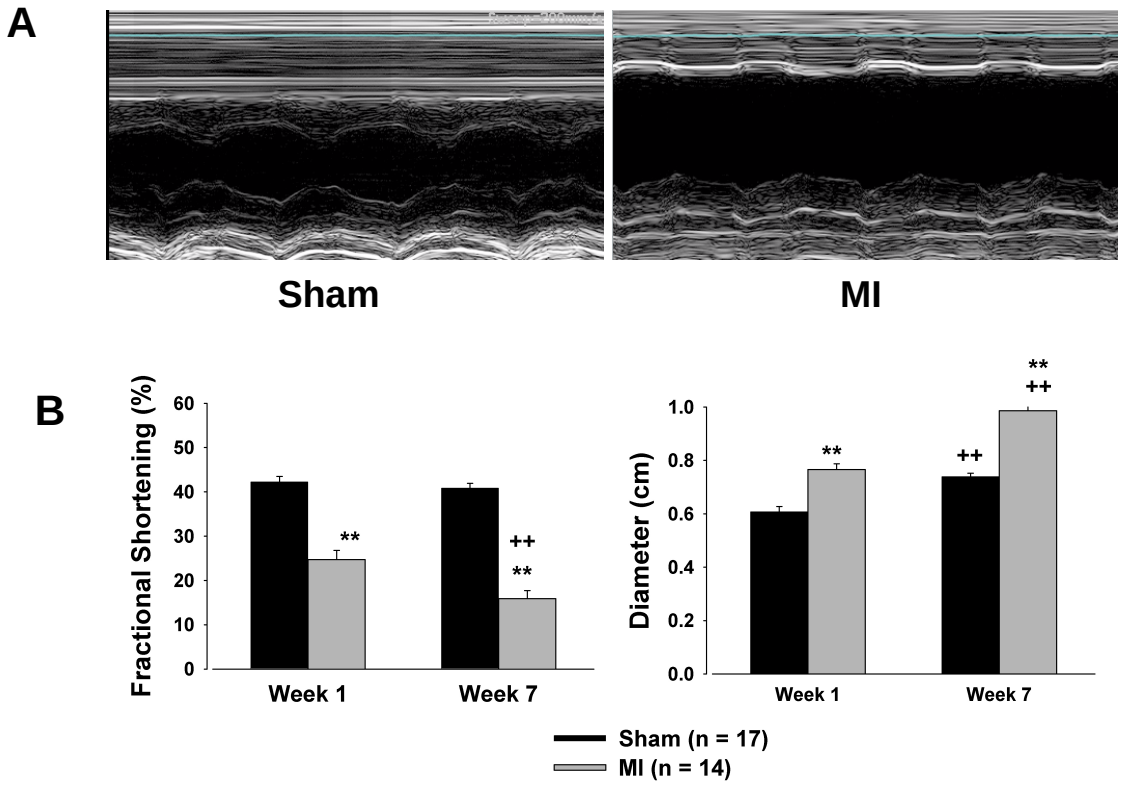

Figure 2. Left ventricular function (Specific Aim 1). Representative M-mode recordings from sham (left) and MI rats (right), showing consecutive cardiac cycles over time (A). Note increased chamber size and lesser change in ventricle size during systole in MI rats. Left ventricular fractional shortening (left) and left ventricular diastolic diameter (right) measured 1 and 7 weeks after MI or sham ligation surgery (B). Data are group means ± SEM. A 2-way ANOVA with repeated measures used to assess group differences in FS over time revealed a surgery x time interaction [$F(1,29) = 6.21$, $P<0.05$], due to an decrease in fractional shortening over time in MI rats, but not sham-operated rats. A main effect of MI [$F(1,29) = 171.56$, $P<0.01$] was observed due to a decrease in

fractional shortening in MI rats vs. sham-ligated rats. A main effect of time [$F(1,29) = 11.95$, $P<0.01$] was also observed. A 2-way ANOVA with repeated measures examining the effect of surgical treatment on left ventricular diastolic diameter over time revealed a surgery x time interaction [$F(1,29) = 4.47$, $P<0.05$] due a greater increase in LVDD over time in MI rats than sham-operated rats. A main effect of surgery [$F(1,29) = 58.18$, $P<0.01$] was due to an increase in LVDD in MI rats vs. sham-operated rats. A main effect of time [$F(1,29) = 69.84$, $P<0.01$] was also observed. Between- and within-group comparisons were made with Tukey's *post hoc* tests. **$P<0.01$ compared to sham, $^{++}P<0.01$ compared to week 1.

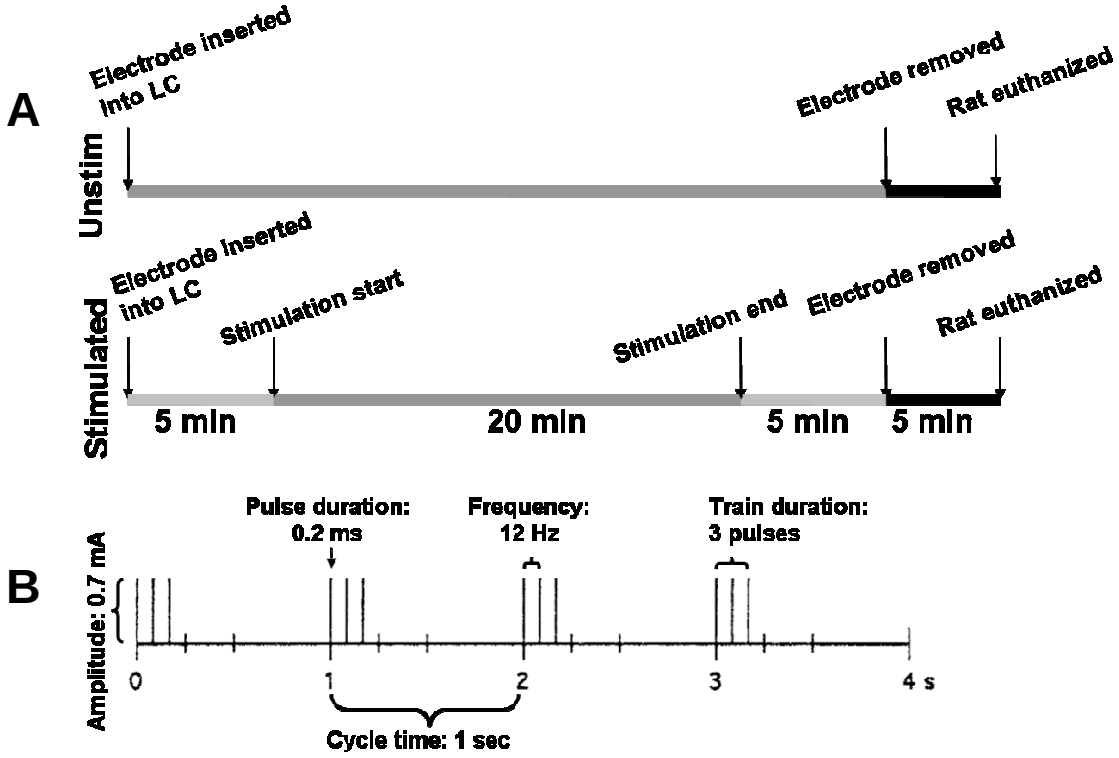

Figure 3. Locus coeruleus stimulation parameters. Time course of experiment for rats instrumented with an LC electrode and subjected to stimulation (Stimulated) or no stimulation (Unstim) (A). Four-second example of the stimulation pattern administered to rats for 20 minutes (B).

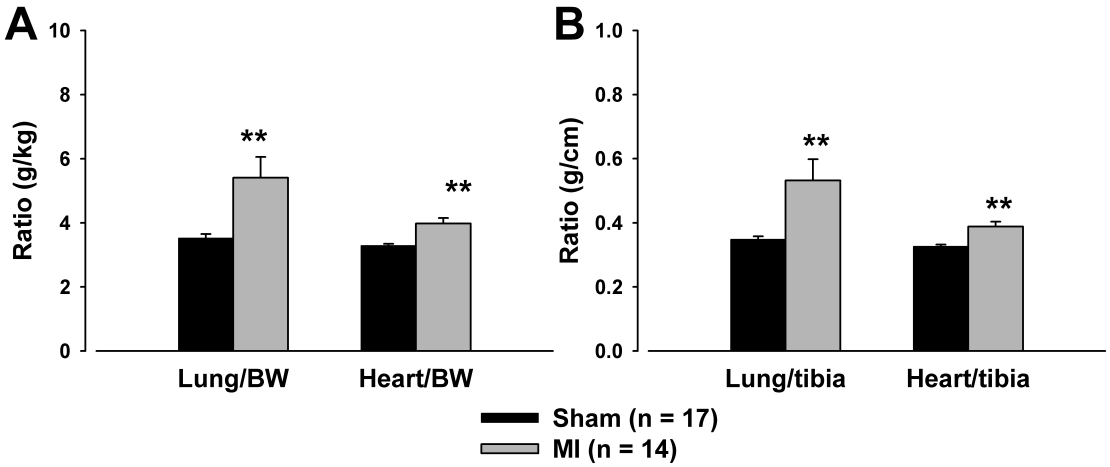

Figure 4. Terminal measures of congestion and remodeling (Specific Aim 1). Ratios of lung and heart weight to body weight (A) and to tibia length (B). Values are group mean ± SEM. Student's t-tests revealed significantly increased lung-to-body weight ratio [$t(29) = 3.14$, $P<0.05$] and heart-to-body weight ratio [$t(18) = 4.16$, $P<0.01$], as well as lung-to-tibia ratio [$t(29) = 2.53$, $P<0.05$] and heart-to-tibia ratio [$t(29) = 4.30$, $P<0.01$] in MI rats. **$P<0.01$ vs. sham-ligated rats.

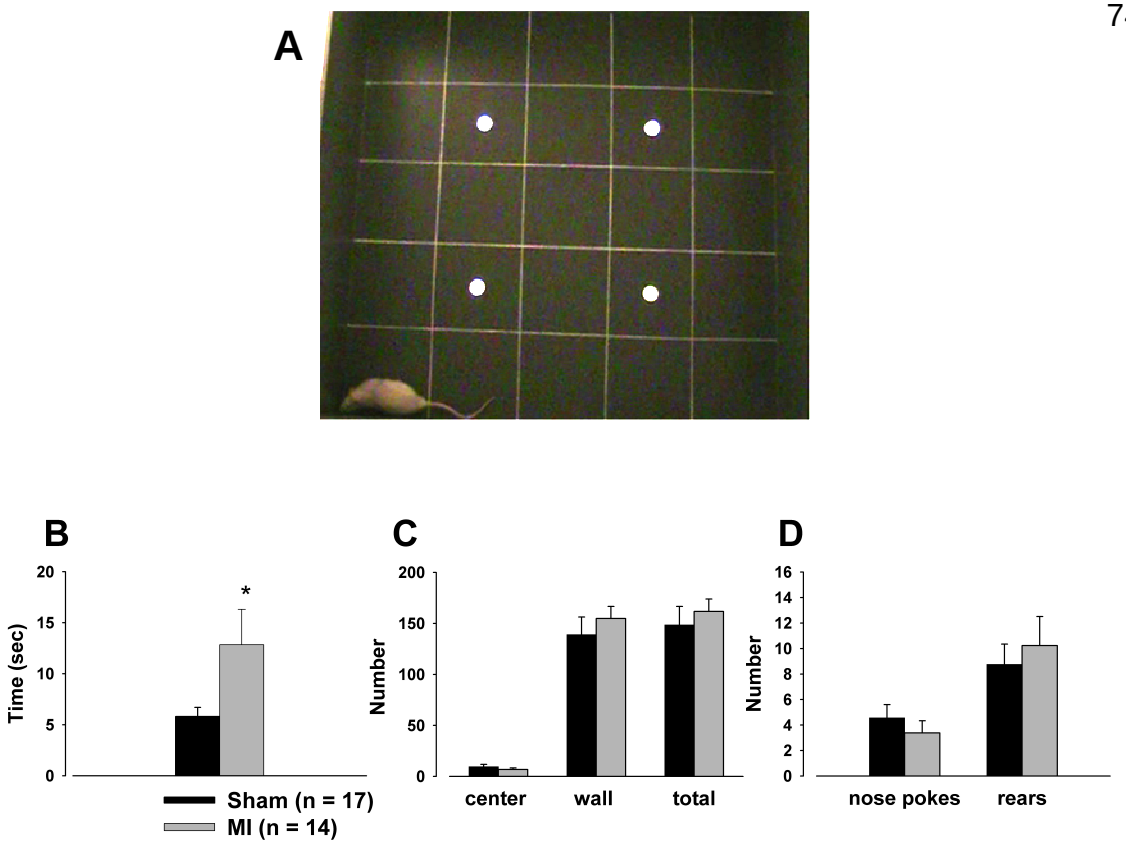

Figure 5. Open field test for anxiety and neophobia. The open field apparatus used for this study (A). Time to leave center square of apparatus at beginning of test (B). Number of each square type entered (center, wall, and total) during 12-minute test (C). Number of rears (standing on hind-legs) and nose hole pokes emitted during test (D). Values are group means ± SEM. Student's t-test revealed that MI rats took significantly longer to leave the center square of the apparatus at the beginning of the test [$T(27) = 2.16$, $P<0.05$]. *$P<0.05$ between groups.

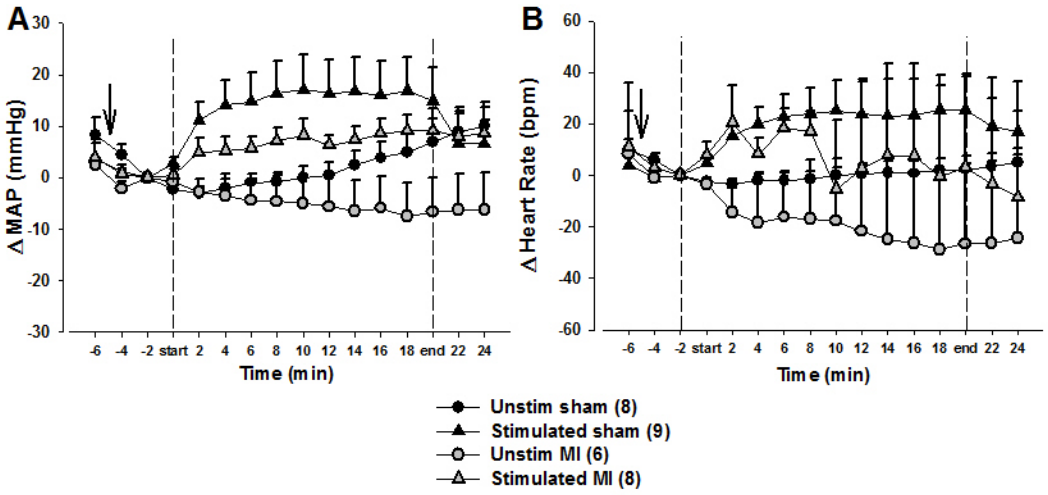

Figure 6. Blood pressure and heart rate responses to locus coeruleus stimulation. Change in mean arterial pressure (MAP, A) and change in heart rate (B). Values are mean ± SEM. Dashed lines indicate start and end of stimulation, and arrow indicates lowering of electrode into the locus coeruleus (LC). A 3-way ANOVA with repeated measures examining the effect of surgery and stimulation on MAP over time revealed a 3-way interaction of surgery, stimulation, and time [$F(1,27) = 3.29$, $P<0.05$] due to a greater increase in MAP over time in stimulated sham rats than stimulated MI rats. A surgery x time interaction [$F(1,27) = 1.97$, $P<0.05$] and a stimulation x time interaction [$F(1,27) = 5.89$, $P<0.01$] were also observed. This analysis also revealed a main effect of stimulation [$F(1,27) = 8.83$, $P<0.01$], and a main effect of time [$F(1,27) = 3.21$, $P<0.01$]. A 3-way ANOVA with repeated measures examining the effects of surgery and stimulation on heart rate over time showed no interactions or main effects. A separate 3-way ANOVA examining the effect of surgery and

stimulation on MAP over time in the 3 time points prior to stimulation revealed a main effect of time, due to a decrease in MAP in all groups in response to lowering the electrode into the LC. No effects of surgery, stimulation, or time on heart rate were observed prior to stimulation.

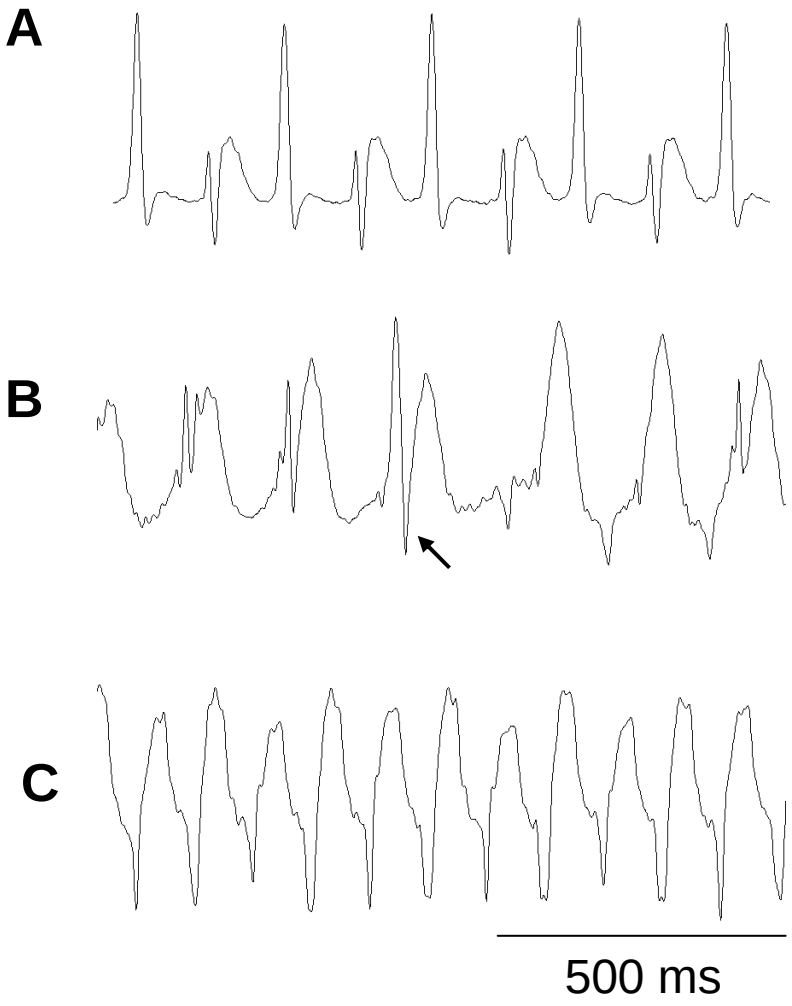

Figure 7. Representative arrhythmia waveforms. Typical waveforms observed during ventricular arrhythmias in MI rats and sham-ligated rats during LC stimulation (and some MI rats at baseline). Arrhythmias include bigeminy (A), premature ventricular contractions (B, arrow), and ventricular tachycardia (C).

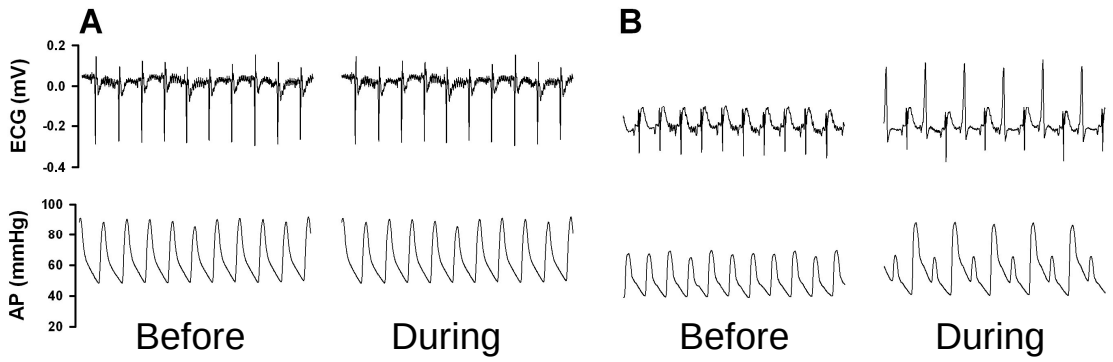

Figure 8. ECG and arterial pressure during locus coeruleus stimulation. Representative simultaneous ECG and arterial pressure from a sham (A) and MI rats (B) before and during LC stimulation. Note bigeminy in MI rat during stimulation, evident by PVC (large upward deflection) in ECG preceding extrasystole in arterial pressure recording.

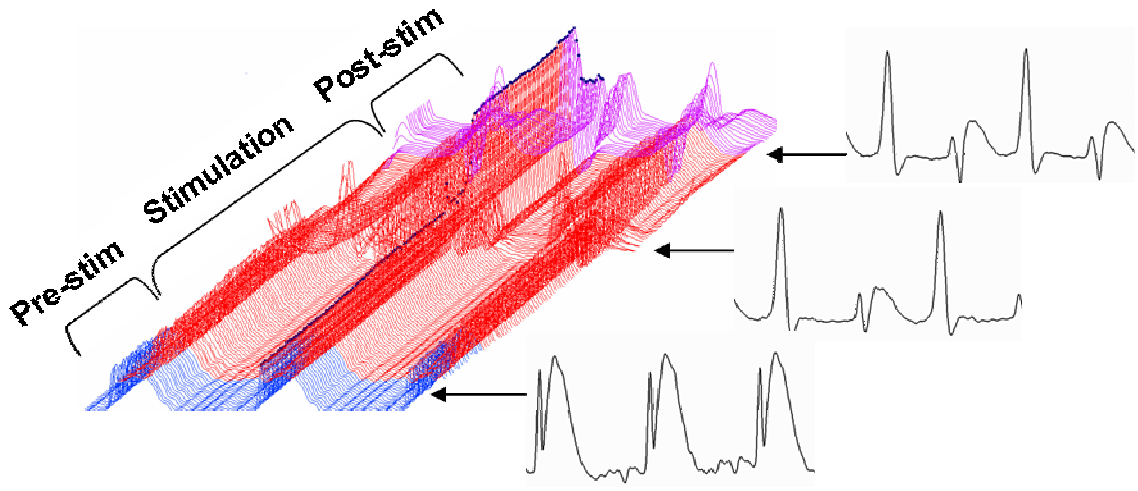

Figure 9. Sequential ECG waveforms. Sequential ECG waveforms (500 ms) from representative MI rat subjected to LC stimulation Note waveform disturbance beginning about 10 minutes after start of 20-minute stimulation period in rat subjected to stimulation.

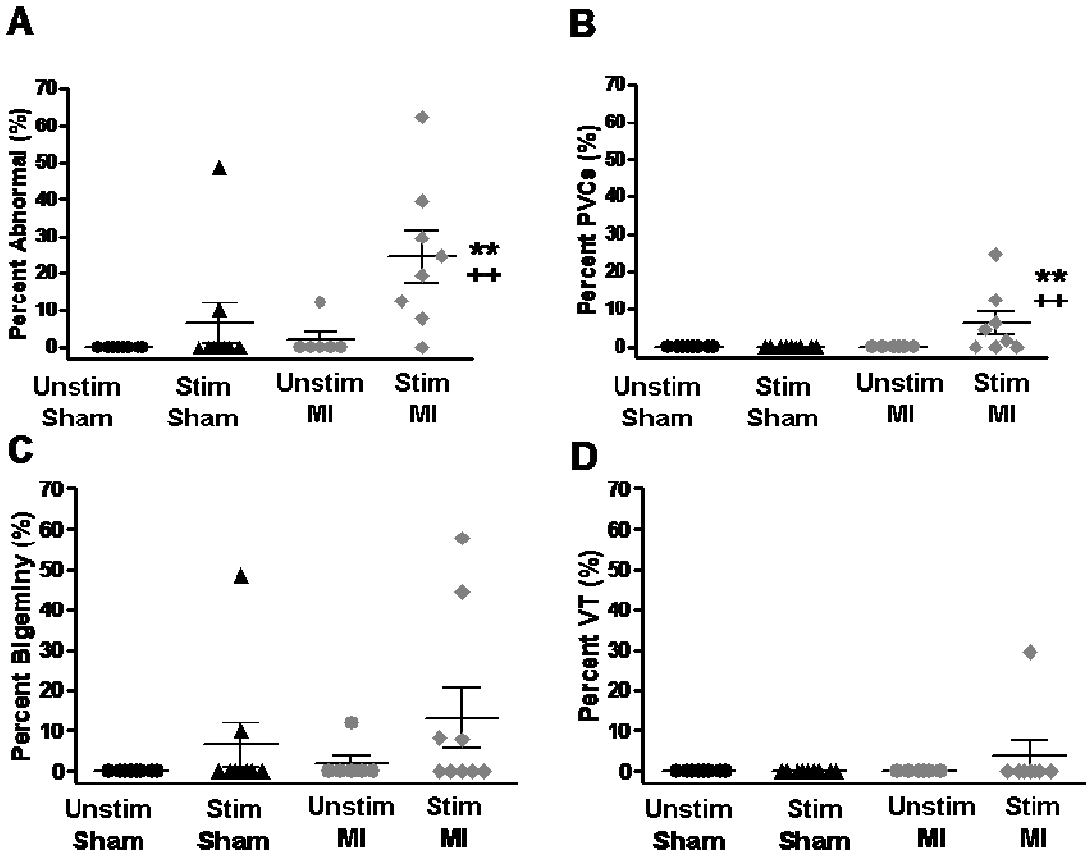

Figure 10. Quantification of locus coeruleus stimulation-associated arrhythmias. Percentage of novel arrhythmic beats (arrhythmia waveforms not observed during baseline, divided by total waveforms) during period of stimulation. All arrhythmias pooled (bigeminy, preventricular contractions, and venticular tachycardia (A), isolated preventricular contractions (PVCs) only (B), bigeminy only (C), and ventricular tachycardia (VT) only (D). Values represent individual rats with mean shown by horizontal bar, and SEM shown as the smaller horizontal error bar cap. For all 3 arrhythmia types pooled (A), 2-way ANOVA on ranks revealed main effects of surgery [$F(1,27) = 12.987$, $P<0.01$] and stimulation [$F(1,27) = 9.958$, $P<0.01$] due to increased arrhythmias in

response to both MI and stimulation. For isolated PVCs (B), 2-way ANOVA on ranks revealed a significant interaction of surgery and stimulation [$F(1,27) = 4.545$, $P<0.05$] due to a significant increase in arrhythmias in MI rats (but not sham-ligated rats) in response to stimulation, as well as main effects of surgery [$F(1,27) = 12.003$, $P<0.01$] and stimulation [$F(1,27) = 4.545$, $P<0.05$]. No significant interactions or main effects were observed for bigeminy or ventricular tachycardia (D). Tukey *post hoc* tests were used for pair-wise comparisons. **$P<0.01$ vs. MI control, $^{++}P<0.01$ vs. sham stimulated.

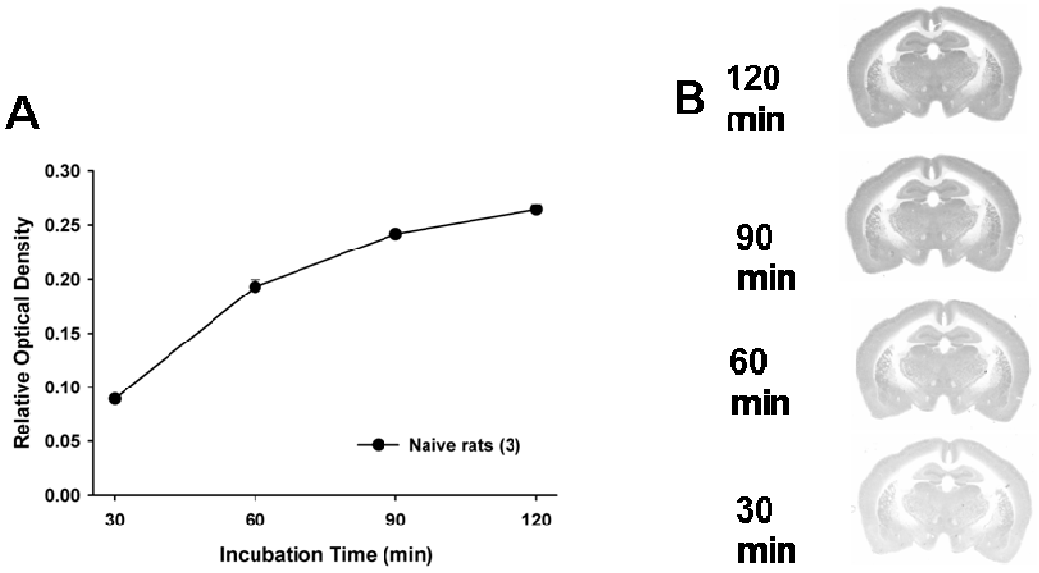

Figure 11. Incubation curve for cytochrome oxidase histochemistry.

Relative optical density of cytochrome oxidase (CO) determined in the basolateral amygdala (BLA) of naïve rats (A). Typical staining in BLA-containing sections incubated in CO staining solution for 30, 60, 90, and 120 minutes (B).

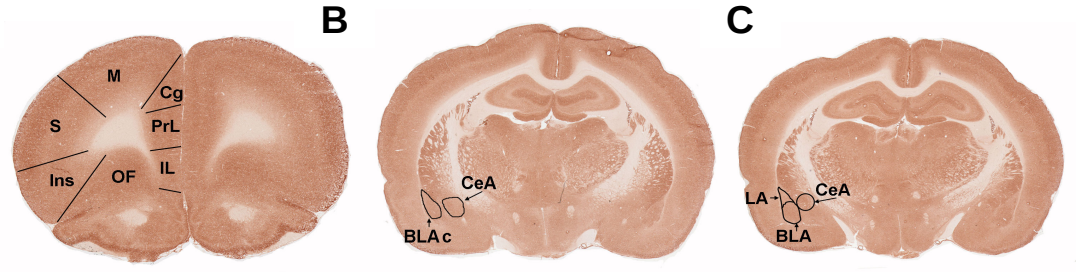

Figure 12. Representative sections showing cytochrome oxidase staining. Sections outlined are representative of those used for densitometry measurements. In prefrontal cortex sections (~3 mm rostral to Bregma), regions assessed included the infralimbic (IL) cortex, prelimbic (PrL) cortex, cingulate (Cg) cortex, primary and secondary motor (M) cortices, somatosensory (S) cortex, insular (Ins) cortex, and orbitofrontal (OF) cortex (A). In sections ~1.8 mm caudal to Bregma, regions assessed were the central nucleus (CeA) of the amgydala and the basolateral complex (BLAc) of the amygdala (B). In sections ~2.2 mm caudal to Bregma, regions assessed were the central nucleus (CeA), the lateral nucleus (LA), and the basolateral nucleus (BLA) of the amygdala (C).

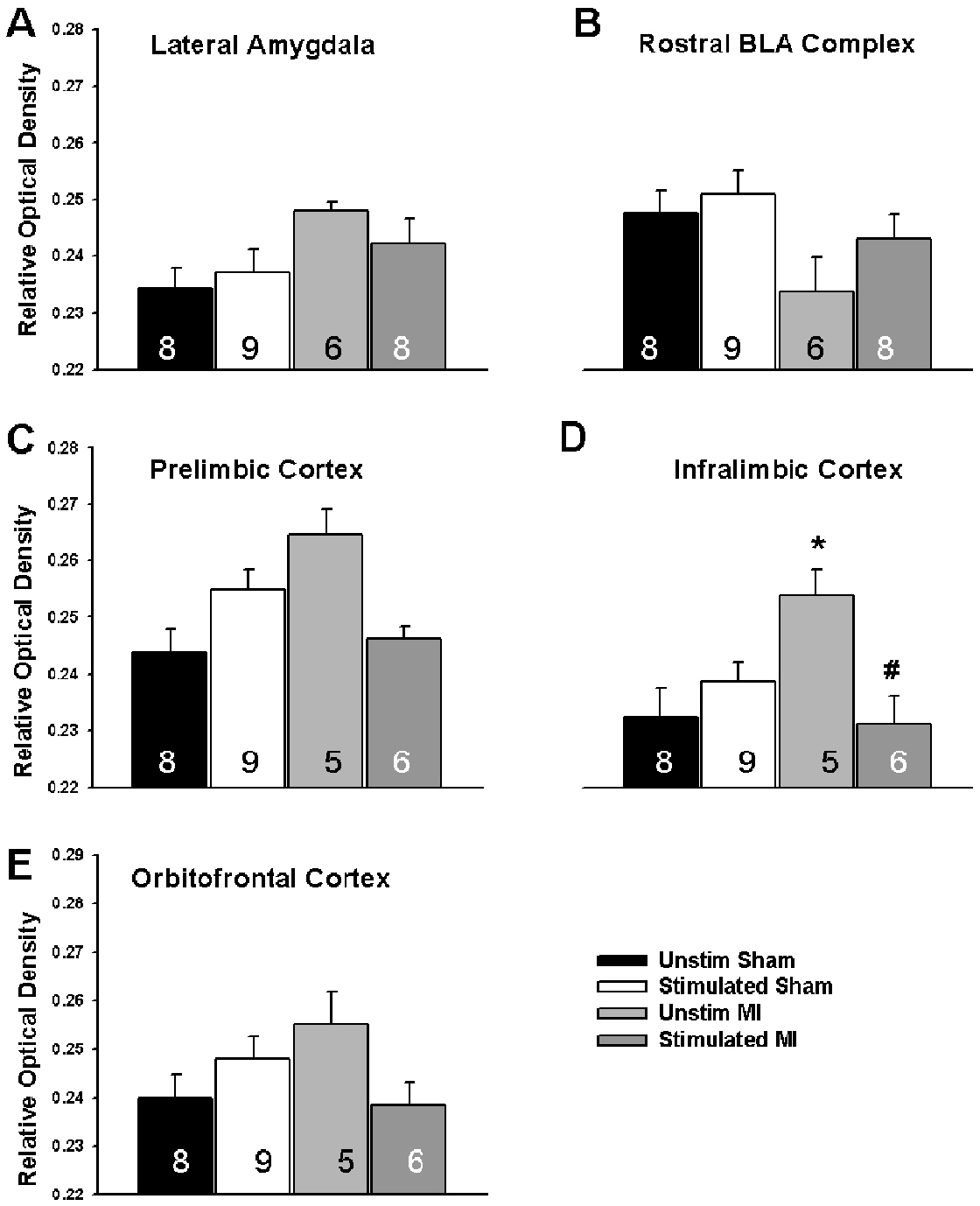

Figure 13. Cytochrome oxidase activity. Values are group mean ± SEM. A two-way ANOVA examining the effect of MI and stimulation on relative optical density (ROD) of cytochrome oxidase staining revealed a main effect of surgery

[F(1.27) = 5.74, P<0.05] in the lateral nucleus of the amygdala (A) due to increased ROD in MI rats. There was also a main effect of surgery [F(1,26) = 5.73, P<0.05] in the rostral basolateral complex of the amygdala due to decreased ROD in MI rats (B). There were surgery x stimulation interactions in the prelimbic cortex (C), [F(1,24) = 6.03, P<0.05], infralimbic cortex (D), [F(1,24) = 9.66, P<0.01], and orbitofrontal cortex (E), [F(1,24) = 5.68, P<0.5] due to increased ROD in unstimulated MI rats vs. unstimulated shams, but decreased ROD in stimulated MI rats vs. unstimulated MI rats. Tukey's *post hoc* test was used to make pairwise comparisons of group means. *P<0.05 vs. unstimulated sham, $^{\#}$P<0.05 vs. unstimulated MI.

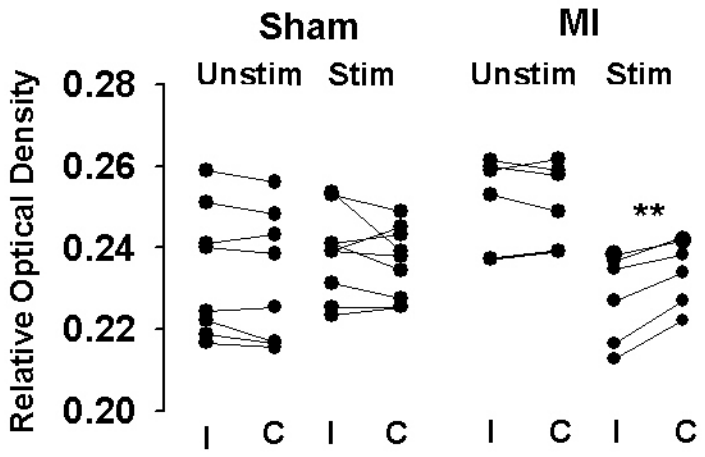

Figure 14. Cytochrome oxidase activity: ipsi- vs. contralateral infralimbic cortex. Relative optical density of cytochrome oxidase staining in IL cortex ipsilateral (I) and contralateral (C) to locus coeruleus stimulating electrode. A 3-way ANOVA with repeated measures revealed a 3-way interaction of surgery, stimulation, and side of brain [$F(1,24) = 5.01$, $P<0.05$]. As in the preceding analysis, here we found a surgery x stimulation interaction [$F(1,24) = 15.71$, $P<0.01$] due to increased ROD in unstimulated MI rats compared to unstimulated shams, but decreased ROD in stimulated MI rats. An MI x side of brain interaction [$F(1,24) = 6.49$, $P<0.05$] was observed due to decreased ROD in the ipsi- vs. contralateral side in stimulated MI rats but no ipsi- vs. contralateral differences in sham operated rats or unstimulated MI rats. A paired t-test revealed that IL ROD in the stimulated side was lower than the contralateral side in stimulated MI rats [$T(6) = 5.61$, $P<0.01$].

	Unstim Sham	Stim Sham	Unstim MI	Stim MI
M cortex	22.70 ± 0.43	23.36 ± 0.32	22.43 ± 0.54	23.08 ± 0.39
SM cortex	21.90 ± 0.45	22.37 ± 0.28	21.29 ± 0.39	21.84 ± 0.45
Ins cortex	22.04 ± 0.38	21.79 ± 0.20	21.19 ± 0.61	21.17 ± 0.39
Cg cortex	24.07 ± 0.37	24.69 ± 0.45	25.09 ± 0.62	24.22 ± 0.62
BLA nuc	26.86 ± 0.39	27.16 ± 0.40	27.69 ± 0.31	27.01 ± 0. 29
CeM	22.03 ± 0.48	22.65 ± 0.37	21.78 ± 0.59	21.86 ± 0 .85
CeL	25.77 ± 0.32	26.74 ± 0.57	25.36 ± 0.48	26.22 ± 0.50

Table 1. Cytochrome oxidase activity (NS). Relative optical density in regions measured for cytochrome oxidase activity in which group differences were not observed: Motor (M), somatosensory (SM), insular (Ins), cingulate (Cg) cortices, basolateral nucleus of the amygdala (BLA nuc), medial division of the central nucleus of the amygdala (CeM), and lateral division of the central nucleus of the amygdala (CeL). Values are mean ± SEM.

Discussion

In the present study, echocardiography data demonstrate profound left ventricular dysfunction in rats subjected to myocardial infarction (MI). Compared to sham-operated rats, MI rats had decreased fractional shortening after MI, indicating deficits in contractility, and a decrease in fractional shortening at week 7 compared to week 1 post-surgery, indicating a worsening of function over time. MI rats also exhibited dramatically elevated left ventricular diastolic diameter compared to sham-operated rats, indicating dilatation. Left ventricular diastolic diameter significantly increased between week 1 and 7 in MI rats, indicating increased dilatation over time and ventricular remodeling. In sham-oprated rats, diastolic diameter also increased slightly over time. However, this increase in diameter in sham-operated rats may have been due to growth of the rats over the course of the experiment, since this measurement did not account for body weight. In this study, lung and heart wet weights were elevated in MI rats, relative to both tibia length and body weight. This increase in heart weight suggests ventricular remodeling, and this increase in heart weight suggests pulmonary edema due to volume overload, likely due to the neurohumoral activation that is characteristic of progression to heart failure (Francis et al., 2001a).

In both MI and sham-ligated rats, electrical stimulation of the locus coeruleus (LC) resulted in an increase in arterial blood pressure. Others have demonstrated similar pressor responses to electrical stimulation of the LC

(Berecek and Mitchum, 1986; Drolet and Gauthier, 1985) While both MI and sham-ligated rats exhibited an increase in mean arterial pressure during stimulation, this pressor response was larger in sham-ligated rats. This effect is likely due to decreased cardiac output in MI rats and a desensitization of cardiac β-adrenergic receptors to catecholamine stimulation that is typical in heart failure (Kompa et al., 1999; Francis et al., 2001a).

Previous studies using catecholamine lesion and adrenal demedullation techniques implicate both epinephrine release from the adrenal medulla and sympathetically-mediated vasoconstriction in mediating the pressor effect of LC stimulation (Drolet and Gauthier, 1985). Drolet et al. also reported that midbrain transection of the dorsal nadrenergic ascending bundle (the projection of the LC to the forebrain, including the prefrontal cortex) abolished the vasomotor component, but not the adrenal medullary component of the pressor response. This suggests that ascending projections to the forebrain and descending projections to the spinal cord both contribute to sympathetic activation by the LC, but these projections mediate distinct components of the sympathetic response.

There has been debate whether the pressor response to electrical stimulation of the LC is mediated by the LC itself, or by adjacent nuclei or fibers of passage, since chemical stimulation of the LC sometimes elicits a depressor effect (Sved and Felsten, 1987; Murase et al., 1993). However, preliminary data from our lab indicate that the blood pressure response to chemical stimulation of the LC is anesthesia-specific, as the excitatory amino acid, D,L-homocysteine,

elicited a depressor response under sodium pentobarbital anesthesia, but a pressor response under chloral hydrate anesthesia. Additionally, selective lesion of catecholamine-containing fibers in the LC does not completely abolish the pressor response to electrical stimulation (Sved and Felsten, 1987; Crawley et al., 1980), suggesting a role of adjacent nuclei and fibers of passage in the responses to electrical stimulation. However, compared to chemical stimulation, electrical stimulation more closely simulates the pattern of activation in the LC in response to a mild stressor, and has been shown to evoke NE release in the forebrain (Abercrombie and Jacobs, 1987; Berridge and Abercrombie, 1999).

Analysis of waveforms unique to the 20-minute stimulation period revealed that stimulated MI rats developed a greater amount of ventricular arrhythmias (including bigeminy, PVCs, and VT) than unstimulated MI rats. The only rats that developed VT unique to the 20-minute stimulation period were the stimulated MI rats. Two sham-ligated rats developed bigeminy during LC stimulation, but the latency to develop bigeminy was longer in these two sham-ligated rats compared to the average latency of MI rats, suggesting that MI decreases the threshold for bigeminy generation. Sham-ligated rats that were not subjected to stimulation did not develop any ventricular arrhythmias, providing further support that activation of the LC promotes the generation of ventricular arrhythmias. Together, these results suggest that psychological stressors that activate the LC can induce cardiac arrhythmias, and MI increases both the susceptibility (i.e.

latency and number of abnormal beats) and severity of stress-induced arrhythmia (i.e. VT vs. bigeminy).

Increased sympathetic drive is thought to be responsible for arrhythmia generation after MI, as cardiac sympathetic nerve stimulation results in arrhythmias in rats subjected to MI, and βAR blockade prevents this effect (Du et al., 1999). LC activation increases sympathetic output, though the mechanism is unclear. Although the LC does project to the rostral ventrolateral medulla (RVLM), a region providing tonic excitation of sympathetic preganglionic neurons of the spinal cord, this projection is thought to be primarily inhibitory by virtue of the action of NE on α_2ARs (Van Bockstaele et al., 1989; Hayar and Guyenet, 1999). However, the LC does project directly to the spinal cord (Proudfit and Clark, 1991), and may increase sympathetic activity in this manner. It is also possible that the LC may increase sympathetic drive through its projections to cardioregulatory forebrain regions, such as the amygdala. The central nucleus of the amygdala regulates autonomic responses to stressful stimuli via direct projections to the RVLM and NTS (Cassell and Gray, 1989; Zardetto-Smith and Gray, 1990; Hopkins and Holstege, 1978) (Cassell and Gray, 1989; Zardetto-Smith and Gray, 1990; Hopkins and Holstege, 1978). The mPFC has also been shown to contribute to sympathoexcitation in response to stressors, as lesion of the ventral mPFC results in the attenuation of the sympathetically-mediated tachycardic response to a tone previously paired with footshock (Skinner and Reed, 1981; Frysztak and Neafsey, 1994), through its projections to

cardioregulatory regions of the brainstem (NTS, RVLM, dorsal vagal motor nucleus) and spinal cord (Neafsey et al., 1986; Hurley et al., 1991). Furthermore, trans-synaptic labeling studies using pseudo-rabies virus have demonstrated pathways from the PFC (IL, PrL, Cg, and Ins) to the left myocardium (Ter Horst, 1999), providing further support for potential mPFC control of the heart.

In the open field test, MI rats took longer than sham-operated rats to leave the center square of the apparatus at the beginning of the test. These results suggest an enhanced anxiety response to novelty in MI rats, as a previous study demonstrated that increased latency to begin exploring an open field apparatus was correlated with increases in other anxiety-like behaviors, including enhanced acoustic startle (McAuley et al., 2009). In another study, central blockade of of corticotropin-releasing factor decreased the latency to begin exploring an open field apparatus (Takahashi et al., 1989), further supporting enhanced exploration latency as an index of anxiety in response to novelty. However, we observed no difference between MI and sham-ligated rats in the number of entries into wall squares or center squares. MI and sham-ligated rats also displayed similar amounts of nose pokes and rears, indicating similar exploratory behavior in these two groups. Unlike the elevated plus maze, which contains an element of danger (the height of the open arms) in addition to its novelty, the open field apparatus is dimly lit and fully enclosed. Therefore, this stimulus, though novel, may not have been sufficient to elicit a robust anxiety-like response in MI rats. A previous study also found a lack of differences in anxiety-like behaviors between MI and

sham-ligated rats in a traditional open field test. However, when the open field test included an opportunity for escape, MI rats displayed increased escape behavior (Prickaerts et al., 1996). Additionally, a baseline level of stress in sham-ligated rats due to social isolation may have masked any group differences in anxiety-like responses in the present study.

Cytochrome oxidase (CO) histochemistry was used to assess both chronic changes in metabolic activity in response to MI and acute changes in metabolic activity in response to locus coeruleus (LC) stimulation. Because CO activity changes in accordance with the energy needs of neurons, measurements of optical density of CO staining have long been used as an index of changes in oxidative metabolism in response to chronic interventions (Wong-Riley, 1989; Wong-Riley, 1979). More recently, CO staining has been used to assess changes in metabolic activity in response to acute stimulation (Tseng et al., 2006).

In the lateral nucleus of the amygdala (~Bregma -2.5), CO activity was increased in MI rats with no further effect of LC stimulation. The lateral nucleus of the amygdala is necessary for acquisition and maintenance of associations between fearful stimuli and environmental cues (Romanski et al., 1993). Since post-MI patients often exhibit enhanced emotional reponses and anger (Frasure-Smith and Lesperance, 2003), the fact that MI rats had an increase in metabolic activity in this region suggests that enhanced lateral nucleus (LA) activity may contribute to these exaggerated responses. The LA has no direct projections to

the medial division of the central nucleus (CeM), and therefore must relay through the basolateral nucleus to influence CeM output (Pitkanen et al., 1997; Savander et al., 1995). In the basolateral complex (~Bregma -2.0 mm), cytochrome oxidase activity was decreased in MI rats, with no further effect of LC stimulation. The BLA complex provides an excitatory projection to the CeM, as well as to the intercalated cell masses which inhibit the CeM (Savander et al., 1995). The functional effect of the observed decrease in basolateral complex activity is difficult to predict, since it could result in either excitation or inhibition of the CeM output neurons. No changes were observed due to MI or stimulation in the caudal basolateral nucleus (~Bregma -2.5), nor in either the medial or lateral divisions of the CeA.

These results suggest that basolateral nucleus and central nucleus activity are not modulated by MI or by LC stimulation. However, it cannot be ruled out that anesthesia masked potential changes in neuronal activation in these regions, or that extrinsic excitation of these regions was met with local inhibition, resulting in no net change in activation (Ehrlich et al., 2009). Moreover, intercalated neurons are involved in extinction of conditioned fear and their modulation might only be apparent during extinction procedures. We were not able to measure cytochrome oxidase activity in the intercalated cell masses because these clusters of neurons are small, dispersed, and must be identified by their GABA or mu opioid receptor content (Royer et al., 1999).

The infralimbic (IL) cortex of MI rats also displayed increased baseline CO activity compared to sham-operated rats. However, in response to LC stimulation that mimics a mild stressor, MI rats exhibited a decrease in metabolic activity in this region (i.e., a surgery x stimulation interaction). This effect was most profound in the IL cortex. No significant changes in cytochrome oxidase activity due to MI or stimulation were observed in the motor cortex, somatosensory cortex, cingulate, or insular cortex. This lack of change confirms the regional specificity of changes observed in the IL PrL, and OF cortices.

The IL is necessary for the extinction of learned fear and when activated inhibits stress responses initiated by the amygdala through excitatory projections to the ICM which, in turn, inhibit output from the CeA (Sierra-Mercado et al., 2011; Muigg et al., 2008). In a simplified view, the enhanced IL activity at baseline in MI rats might suggest a suppression of inappropriate fear responses. However, the overall activity of the mPFC is modulated by GABA-ergic interneurons that influence pyramdial projection neurons. In particular, parvalbumin-containing, fast-spiking interneurons help to maintain proper oscillations of pyramidal neuronal activity, that are necessary for synchronization of cortical neurons and cognitive processing, including attention to relevant stimuli (Volman et al., 2011). Dysregulation (e.g., reduced activity) of interneurons in the PFC (including the OF cortex) is thought to contribute to the deficits in attention and cognitive processing in multiple neuropsychiatric disorders, including schizophrenia and attention disorders (Paine et al., 2011;

Quirk et al., 2009). A lack of proper “tuning” of PFC activity may also contribute to attentional and cognitive aspects of depression and anxiety, as symptoms of these disorders often include deficits in classification of stimuli as threatening or safe (Britton et al., 2011). Therefore, it is probable that the increased metabolic activity we observed in the IL cortex of MI rats at baseline reflects a deficit in inhibition by interneurons, and this dysregulation may contribute to the development of post-MI anxiety. The IL mPFC is also contributes to sympathoexcitatory responses to learned fear, as lesion of the mPFC abolishes sympathetically-mediated tachycardia in response to tones previously paired with footshock (Frysztak and Neafsey, 1994). Therefore, alternatively, this increase in IL metabolic activity may reflect IL-mediated sympathoexcitation that contributes to the increase in sympathetic drive that is both typical after MI and accompanies anxiety disorders (Hasking et al., 1986; Esler et al., 2008).

Whatever the cause of this baseline increase, MI rats exhibited an altered response to norepinephrine in the mPFC (most profoundly in the IL cortex). This norepinephrine-induced decrease in mPFC metabolic activity in MI rats may result in a deficit in the normal gating of amygdala-mediated cardiovascular and behavioral responses specifically during exposure to novel stimuli, changes in stimulus salience or times of stress when increases in LC neuron firing rate are typically observed.

The effect of norepinephrine release in the PFC depends on the adrenergic receptor profile of the target tissue where it is released. The mPFC

contains α_2-adrenergic receptors, which mediate inhibition through Gαi, α_1-adrenergic receptors (which mediate excitation through Gαq), and βARs, which mediate excitation through Gαs (Flugge, 1996; Andrade and Aghajanian, 1985; Kreiner et al., 2011; Docherty, 2010; Rainbow et al., 1984; Wessels et al., 1978). Reduction in forebrain norepinephrine release through catecholamine-specific lesion of the LC and medial forebrain bundle results in an increase in firing rate of mPFC pyramidal neurons, suggesting that NE usually serves to inhibit mPFC activity. The fact that intra-mPFC infusion of an α_2AR agonist decreases the firing rate of mPFC pyramidal neurons indicates that activation of α_2ARs contributes to the inhibition of mPFC activity by norepinephrine (Wang et al., 2010).

Although it is well documented that norepinephrine is released in the PFC in response to novel or stressful stimuli, the role of noradrenergic signaling in the mPFC is not well established. Norepinephrine in the mPFC modulates attention and working memory processes, as depletion of norepinephrine in this region (IL, PrL, and cingulate) impairs a rat's performance in an attentional task (Milstein et al., 2007). The facilitory effect of NE on attention processes is thought to be mediated through α_2ARs, since systemic treatment with the α_2AR agonist, guanfacine, improves performance in an attentional task requiring the PFC. Conversely, mice with a mutation in the α_{2a}AR, that disrupts receptor function, exhibit deficits in this task (Franowicz et al., 2002). While NE signaling through α_2ARs is thought to facilitate working memory, β_1AR activation in the mPFC is

thought to impair working memory. This idea is supported by the fact that infusion of the β_1AR antagonist, betaxolol, into the mPFC (dorsal IL and ventral PrL) improves performance in a working memory task (Ramos et al., 2005). It is thought that β_1ARs and β_2ARs may mediate opposing effects in the mPFC, as infusion of the β_2AR agonist, clenbuterol, improves performance in a working memory task in aged rats, but this effect is reversed by the β_2AR antagonist, ICI-118,551 (Ramos et al., 2008).

Even fewer studies have examined the role of mPFC noradrenergic signaling in stress responses. Selective lesion of noradrenergic nerve terminals specifically in the PrL cortex has been shown to enhance restraint stress-induced Fos expression in the PrL (Radley et al., 2008), suggesting that NE release during stress normally inhibits neuronal activation in the PrL. Blockade of noradrenergic signaling through βARs in the IL has been shown to impair retrieval of conditioned fear extinction (Mueller et al., 2008), suggesting that reduced NE signaling through βARs in the IL may negatively influence both the association of danger signals with neutral cues and the extinction of this association.

Reduced activity in the PFC in response to LC stimulation may also result from an increase in post-synaptic α_2ARs. Chronic psychosocial stress in tree shrews results a transient decrease followed by a sustained increase in α_2AR expression (Flugge, 1996). Given that both social stress and MI activate the LC, it is possible that chronic activation of the LC after MI results in α_2AR

upregulation and/or βAR downregulation in the mPFC, leading to inhibition of metabolic activity in response to further LC stimulation.

In conclusion, the present study demonstrates that MI results in long-term changes in activation in brain regions governing stress responses: the amygdala and prefrontal cortical regions. This study also demonstrated changes in the response of the infralimbic, prelimbic, and orbitofrontal cortices to stress-like locus coeruleus stimulation in MI rats. MI rats also displayed neophobia in the open field test and developed more ventricular arrhythmias during locus coeruleus stimulation. Thus, the changes we observed in the PFC and amygdala may contribute to exaggerated stress responses in MI patients and may increase susceptibility to arrhythmias. However, it remains unknown what adrenergic receptor subtypes are mediating this response. Thus, studies presented in Chapter 4 examined changes in β-adrenergic receptor number and coupling in these regions following MI.

CHAPTER 4

ALTERATIONS IN BETA-ADRENERGIC RECEPTORS AFTER MYOCARDIAL INFARCTION

Abstract:

After myocardial infarction (MI), humans tend to develop depression and anxiety that are associated with increased morbidity and mortality. Excess noradrenergic drive and abnormalities in noradrenergic signaling through CNS β-adrenergic receptors (βARs) have been implicated in exaggerated stress responses and the development of anxiety disorders. Excess noradrenergic drive occurs after MI and results in desensitization of cardiac βARs, worsening cardiac function. In the studies reported in Chapter 3, we observed an altered effect of locus coeruleus stimulation on forebrain metabolic activity in rats subjected to MI. However, it is not known whether alterations in central nervous system βAR density and coupling occur after MI. Therefore, this study used quantitative receptor autoradiography to assess changes in βAR density and functional coupling in the amygdala and PFC after MI. Slide-mounted brain tissue from rats subjected to MI or sham ligation 8 weeks prior was incubated with 20 pM ^{125}Iodocyanopindolol (ICYP) to label βARs. Parallel incubations included competing drugs to determine both the density of β_1ARs and their G protein coupling state.

Rats subjected to MI had decreased fractional shortening, increased left ventricular diastolic diameter, and increased heart and lung weight compared to sham-ligated rats. In the infralimbic cortex, MI rats exhibited a decrease in β_1AR density. In the lateral amygdala, MI rats displayed a decrease in β_1AR density, and an increase in β_2AR density. In the rostral basolateral amygdala complex, MI rats displayed a decrease in both overall βAR and β_1AR density. Together these data suggest the intriguing possibility that increased noradrenergic drive may cause downregulation of β_1AR in the amygdala and infralimbic cortex.

Introduction:

After myocardial infarction (MI), humans are more likely to be diagnosed with depression and anxiety. As described in Chapter 2, the development of depression or anxiety after MI is associated with increased cardiovascular morbidity and mortality (Dickens et al., 2008), suggesting that MI precipitates changes in the central nervous system that lead to the development of depression and anxiety, as well as worsening of cardiac function and risk of sudden cardiac death.

An excess activation of the sympathetic nervous system occurs both in MI patients and those suffering from anxiety disorder (Esler et al., 2004; Ramchandra et al., 2009; Jardine et al., 2005). The NE released from sympathetic nerve terminals and epinephrine released from the adrenal medulla as a result of sympathetic activation bind to cardiac βARs to mediate increases in

heart rate and contractility. However, chronic stimulation of cardiac βARs by NE and epi after MI leads to desensitization of cardiomyocytes to subsequent catecholamine stimulation, resulting in further decreases in contractility (Kompa et al., 1999; Sethi and Dhalla, 1995).

Noradrenergic signaling through βARs in the CNS is also thought to play a role in the encoding and maintenance of fear-related memories, with dysregulation of these pathways leading to exaggerated emotional responses to fear-associated stimuli. Abnormally persistent emotional responses to innocuous stimuli once associated with threatening stimuli are the hallmark of some anxiety disorders, including PTSD and phobias. Treatment with lipophilic βARs antagonists has been shown to alleviate the symptoms of PTSD and phobias (Pitman et al., 2002; Heaton et al., 2010). PTSD patients treated with propranolol soon after a traumatic event were shown to exhibit attenuated physiological responses (blood pressure, heart rate, and skin conductance) in response to trauma-related imagery compared to placebo-treated patients (Pitman et al., 2002). Propranolol has also been shown to attenuate subsequent responses to trauma-related imagery when given during reactivation of traumatic memories (Brunet et al., 2008). These data suggest that suppression of βAR activation during trauma and retrieval results in CNS plasticity that attenuates subsequent physiological and behavioral responses to fear-related stimuli.

These findings have been corroborated in animal models. For example, infusion of propranolol into the lateral amygdala during reconsolidation of fear

conditioning reduces freezing in response to presentation of a fear-associated cue (Debiec and LeDoux, 2006). Similarly, inhibition of β_1ARs in the BLA results in decreased freezing in response to a tone previously paired with footshock (Fu et al., 2008), and transient downregulation BLA β_1ARs impairs retrieval of auditory fear memory (Fu et al., 2007). Chronic systemic treatment with desipramine (a NE reuptake inhibitor) or isoproterenol (a βAR agonist) have been shown to downregulate βAR expression in multiple brain regions (Ordway et al., 1988). These results suggest that, as in the heart, chronic agonist stimulation may alter subsequent responses through downregulation of receptor density or sensitivity.

The role of noradrenergic signaling through βARs in the mPFC is not well established, though βARs in the IL have been implicated in extinction learning. Specifically, blockade of βARs in the IL cortex has been shown to impair retrieval of fear extinction learning (Mueller et al., 2008). Relatively little is known about the distribution of βAR subtypes in the mPFC and their roles in cognitive processes and stress responses.

β_1ARs comprise about 70% of the overall receptor population in the cortex and are distributed primarily in the outer lamina (Rainbow et al., 1984).The role of β_2ARs is not well known. Although β_2ARs have been observed on dendrites of both pyramidal neurons and interneurons in the monkey PFC (Aoki et al., 1998), β_2ARs are also expressed on astrocytes, where they are thought to regulate glutamate uptake and glucose availability (Hansson and Ronnback, 1991; Fillenz

et al., 1999). Whatever the localization of β_2ARs in the PFC, it is thought that β_2ARs and β_1ARs may mediate opposing roles in the PFC, since both a β_1ARs antagonist and a β_2ARs agonist were shown to improve performance in a working memory task (Ramos et al., 2005).

Receptor agonists, including neurotransmitters, must bind to receptors coupled to their heterotrimeric G protein in order to mediate their effects. When an agonist binds, a transient ternary complex is formed between the agonist, the receptor, and the Gα subunit of the heterotrimeric G protein. Upon agonist binding, the GDP bound to the Gα subunit is exchanged for GTP, and the Gα protein dissociates from the receptor. Additionally, the β and γ subunits that also comprise the heterotrimeric G protein dissociate from the α subunit (Hepler and Gilman, 1992) βARs are primarily coupled to the $G\alpha_s$ isoform of the Gα protein, the activation of which leads to adenylyl cyclase stimulation and thus formation of the second messenger, cAMP. Increases in cAMP lead to subsequent increases in cell excitability and synaptic strength through, among other mechanisms, phosphorylation of transcription factors by PKA (Pedarzani and Storm, 1993). Agonists typically exhibit differential affinity for G-protein receptors expressed on the cell surface depending upon whether the receptor is coupled to its associated heterotrimeric G-protein. At low concentrations a receptor agonist will bind preferentially to coupled receptors. In contrast, receptor antagonists and high concentrations of agonists bind coupled and uncoupled receptors less discriminately (Lefkowitz et al., 1976; Kent et al., 1980). Thus, in radioligand

binding studies, the amount of inhibition of radiolabeled antagonist binding induced by an agonist can be used as an index of the coupling state of a receptor in a given region. The nonhydrolyzable analog of GTP, Gpp[NH]p, can also be useful in assessing the coupling state of receptors in radioligand binding studies. For multiple receptor types, Gpp[NH]p serves to uncouple receptors, thereby inhibiting agonist binding without affecting antagonist binding (Lefkowitz et al., 1976).

Currently, it is unknown how the density and G protein coupling of βARs in brain regions that contribute to anxiety after MI. Therefore, this study sought to assess changes in βAR density and functional coupling in the amygdala and PFC in response to MI using quantitative receptor autoradiography.

Materials and Methods:

Animals

All experiments were performed in accordance with the American Physiological Society Guiding Principles for Research Involving Animals and Human Beings (2002) and were approved by the University's Institutional Animal Care and Use Committee. Male Sprague-Dawley rats between 275 and 299 g (Harlan, Indianapolis, IN) were acclimated to the virarium for one week prior to surgery with ad libitum access to food and water. Rats were housed at a constant temperature of 22 ± 2℃ with a 12/12 hour light/dar k cycle.

Coronary Artery Ligation

After one week, rats were anesthetized with ketamine/xylazine (100 mg/kg + 7 mg/kg, im) and were subjected to MI by coronary artery ligation or underwent sham ligation surgery as described in Chapter 3.

Echocardiography

One and 7 weeks after surgery, rats were anesthetized with ketamine/xylazine (100 mg/kg + 7 mg/kg, im) and subjected to echocardiography (Acuson Sequoia C256, Siemens AG) to determine left ventricular function, as described in detail in Chapter 3.

Euthanasia and Tissue Collection

Eight weeks after MI or sham surgery, rats were euthanized by rapid decapitation without anesthesia. This method of euthanasia was necessary for assays of functional G protein receptor coupling because anesthesia has been shown to influence the affinity state of receptors. Several studies have shown both increases and decreases in receptor affinity for radioligands in response to multiple types of injectable and inhaled anesthetics (Elfving et al., 2003; Rada et al., 2003; Ginovart et al., 2002). Therefore, this euthanasia method was necessary to obtain optimal samples for this assay. After decapitation, the brain was rapidly removed, cooled in -30^{o}C isopentane, frozen in powdered dry ice, and stored at -80^{o}C until sectioning. The heart, lungs, and left tibia of each rat

was removed and weighed or measured. Brains were cut in16 μm sections using a cryostat (chamber temperature -16℃, object temperat ure -14℃), Samples were collected through the extent of the medial prefrontal cortex and amygdala and serially thaw-mounted onto Superfrost Plus slides. In order to compare as many animals as possible in the same film cassette to avoid inter-film variability, 2 adjacent sections from 2 different rats were mounted on each slide (i.e. 2 sections from an MI rat, 2 sections from 1 sham-operated rat on each set of slides). Specimen slides were stored at -20^{o}C (in sealed plastic slide boxes with dessicators) until autoradiography.

Receptor Autoradiography

Quantitative βAR autoradiography was performed as described previously (Rainbow et al., 1982; Ordway et al., 1991; Grimm et al., 1992) with modifications to determine receptor coupling states with agonist inhibition of radiolabeled antagonist binding. Specifically, after thawing and drying overnight, slide-mounted sections were incubated for 2 hours in a solution containing ^{125}ICYP at 20 pM, its approximate Kd in the cortex and amygdala (Tiong and Richardson, 1990a; Tiong and Richardson, 1990b) and 1 μM serotonin (in creatinine sulfate complex, to preclude ^{125}ICYP binding to serotonin receptors) in a room-temperature assay buffer. The assay buffer consisted of 50 mM Tris, 135 mM NaCl, 5 mM $MgCl_2$, 10 μM pargyline (to inhibit oxidation of serotonin and isoproterenol), and 0.02% ascorbic acid, pH 7.6 (all reagents from Sigma). Five

sets of slides were incubated in this solution in the presence and absence of various competing drugs. Nonspecific binding was determined in the presence of 1μM L-propranolol (Tocris). See Figures 15 and 16 for schematics of all incubation conditions.

Binding to β_1ARs was determined in the presence of 5 nM ICI-118,551 (Tocris), a selective β_2AR antagonist. Previous autoradiography studies have used up to 70 nM ICI-118,551 to determine β_1AR binding (Ordway et al., 1988; Grimm et al., 1992). However, in pilot studies we found this concentration of ICI-118,551 to be excessive, in that β_1AR binding was much less than the 60–70% of total binding reported in the literature (Rainbow et al., 1984; Ordway et al., 1988; Tiong and Richardson, 1990b). The Kd of ICI-118,551 is 0.549 nM for β_2ARs, and 302 nM for β_1ARs (Baker, 2005). We used the fractional occupancy (FO) formula below to determine a concentration that would maximize binding to β_2ARs while minimizing β_1AR binding.

$$FO = 1/(1+Kd/[ligand])$$

Based on our calculations, we chose to use 5 nM of ICI-118,551, since this concentration would bind to 90.2% of β_2ARs and 1.6% of β_1ARs, allowing us to block the majority of β_2ARs in order to visualize β_1AR binding. Although β_3ARs are present in many brain regions (Silberman et al., 2010), ^{125}ICYP's affinity for β_3ARs is at least 100 times lower than for β_2ARs or β_1ARs (Niclauss et al., 2006; Neve et al., 1986). Therefore, based on fractional occupancy calculations,

binding to β_3ARs should account for less than 4% of total ^{125}ICYP binding. In contrast, ^{125}ICYP's affinity is only 2–4 times higher for β_2ARs than β_1ARs.

Two additional sets of slides were incubated with ICI-118,551 and competing drugs to determine the G protein coupling of β_1ARs. In one solution -(-) isoproterenol (Sigma), a βAR agonist with equal affinity for β_1AR and β_2ARs, was used at 10 nM, a concentration selective for receptors in the high-affinity state. Previous studies have demonstrated isoproterenol to have a K_dH of 4.9 nM and a K_dL of 249 nM in rat amygdala (Tiong and Richardson, 1990b). Based on FO calculations, we chose 10 nM in order to maximize binding at high-affinity sites (67.1%), and minimize the binding at low-affinity sites (3%). The second solution contained both 10 nM isoproterenol and the non-hydrolyzable GTP analog, Gpp[NH]p (100 μM, Sigma) in order to uncouple βARs. The rationale is that by uncoupling receptors in the high-affinity state, Gpp[NH]p would prevent the inhibition of ^{125}ICYP binding by isoproterenol at this relatively low concentration.

After incubation, the slides were washed twice in ice-cold assay buffer for 10 minutes, briefly dipped in ice-cold deonized water to remove buffer salts, and then immediately dried with cool air. Slides were stored overnight in sealed plastic slide boxes containing dessicator pellets. The following day, slides were taped to mat boards cut to the size of the cassettes, and a slide map was created to enable film labeling after exposure. Slides were apposed to film (Kodak Biomax MR) in Monotec cassettes (Spectronics Corporation, Westbury, NY) in

total darkness and stored at 4℃ for 48 hours. Iodine- 125 microscale standards (American Radiolabeled Chemicals, St. Louis, MO) were exposed with the slides in each cassette to enable calibration of the optical density to the activity of the radioligand. Film cassettes were allowed to warm to room temperature for one hour before films were developed with an SRX-101A autoprocessor (Konica Minolta, Wayne, NJ).

Autoradiograms were labeled and scanned with a Microtek Scanmaker i900 to enable image analysis with NIH ImageJ software. Optical densities (OD) in amygdala and prefrontal cortical regions were determined with ImageJ's polygon tool, using the same anatomical boundaries as described in detail in Chapter 3. The ODs were fit to a standard curve relating optical density (grayscale value 0–255) and radioactivity (nCi/mg), which was generated for each film with the polymer standards. The specific activity was used to convert nCi/mg to fmol/mg protein with the following conversions:

DPM = nCi/mg * 2.22 *1000

fmol/mg tissue equivalent = DPM / Specific activity of ligand at exposure * 0.48

fmol/mg protein = fmol/mg tissue equivalent / 0.05

In these conversions, 2.22 represents the conversion from decays per minute (DPM) to picocuries. In the conversion to fmol/mg tissue equivalent, 0.48

represents the conversion between polymer standards and brain tissue (provided in microscale standard specification sheets).

Determination of Specific Binding to Overall βARs, β_1ARs and β_2ARs

Specific ^{125}ICYP binding to overall βARs (i.e., β_1ARs and β_2ARs) in each brain region was defined as the difference in ^{125}ICYP binding in the presence and absence of 1 μM propranolol . Specific binding to β_1ARs was defined as the difference between ^{125}ICYP binding in the presence of 5 nM ICI-118,551 and ^{125}ICYP binding in the presence of 1 μM propranolol. Specific binding to β_2ARs was defined as the difference between ^{125}ICYP binding in the presence and absence of 5 nM ICI-118,551.

Determination of Agonist-Induced Inhibition of ^{125}ICYP Binding to G Protein-Coupled β_1ARs

Inhibition of ^{125}ICYP binding by isoproterenol (a measure of receptor coupling) was determined by the following equations:

$$\%\ \text{agonist-induced inhibition of } {}^{125}\text{ICYP binding to } \beta_1\text{ARs} = \frac{(\text{Total } \beta_1\text{AR binding} - \beta_1\text{AR binding with iso})}{\text{Specific } \beta_1\text{AR binding}} * 100$$

$$\%\ \text{agonist-inhibition of } {}^{125}\text{ICYP binding to } \beta_1\text{ARs in the presence of GppNHP} = \frac{(\text{Total } \beta_1\text{AR binding} - \beta_1\text{AR binding with iso and Gpp[NH]p})}{\text{Specific } \beta_1\text{AR binding}} * 100$$

$$\%\ \text{inhibition relative to uncoupled} = \frac{(\beta_1\text{AR binding with iso and GppNHp} - \beta_1\text{AR binding with iso})}{\text{Specific } \beta_1\text{AR binding}} * 100$$

Statistical Analysis

For echocardiography data, two-way ANOVA with repeated measures were used to assess differences between MI and sham-ligated rats over time in fractional shortening and left ventricular diastolic diameter (as in Chapter 3). Tukey *post hoc* tests were used for further analysis of interactions and main effects. For measures of congestion and remodeling, Student's t-tests were used to assess group differences in the ratios of heart and lung weight to both body weight and tibia length (as in Chapter 3). For autoradiography, Student's t-test was used to assess differences between MI and sham-ligated rats in specific binding of ^{125}ICYP to overall βARs, β_1ARs, and β_2ARs. Student's t-tests were also used to compare the percent inhibition of ^{125}ICYP binding to β_1ARs by isoproterenol (indicative of G protein coupling).

Results

Echocardiography and Terminal Congestion Measurements

Similar to the results reported in Chapter 3, MI rats had significantly lower fractional shortening than sham-ligated rats both 1 and 7 weeks after surgery, as

shown in Figure 17A. In contrast, there was a tendency for FS to increase over time in sham-operated rats. At both 1 and 7 weeks after surgery, MI rats had significantly higher left ventricular diastolic diameter than sham-ligated rats, and diastolic diameter was increased in MI rats at week 7 compared to week 1 (Figure 17B). Eight weeks after surgery, sham-ligated rats weighed an average of 420 ± 9 grams, and MI rats weighed an average of 417 ± 7.4 grams. MI rats exhibited elevated post-mortem lung and heart weight compared to sham-ligated rats. Lung and heart wet weights were elevated in MI rats when normalized to both body weight and to tibia length (Figure 18).

Specific ^{125}ICYP Binding in Prefrontal Cortex

^{125}ICYP-incubated specimen slides generated autoradiograms typical of those shown in Figure 19. Incubation with an excess of propranolol generated a very light nonspecific signal (Figure 19C), and incubation with the β_2AR specific antagonist ICI-118,551 reduced the total signal (Figure 19A,B). Simultaneously exposed microscale standards ranged from 0.27–143.1 nCi/mg (corrected for decay). Radioactivity was related to grayscale values (0–255) obtained after exposure with an exponential function, shown in Figure 20. When grayscale values for regions of interest were calibrated to nCi/mg using the standard curve, values for total binding for all regions surveyed fell mid-range in the standard curve (8–14 nCi/mg).

In the infralimbic cortex (all cortical layers quantified together), MI rats exhibited decreased β_1AR density compared to sham-operated rats, with no significant group differences in overall βAR binding or β_2AR binding. No significant group differences in specific ^{125}ICYP binding were observed in any other cortical regions surveyed (Table 2).

Specific ^{125}ICYP Binding in the Amygdala

A 2-day exposure of ^{125}ICYP-incubated specimen slides generated autoradiograms as shown in Figure 21. When grayscale values for regions of interest in the amygdala were calibrated to nCi/mg using the standard curve, values for total binding for all regions surveyed fell mid-range in the standard curve (8–14 nCi/mg). These values were then converted to fmol sites per mg protein using the equations described in the Methods section.

In the BLA complex, MI rats had decreased density of overall βARs and β_1ARs compared to shams. The lateral nucleus of the amygdala in MI rats showed reduced specific β_1AR binding, and increased β_2AR binding compared to shams. No significant group differences in specific ^{125}ICYP binding to overall βARs, β_1ARs, or β_2ARs were observed in the basolateral nucleus of the amygdala (Table 2).

Agonist-Induced Inhibition of ^{125}ICYP Binding to G Protein-Coupled β_1ARs in the Prefrontal Cortex

In the prefrontal cortex, incubation with 10 nM isoproterenol (a concentration specific for high-affinity βARs) slightly reduced ^{125}ICYP binding. The addition of the non-hydrolyzable GTP analog, Gpp[NH]p, partially reversed the inhibition of binding by the agonist. No significant group differences in isoproterenol inhibition of ^{125}ICYP binding were observed in the infralimbic, prelimbic, or orbitofrontal cortices (Table 3).

Agonist-Induced Inhibition of ^{125}ICYP Binding to G Protein-Coupled β_1ARs in the Amygdala

In the amygdala, incubation with 10 nM isoproterenol (a concentration specific for high-affinity βARs) slightly reduced ^{125}ICYP binding. As in the prefrontal cortex, addition of Gpp[NH]p partially reversed this inhibition of binding. In the basolateral complex, MI rats had significantly more inhibition of ^{125}ICYP binding by isoproterenol than sham-operated rats (Table 3). Neither the basolateral nucleus nor the lateral nucleus exhibited significant group differences in isoproterenol inhibition of ^{125}ICYP binding.

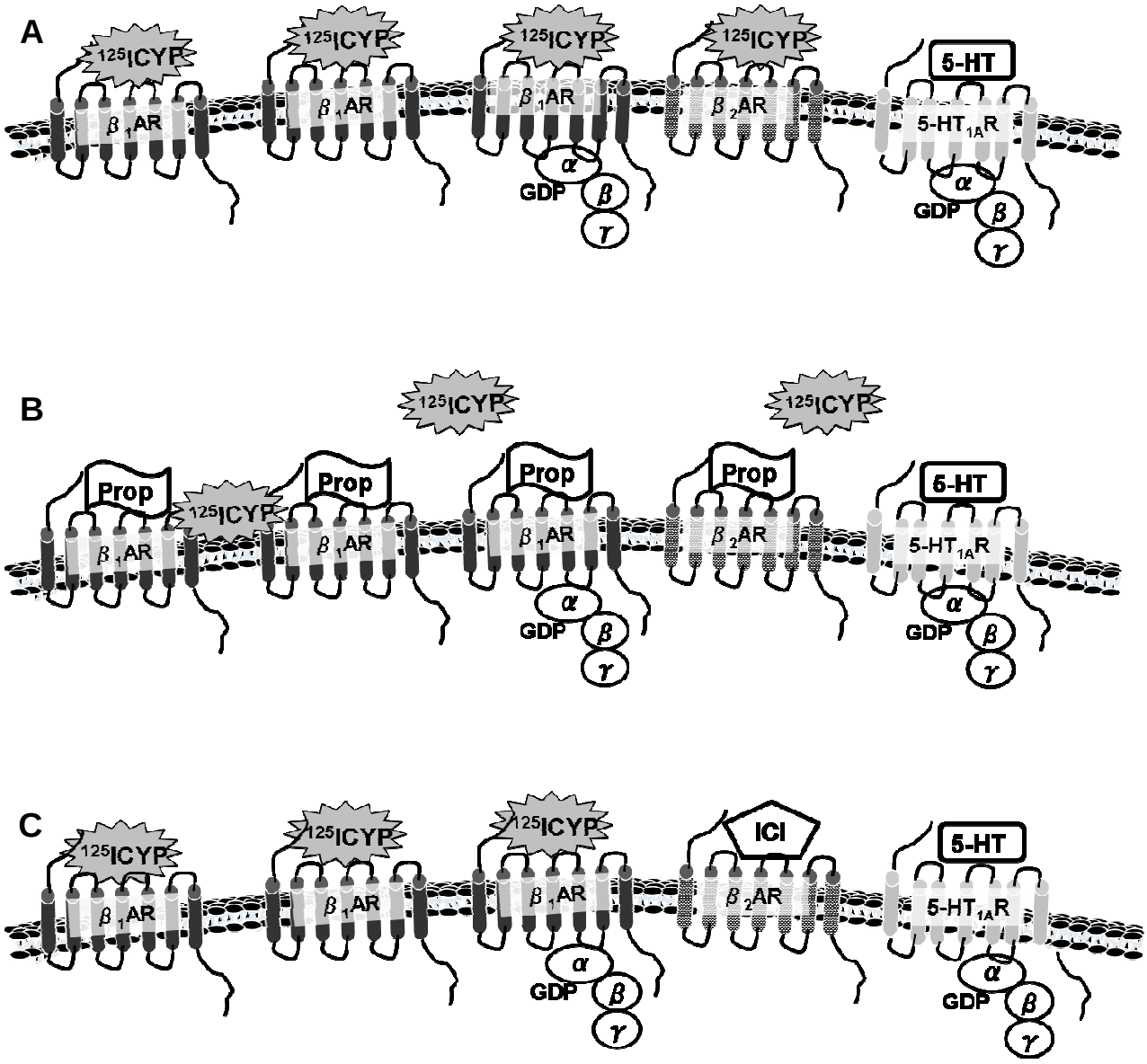

Figure 15. Schematics of autoradiography incubations to determine specific binding. All incubation conditions include ^{125}ICYP and serotonin (5-HT) to block serotonin receptors, e.g. 5-HT$_{1A}$. The total binding condition includes no other competing drugs (A). An excess of the βAR antagonist, propranolol (prop),

was used to determine nonspecific binding to the plasma membrane (B). The β_2AR antagonist, ICI-188,551(ICI), was used to determine β_1AR binding (C).

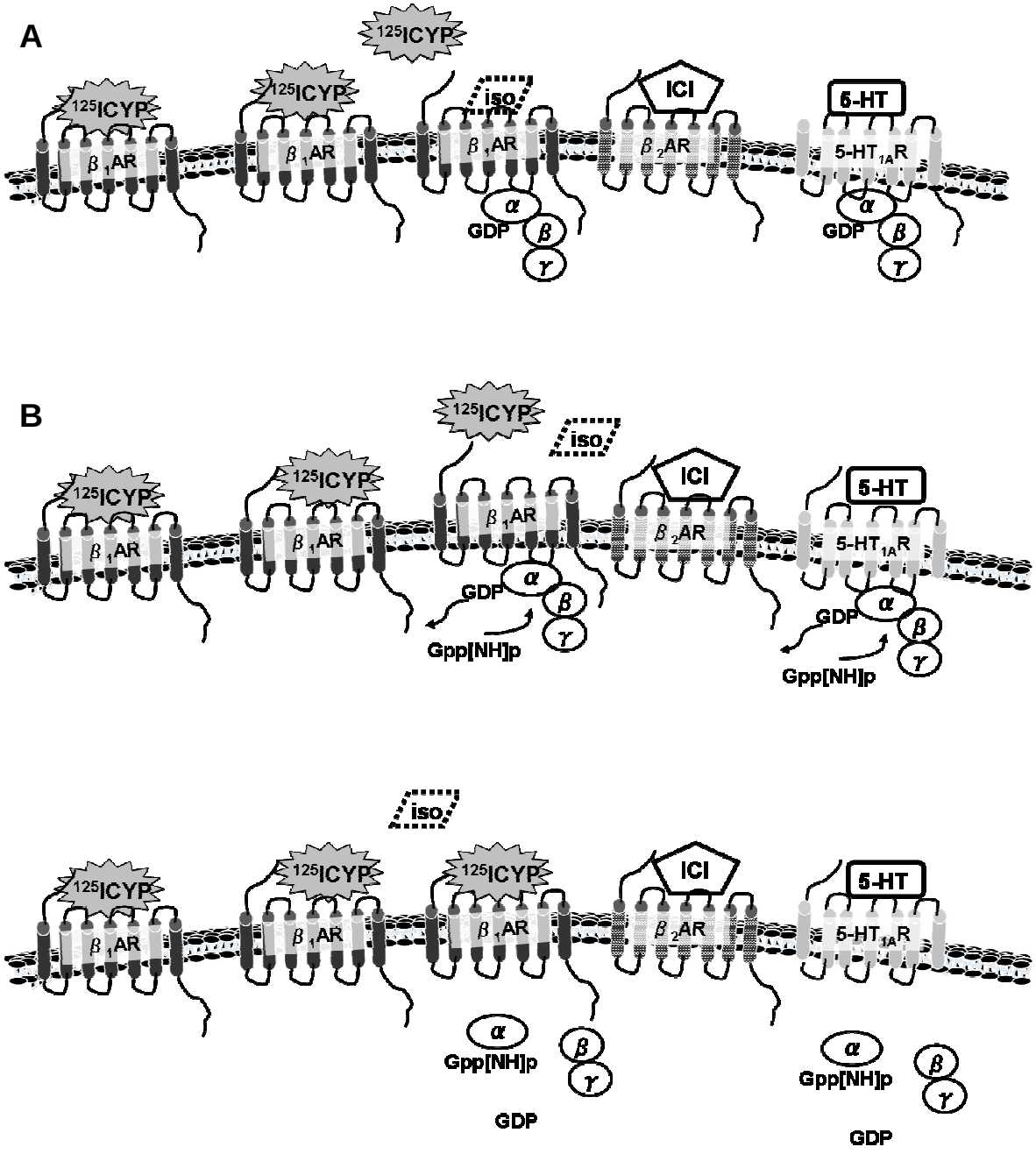

Figure 16. Schematics of ^{125}ICYP solutions to determine agonist inhibition of β_1AR binding. All incubation conditions include ^{125}ICYP and serotonin (5-HT) to block serotonin receptors (e.g. 5-HT_{1A}) and ICI-118,551 (ICI) to block β_2AR

binding. The agonist inhibition condition includes isoproterenol (iso) at a concentration selective for high-affinity receptors (A). The uncoupled binding condition includes the non-hydrolyzable GTP analog, Gpp[NH]p in addition to isoproterenol. Gpp[NH]p uncouples the high-affinity receptors and reverses isoproterenol's inhibition of ^{125}ICYP binding (B).

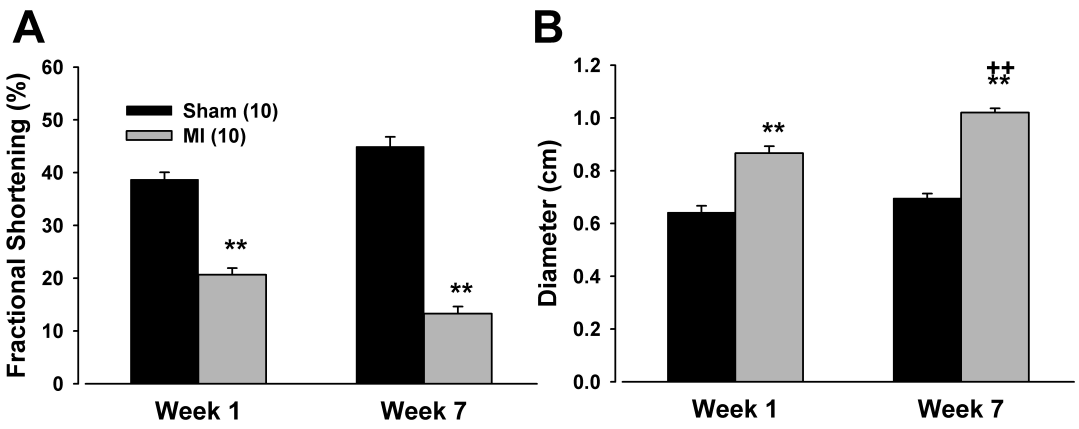

Figure 17. Left ventricular function (Specific Aim 2). Left ventricular fractional shortening (FS, A) and left ventricular diastolic diameter (LVDD, B) measured 1 and 7 weeks after MI or sham ligation surgery. Data are group means ±SEM. A two-way ANOVA with repeated measures used to assess group differences in fractional shortening over time revealed a surgery x time interaction [$F(1,18) = 21.69$, $P<0.01$] due to a tendency for decreased fractional shortening over time in MI rats, but increased fractional shortening over time in sham-ligated rats. A main effect of surgery [$F(1,18) = 283.01$, $P<0.01$] on FS was also observed due to significantly decreased fractional shortening in MI rats vs. sham-operated rats. A separate two-way ANOVA with repeated measures examining the effect of surgery on left ventricular diastolic diameter over time revealed a surgery x time interaction [$F(1,18) = 7.11$, $P<0.05$] due to a significant increase in diastolic diameter over time in MI rats but not sham-operated rats. A main effect of surgery [$F(1,18) = 126.78$, $P<0.01$] was also observed due to increased LVDD in MI rats vs. sham-operated rats. Between- and within-group comparisons were made with Tukey's *post hoc* test. **P<0.01 vs. sham, $^{++}$P<0.01 vs. week 1.

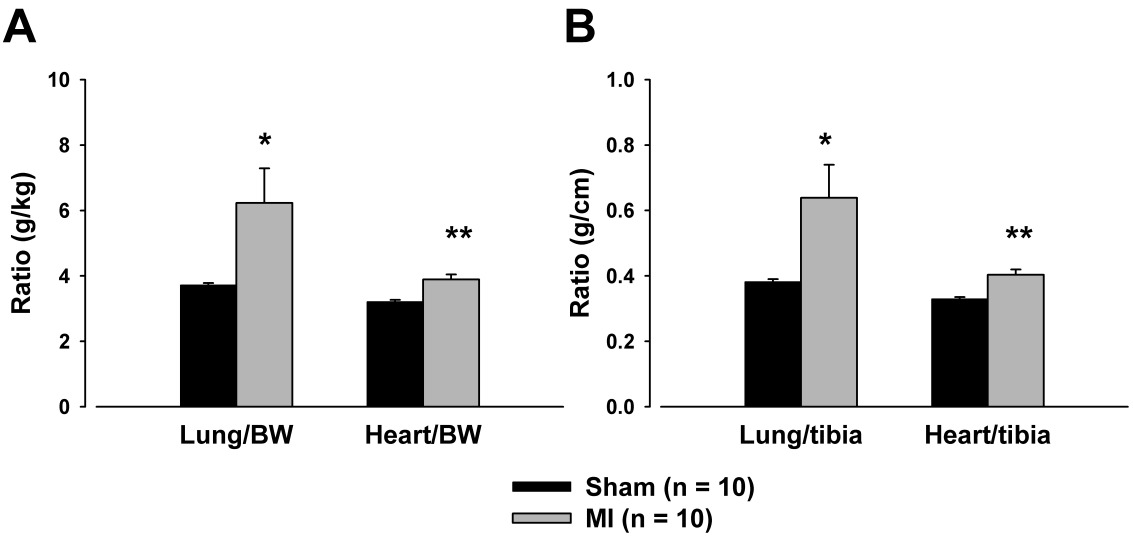

Figure 18. Terminal measures of congestion and remodeling

(Specific Aim 2). Ratios of lung and heart weight to body weight (A) and to tibia length (B). Values are group mean ± SEM. Student's t-tests revealed significantly increased lung-to-body weight ratio [$t(18) = 2.36$, $P<0.05$] and heart-to-body weight ratio [$t(18) = 4.10$, $P<0.01$] in MI rats vs. shams. Lung-to-tibia ratio [$t(18) = 3.03$, $P<0.01$] and heart-to-tibia ratio [$t(18) = 4.16$, $P<0.01$] were also elevated in MI rats. **P<0.01 vs. sham, *P<0.01 vs. sham.

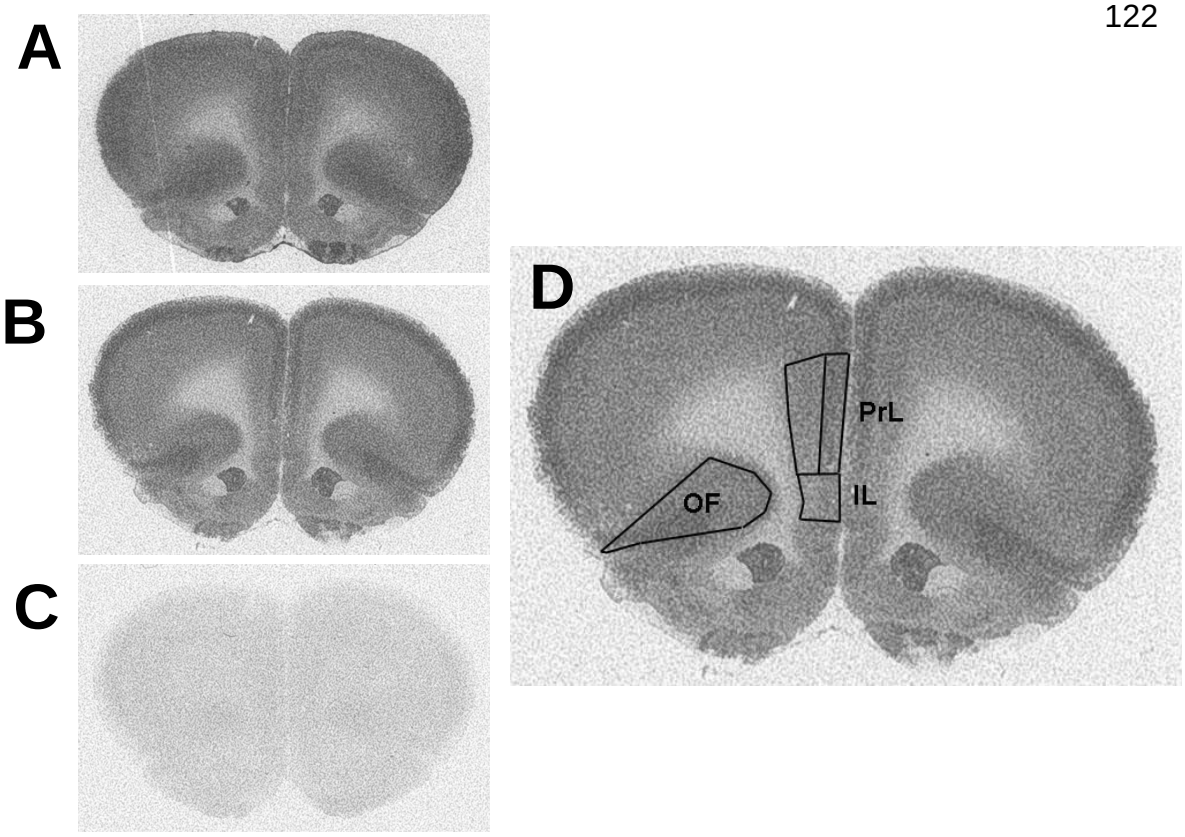

Figure 19. Representative ^{125}ICYP autoradiograms used to determine βAR binding in the prefrontal cortex. Dark areas indicate regions of higher density of ^{125}ICYP binding. ^{125}ICYP binding to β_1ARs and β_2ARs is shown in A. . Binding to β_1ARs (determined in the presence of 5 nM ICI-118,551) is shown in B. Nonspecific binding is shown in C. Binding to β_1ARs is also shown in D, enlarged and with measured regions labeled: infralimbic (IL), prelimbic (PrL, outer and inner lamina), and orbitofrontal cortices.

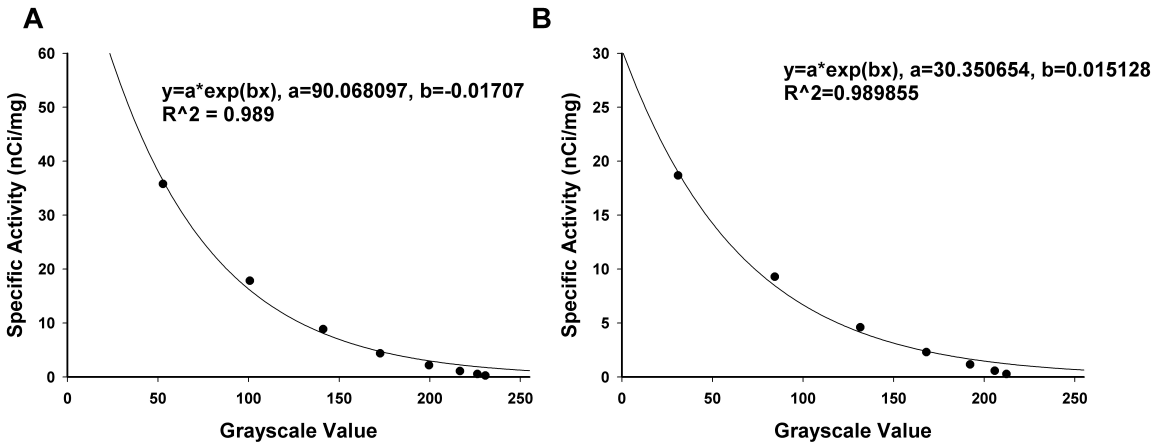

Figure 20. Standard curves relating specific activity and optical density. Curves are exponential functions fit to grayscale values of microscale standards with known specific activity for prefrontal cortex (A) and amygdala sections (B). Functions are displayed on each graph.

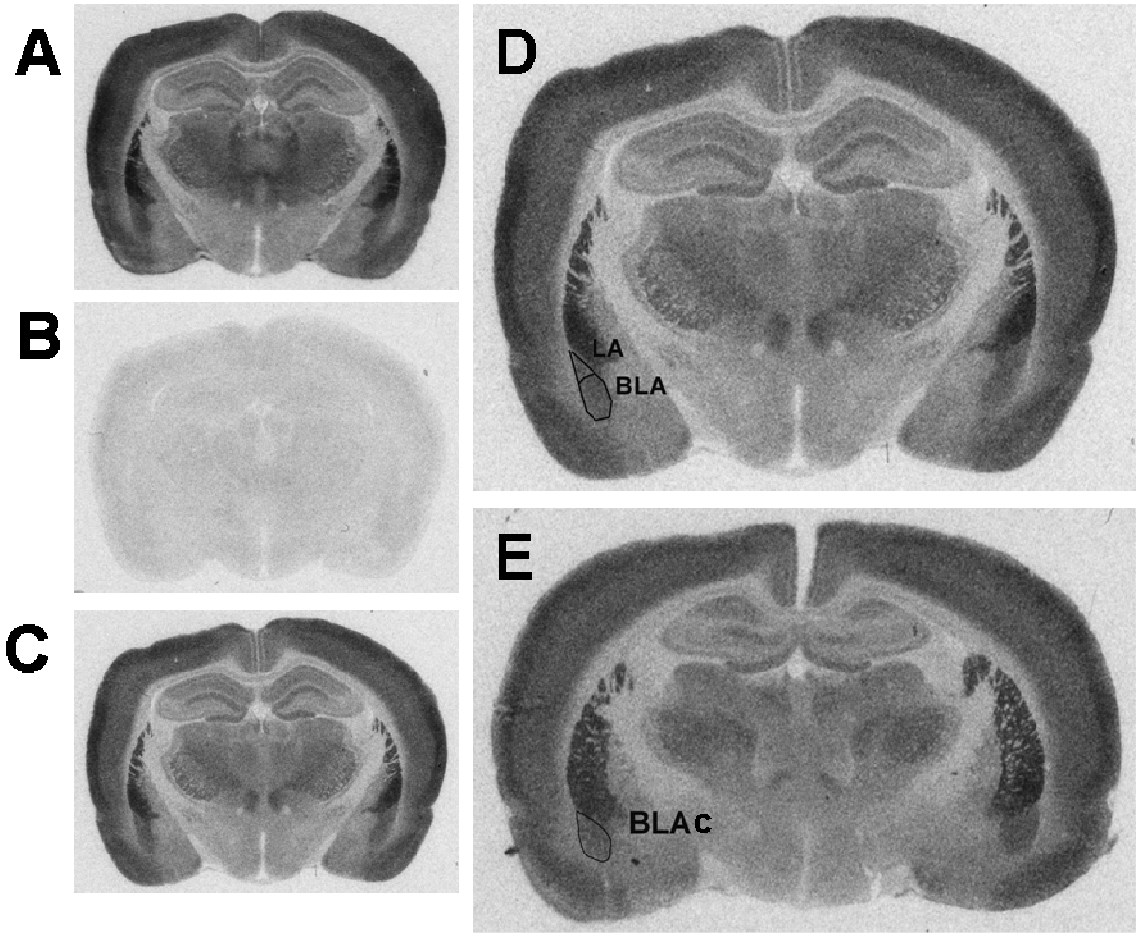

Figure 21. Representative ^{125}ICYP autoradiograms used to determine βAR binding in the amygdala. Dark areas indicate regions of higher density of ^{125}ICYP binding. ^{125}ICYP binding to β_1ARs and β_2ARs is shown in A. Binding to β_1ARs (determined in the presence of 5 nM ICI-118,551) is shown in B. Nonspecific binding is shown in C. Binding to β_1ARs is shown again in D and E, with measured areas labeled: lateral amygdala (LA) and basolateral nucleus (BLA) in D, basolateral complex (BLAc) in E.

	β_1ARs + β_2ARs (fmol/mg protein)		β_1ARs (fmol/mg protein)		β_2ARs (fmol/mg protein)	
	Sham (10)	**MI (10)**	**Sham (10)**	**MI (10)**	**Sham (10)**	**MI (10)**
IL (all)	45.4±1.1	43.5±1.3	32.8±1.0	29.2±1.3* (↓)	12.7±0.8	14.2±2.0
PrL (outer)	58.4±1.4	57.8±0.8	43.4±0.9	44.8±0.7	15.0±1.5	13.1±0 .6
PrL (inner)	51.7± 0.8	49.6±1.1	33.3±0.8	34.1±0.6	18.4±1.8	15.5± 1.2
OF (all)	62.2±2.6	61.0±2.0	40.5±1.3	41.6±1.3	21.7±1.9	19.5±2 .0
BLA cplx	40.0±0.6	36.9±0.8* (↓)	31.7±0.4	29.4±0.9* (↓)	8.3±0.9	7.5±0.8
BLA nuc	49.4±1.0	50.8±1.3	34.5±0.9	33.7±0.8	14.9±0.6	17.1±0 .9
LA	44.1±1.0	44.6±0.9	35.3±0.8	32.9±0.4* (↓)	8.8±0.8	11.6±3.9* (↓)

Table 2. Specific ^{125}ICYP binding in prefrontal cortical and amygdala regions. Values are means ± SEM and are presented as fmol sites per mg protein with group n indicated in parentheses. For prefrontal cortical regions, layers of cortex quantified are indicated in parentheses. In the infralimbic cortex (IL) when all cortical layers were quantified together, Student's t-test revealed decreased density of β_1ARs in MI rats vs. sham-operated rats. In the basolateral complex of the amygdala (BLA cplx), Student's t-test revealed significant decreases in overall βAR density and β_1AR density in MI rats vs. sham-operated rats. In the lateral nucleus of the amygdala (LA), Student's t-test revealed a significant decrease in β_1AR density, but a significant increase in β_2AR density in MI rats vs. sham-operated rats. No significant group differences were observed in specific ^{125}ICYP binding in the prelimbic (PrL) cortex outer or inner layers, orbitofrontal (OF) cortex, or basolateral nucleus (BLA nuc). *P<0.05 vs. sham.

		IL (all)	PrL (outer)	PrL (inner)	OF (all)	BLA cplx	BLA nuc	LA
% Inhibition of β_1AR binding (+iso)	Sham (10)	32.4±3.8	29.9±3.5	33.5±1.0	26.9±1.7	32.4±2.3	33.1±2.8	31.4±3.2
	MI (10)	37.6±4.2	28.6±1.5	33.5±1.4	28.9±2.2	37.8±3.0	34.5±2.6	32.3±2.7
% Inhibition of β_1AR binding (+iso and G)	Sham (10)	17.7±4.0	15.6±0.6	20.8±2.4	15.1±2.2	28.9±2.1	22.7±2.8	23.5±2.0
	MI (10)	22.3±2.4	19.7±1.4	20.8±1.2	18.8±1.4	27.5±4.0	20.2±3.7	17.6±3.0
% Change in inhibition	Sham (10)	14.74±1.6	14.34±3.8	12.72±2.8	11.84±2.3	3.48±1.7	10.40±2.8	7.91±3.9
	MI (10)	15.3±2.4	9.0±1.3	12.8±1.1	10.1±1.8	10.3±2.1*	14.3±2.8	14.7±2.5

Table 3. Isoproterenol inhibition of ^{125}ICYP binding. Values are group mean percent inhibition ± SEM. Left-most column shows percent inhibition of β_1AR binding in the presence of 10 nM isoproterenol (an index of the percentage of β_1ARs that are G protein coupled). Center column shows percent inhibition of β_1AR binding in the presence of isoproterenol and Gpp[NH]p. Right-most column displays the difference in isoproterenol-mediated inhibition of ^{125}ICYP binding of β_1ARs in the presence and absence of Gpp[NH]p (an index of binding to G protein-coupled β_1ARs). Student's t-test revealed a significant increase in percent inhibition of ^{125}ICYP binding by isoproterenol relative to ^{125}ICYP binding of β_1ARs in the presence of Gpp[NH]p [$T(18) = 2.49$, $P<0.05$] in the rostral basolateral complex (BLA cplx) of the amygdala. *$P<0.05$.

Discussion

In this study, rats that developed profound left ventricular dysfunction after MI exhibited exhibited significant changes in β-adrenergic receptor (BAR) density in the prefrontal cortex and amygdala, regions important in regulating responses to stressors. Specificially, in the infralimbic cortex, MI rats exhibited a decrease in β_1AR density. In the lateral amygdala, MI rats displayed a decrease in β_1AR density, with a concomitant increase in β_2AR binding. MI rats displayed a decrease in both overall βAR and β_1AR density in the rostral basolateral complex of the amygdala.

In the present study, echocardiography data demonstrate profound left ventricular dysfunction in MI rats, similar to the studies presented in Chapter 3. Compared to sham-operated rats, MI rats had decreased fractional shortening both 1 and 7 weeks after MI, indicating deficits in contractility. In contrast, fractional shortening in sham-operated rats tended to increase slightly over the course of the study. This increase in FS over time is likely due to an effect of thoracotomy surgery on contractility that recovered once rats were completely healed from surgery. Thoracotomy can result in pericardial effusions (evident in 1 week post-surgical echo) and mild lung inflammation (Nakamura et al., 2006), and mild pericardial effusions have been shown to reduce fractional shortening (Movahed et al., 2006). MI rats also exhibited dramatically elevated left ventricular diastolic diameter compared to shams at both 1 and 7 weeks after surgery, indicating chamber dilatation. Diastolic diameter significantly increased

in MI rats between week 1 and 7, indicating increased dilatation over time. In shams, diastolic diameter also increased slightly over time, likely due to growth, as this measurement is not normalized to body weight. Similar to the results in Chapter 3, lung and heart wet weights were elevated in MI rats, relative to both tibia length and body weight, suggesting cardiac remodeling and pulmonary edema in these rats due to volume overload.

These results indicate that rats subjected to MI progressed to heart failure over the course of the 8 week post-surgical period. However, this label must be used with caution, since heart failure is a cluster of several symptoms, including neurohumoral activation and elevated left ventricular end-diastolic pressure, i.e., the pressure in the ventricle at the end of diastole (Francis et al., 2001a). Assessments of left ventricular end-diastolic pressure require catheterization of the left ventricle. This can be performed acutely as a terminal procedure. We did not perform the acute procedure because it would have required anesthesia prior to euthanasia, which could have confounded the autoradiographic assays.

In the rostral basolateral complex of the amygdala, our observation that MI rats displayed a tendency for increased inhibition of ^{125}ICYP binding by the βAR agonist, isoproterenol, at a concentration selective for high-affinity receptors, suggests an increase in G protein coupling of β_1ARs. Although variability precluded a statistically significant group difference in isoproterenol-induced inhibition of ^{125}ICYP binding to β_1ARs (in the absence of Gpp[NH]p, we did observe a significantly greater isoproterenol-induced inhibition of ^{125}ICYP binding

to uncoupled β_1ARs (i.e., in the presence of GppNHp) in MI rats. The tendency for increased coupling in MI rats may reflect two possibilities: either a proportion of the receptor population is in a high-affinity state, or the affinity of the receptor for agonist has increased (Lefkowitz et al., 1976). Either case would suggest the possibility that the β_1ARs in the BLA complex of MI rats would be more responsive to agonist (NE). However, we also observed a decrease in β_1AR density in this region. It is difficult to predict the net functional effect of these opposing changes, though it is possible that increased G protein coupling is compensating for the decrease in β_1AR density in the the BLA complex after MI.

The decrease in β_1ARs we observed in both the LA and BLA complex of MI rats is in contrast to our expectations, since activation of β_1ARs in the BLA and LA is implicated in responses to learned fear. Specifically, β_1ARs have been shown to be upregulated in the BLA after fear conditioning (Fu et al., 2008), and transient downregulation of β_1ARs in the BLA impairs retrieval of auditory fear memory in rats (Fu et al., 2007). Also, blockade of β_1AR and β_2ARs in the LA with propranolol disrupts the reconsolidation of fear memory in rats (Debiec and Ledoux, 2004). However, we do not know whether the downregulation of βARs in these previous studies, or the reduction in β_1ARs that we observed in MI rats is localized to pyramidal cells or interneurons. Thus, it is possible that a reduction in β_1ARs on GABAergic interneurons in the lateral amygdala and basolateral amygdala could still result in increased excitation of the CeA (leading to enhanced stress responses). Though some studies have reported increases in

βARs in the BLA and LA in response to stress, others have reported downregulation, especially in response to chronic stressors. For example, rats subjected to chronic REM sleep deprivation demonstrate significant decreases in both β_1ARs and β_2ARs in multiple brain regions, including the IL, the entorhinal cortex, and the supraoptic nucleus, and the hippocampal dentate gyrus (Hipolide et al., 1998). Another study found that rats subjected to chronic, but not acute, tail shock demonstrate downregulation of βARs in multiple brain regions (Nomura et al., 1981). Chronic mild stress in rats has also been shown to downregulate cortical βAR expression (Papp et al., 1994). Together, these studies suggest that stress, particularly chronic stress, can result in downregulation of βAR expression in multiple brain regions. Given that chronic stress (14 days of restraint stress) results in increased forebrain norepinephrine (Beck and Luine, 2002), our results may indicate receptor desensitization in response to chronic agonist (NE) stimulation.

Investigations of the role of βARs in stress responses have focused primarily on the β_1AR, since this is the most abundant beta receptor subtype expressed in the cerebral and in subcortical structures. Norepinephrine has a 10-fold higher affinity for β_1ARs than β_2ARs (Lands et al., 1967), and norepinephrine binding to β_2ARs results in slower and less pronounced conformational changes than those induced by epinephrine (as determined by fluorescent resonance energy transfer). However, norepinephrine and epinephrine binding to β_2ARs elicits similar adenylyl cyclase activation (Reiner et

al., 2010), suggesting that β_2ARs are, indeed, responsive to norepinephrine. While both β_1ARs and β_2ARs can couple to $G\alpha_s$, resulting in excitation, β_2ARs have been shown to sometimes couple to $G\alpha_i$, leading to decreases in cAMP and hyperpolarization of neurons. After MI, atrial and ventricular β_2ARs have been shown to be coupled to $G\alpha_i$, as treatment with pertussis toxin (which inactivates $G\alpha_{i/o}$), restores reduced inotropic responses to isoproterenol (Kompa et al., 1999). Recent evidence suggests that β_2ARs in the brain may be coupled to $G\alpha_i$ in the brain in some situations. For instance, coupling of β_2ARs to $G\alpha_i$ has been demonstrated in the hippocampus, in which β_2AR activation results in glucocorticoid-dependent impairment of contextual fear memory retrieval (Schutsky et al., 2011). It is not known whether the increased β_2ARs expressed in the LA of rats with MI are coupled to Gαs or Gαi proteins. It is tempting to speculate that altered coupling of β_2ARs receptors contributes to aberrant signal processing.

In contrast to our expectations, the addition of Gpp[NH]p provided only slight reversal of isoproterenol inhibition of ^{125}ICYP binding in all brain regions surveyed. Gpp[NH]p has been shown to successfully uncouple high-affinity ternary complexes to inhibit receptor agonist binding in multiple receptor and tissue types at lower or equivalent concentrations as used in the present study (Appel et al., 1990; Li et al., 1997), including one autoradiographic study labeling βARs (Arango et al., 1990). However, others have found that the ability of Gpp[NH]p to uncouple high-affinity receptors is limited in neuronal βARs (Vickroy

et al., 1983; Garnier et al., 1997). Garnier et al. have proposed that an insensitivity of high-affinity βARs in cerebral cortical neurons to uncoupling by Gpp[NH]p is due to a membrane-bound factor that stabilizes the ternary complex and inhibits the dissociation of Gαs from the receptor (Garnier et al., 1999). These previous studies may explain the limited reversal of isoproterenol-induced inhibition of ^{125}ICYP binding by Gpp[NH]p that we observed in all regions surveyed.

βAR expression in the brain is downregulated in response to chronic agonist stimulation (Ordway et al., 1988). βAR expression also changes in response to stress in particular brain regions (Fu et al., 2008; Hipolide et al., 1998). Chronic, systemic treatment with desipramine has been shown to downregulate β_1AR expression in multiple brain regions, including the BLA, though not any cortical regions, suggesting that chronic increases in NE may suppress β_1AR (but not β_2AR) expression in some brain regions. βARs are also downregulated in response to intracerebroventricular administration of isoproterenol (Ordway et al., 1988). However, isoproterenol, which is a full agonist at both β_1AR and β_2ARs (Lands et al., 1967), induces preferential downregulation of β_2ARs (Ordway et al., 1988). The fact that NE has a 10-fold higher affinity for β_1ARs than β_2ARs (Lands et al., 1967; Reiner et al., 2010) provides a potential explanation for why β_1ARs would be downregulated by increased synaptic NE resulting from desipramine treatment. In response to chronic agonist stimulation, the cell surface expression of many GPCRs,

including the βAR, is downregulated. The classic method of downregulation is through internalization. After agonist stimulation, βARs are phosphorylated by G protein receptor kinases. β-arrestins are recruited by this phosphorylation and target the receptor for internalization and subsequent degradation or recycling (Benovic et al., 1987). Activation of LC neurons (i.e., Fra-like immunoreactivity and hexokinase activity) has been shown to be chronically increased in rats after MI (Patel et al., 1993; Vahid-Ansari and Leenen, 1998), and human heart failure patients show evidence of increased brain NE (Hasking et al., 1986). Therefore, in the present study, the reduction in β_1AR binding observed in the infralimbic cortex, lateral amygdala, and basolateral complex of the amygdala in MI rats may be a result of downregulation due to increased NE release in these areas.

In the IL cortex, is has been shown that βAR blockade with propranolol impairs recall of fear extinction in a PKA-dependent manner (Mueller et al., 2008). In Chapter 3, we reported a decrease in IL metabolic activity in response to LC stimulation in MI rats. This decreased activity in response to NE release could result from either a decrease in βAR-mediated excitation or from an increase in α_2AR-mediated inhibition. Our finding of a decrease in β_1AR density in the IL in MI rats provides evidence that a possible desensitization of IL β_1ARs may contribute to decreases in IL activity during LC activation such as occurs during stress. Taken together, these results identify changes in βAR density and coupling after MI that may contribute to abnormal stress responses and the development of anxiety disorders.

CHAPTER 5

ALTERATIONS IN EXPRESSION AND EXTINCTION OF CONDITIONED FEAR AFTER MYOCARDIAL INFARCTION

Abstract

Post-MI patients display exaggerated physiological and emotional responses to stressors and have an increased prevalence of post-traumatic stress disorder (PTSD). Imaging studies have demonstrated hyperactivity of the amygdala and hypoactivity of the prefrontal cortex (PFC) in PTSD patients. In rodent models of fear extinction, the infralimbic PFC (IL) has been shown to regulate extinction of learned fear. In our prior study described in Chapter 3, we observed increased baseline metabolic activity in the IL in MI rats, but decreased IL metabolic activity in MI rats in response to locus coeruleus (LC) stimulation, suggesting that activation of the LC in response to a stressor results in inhibition of the IL in MI rats. Our findings described in Chapter 4 suggest that a desensitization of IL β_1ARs may contribute to stress-induced IL inhibition. Given our results and the fact that noradrenergic signaling in the IL contributes to the extinction of learned fear responses, this study sought to determine the effect of MI on the acquisition and recall of extinction of conditioned fear. Rats subjected to MI developed left ventricular dysfunction (lower left ventricular fractional shortening and higher left ventricular diastolic diameter than sham-ligated rats).

In response to presentation of a tone previously paired with footshock, MI rats displayed increased freezing behavior compared to sham-operated rats and took more trials than sham-operated rats to extinguish freezing in response to the conditioned stimulus (CS+). While sham-ligated rats exhibited lesser freezing in response to a tone previously unpaired with footshock (CS-), MI rats displayed similar freezing responses to CS+ and CS- for several trials, suggesting a deficit in their ability to discriminate between threatening and safe stimuli. During the testing of recall of extinction the following day, MI rats again displayed increased freezing during initial CS+ presentations compared to shams, indicating a deficit in extinction recall. Taken together with our prior studies, these data indicate that MI results in a deficit in the extinction of learned fear responses that may, in part, be mediated by an inhibition of the IL during stress.

Introduction

Post-MI patients have an increased prevalence of anxiety disorders, including generalized anxiety disorder (Frasure-Smith and Lesperance, 2008) and post-traumatic stress disorder (Gander and von Kanel, 2006). Additionally, panic disorder is associated with coronary artery disease (Fleet et al., 2005). Up to 15% of post-MI patients develop post-traumatic stress disorder (PTSD), which is characterized by intrusive trauma-related thoughts, avoidance of trauma reminders, and chronically heightened physiological and emotional arousal (Wikman et al., 2008; Whitehead et al., 2006). The development of PTSD after

MI is associated with further cardiovascular pathology (Wikman et al., 2008). The neural mechanisms underlying the development of anxiety after MI are largerly unknown.

Classical conditioning can be used in animal models to study the neural substrates that underlie aberrant stress responses and the development of anxiety disorders. In classical conditioning, subjects develop conditioned responses to a neutral stimulus by pairing of the innocuous stimulus with a salient (aversive or appetitive) stimulus. Thus, the neutral stimulus comes to elicit a similar response to the salient unconditioned stimulus (US) and so becomes known as the conditioned response (CS). After repeated presentations of the CS without the US, responses to the CS normally abate. However, this extinction process is often delayed or absent in anxiety disorders, including PTSD. In PTSD, the neutral cues associated with the trauma (the US) continue to elicit intense fear responses long after the trauma has terminated. Aberrant risk assessment, i.e. difficulty discerning cues signaling threats vs. safety, is also a hallmark of depression and generalized anxiety (Britton et al., 2011). Understanding the mechanisms underlying this lack of extinction is key for developing novel therapies to treat post-MI patients with comorbid depression and anxiety disorders.

Several imaging studies in PTSD patients have shown alterations in amygdala and prefrontal cortical activation compared to healthy controls. In male Vietnam veterans, exposure to combat-related pictures and sounds resulted in

increased bloodflow to the amygdala, but decreased bloodflow to the prefrontal cortex (Bremner et al., 1999). Furthermore, in both male and female Vietnam veterans with PTSD, symptom severity was positively correlated with amygdala activation, and negatively correlated with prefrontal cortical activation during script-driven imagery, in which subjects are encouraged to recall sensations associated with the traumatic event while listening to a trauma-related script (Shin et al., 2004).

As reported in Chapter 3, we observed increases in metabolic activity at basline in the infralimbic (IL) cortex of MI rats at baseline. However, in response to locus coeruleus (LC) stimulation in a pattern mimicking a mild stressor, we observed decreased IL metabolic activity in MI rats, suggesting that the norepinephrine (NE) released as a result of LC activation by a stressor has an inhibitory effect in the IL. As reported in Chapter 4, we also observed a decrease in β_1AR density in the IL, as well as the BLA and LA in MI rats. Given that previous studies have demonstrated long-term activation (hexokinase activity and Fra-like immunoreactivity) of the LC in rats after MI (Patel et al., 1993; Leenen, 2007), the decreases in β_1AR density we observed may reflect desensitization induced by chronic stimulation by NE. Since activation β_1ARs is usually excitatory, a decrease in β_1AR availability could contribute to the inhibition of metabolic activity we observed in the IL of MI rats in response to LC stimulation.

Studies using the $GABA_A$ agonist, muscimol, to inhibit discrete brain regions just prior to extinction of auditory conditioned fear have shown that the prelimbic cortex is necessary for the expression of learned fear, the IL cortex is necessary for the acquisition and retention of extinction of learned fear, and the basolateral amygdala is necessary for both expression and extinction of learned fear (Sierra-Mercado et al., 2011). Furthermore, Mueller et al. reported that blockade of βARs in the IL with propranolol prior to fear extinction impairs the retention of extinction memory, and that NE increases the excitability of IL pyramidal neurons in a βAR-dependent manner (Mueller et al., 2008). The LC is activated in response to stress or novelty (Aston-Jones et al., 1991; Aston-Jones et al., 1991; Campeau et al., 1997), and the activation of the LC results in NE release in the mPFC (Florin-Lechner et al., 1996). It has been shown through mPFC microdialysis that NE release in the cortex during exposure to various appetitive and aversive stimuli is proportional to the salience of the stimuli (Ventura et al., 2008). Ventura et al. also demonstrated that lesion of NE nerve terminals in the mPFC prevents conditioned place preference/avoidance only when stimuli are highly salient, indicating that NE signaling in the mPFC is necessary for attributing salience value to stimuli (e.g., threatening vs. innocuous). Given the inhibition of IL activity we observed in response to LC stimulation in MI rats and the known role of the IL in extinction of conditioned fear, we tested the hypothesis that MI results in increased fear responses and deficits in extinction.

Materials and Methods

Animals

All experiments were performed in accordance with the American Physiological Society Guiding Principles for Research Involving Animals and Human Beings (2002) and were approved by the university's Institutional Animal Care and Use Committee. Male Sprague-Dawley rats between 275 and 299 grams (Harlan, Indianapolis, IN) were acclimated to the virarium for one week prior to experiments with ad libitum access to food and water. Rats were housed at a constant temperature of 22 ± 2℃ with a 12/12 h our light/dark cycle. To avoid potential confounds of isolation stress on behavioral measurements, rats in this study were housed in groups of 2 or 3 and were provided with wooden blocks and brightly-colored plastic dumbbells for environmental enrichment. Rats were housed separately for one week following each surgery.

Fear Conditioning

Rats were subjected to auditory fear conditioning as described previously with some modifications (Chang et al., 2009). Rats were transported in their home cages from the animal care facility to a nearby room that was used for fear conditioning and for subsequent extinction and recall testing. For fear conditioning, rats were placed in a Med Associates Inc. operant conditioning (ENV-001, St. Albans, VT) chamber inside a Med Associates inc. sound-attenuating cubicle that had been cleaned with 30% ethanol to provide a distinct

odor. Two rats were conditioned simultaneously in separate side-by-side cubicles. A fan inside each cage supplied low-level background noise. A 10-second tone of either 1000 or 5000 Hz was delivered by a Dell speaker mounted inside the chamber. Each rat was randomly assigned to receive either the 5000-Hz or 1000-Hz tone paired with a foot shock supplied through the grid floor. This tone was designated as the CS+ tone. The other tone was designated at the CS- tone, and was never paired with footshock. Both tones were 80 dB, and the loudness of each tone was confirmed with a decibel meter inside the chamber before each session. Both tone and shock presentation were controlled by ADInstruments software (Chart 5.3).

After placement in the chamber, the rats were exposed to 10 habituation tones (5 CS+, 5 CS-) that were not paired with footshock. All tones were presented in quasi-random order such that no more than two CS- or CS+ trials were presented consecutively. After presentation of the habituation tones, the tone assigned as CS+ was co-terminated with a half-second 0.5 mA footshock applied via the metal floor bars of the cage, which were connected to a Med Associates Inc. stand-alone shock scrambler (ENV-414S). The 18 tone-shock pairings and 18 CS- tones were presented with a variable inter-trial interval (16–140 seconds, average 72 seconds) in order to avoid changes in behavior based on the rats' ability to predict the onset of the tone based on elapsed time. Behavior was recorded for analysis on either a Cannon FS20 camera or a Cannon DC220 camera mounted on a tripod outside the door of the sound-

attenuating chamber. For all behavior analysis, rat identities were coded to allow scoring by an observer blind to the rats' experimental treatment.

After the hour-long conditioning session, rats were removed from the chambers, placed in their home cages, and transported back to the vivarium. After counting the number of fecal boli, the chambers were cleaned with 30% ethanol before the next session. All conditioning trials took place between 8:00am and 3:00pm. For analysis, the freezing time during each tone was scored with a stop-watch. The rat was considered to be freezing if it made no movements except those necessary for respiration for 1 second or more.

Coronary Artery Ligation

One week following fear conditioning, rats were anesthetized with ketamine/xylazine (100 mg/kg + 7 mg/kg, im) and underwent coronary artery ligation to induce MI, or were subjected to sham ligation surgery as described in Chapter 3. Half the rats that received each frequency of CS+ tone were assigned to undergo MI surgery, and the rest were assigned to receive sham ligation surgery. Rats were assigned to MI or sham groups based on body weight, such that rats of similar body weight were assigned to different surgery groups.

Echocardiography

Rats were anesthetized with ketamine/xylazine (100 mg/kg + 7 mg/kg, im) and subjected to echocardiography (Acuson Sequoia C256, Siemens AG) to determine left ventricular function 1 and 7 weeks after CAL or sham ligation surgery, as described in detail in Chapter 3. All sham-ligated rats, as well as MI rats exhibiting FS<25% were implanted with radio telemetry probes to enable recording of blood pressure, heart rate, ECG and locomotor activity during later extinction and recall trials. Rats that did not meet criteria for inclusion in the study were euthanized with an overdose of sodium pentobarbital.

Telemetry Probe Implantation

One to 2 weeks after the first echocardiogram, rats were instrumented with radio-telemetry probes (C50-PXT, Data Sciences International, St. Paul, MN) as described previously (Henze et al., 2008; Brockway et al., 1991). Probes were implanted subcutaneously under isoflurane anesthesia (5% in 100% O_2 for induction, 2% in 100% O_2 for maintenance). Gel-filled blood pressure catheters were placed in the left femoral artery, and ECG leads were sutured subcutaneously to record 2-lead ECG. The positive lead was placed 2 cm to the right of the sternum at the level of the 2nd rib, and the negative lead was placed 1 cm to left of center at the level of the xiphoid process. Rats received buprenorphine (50 µg/kg, s.c.) upon waking from anesthesia and again 16, 24, 40, and 48 hours later.

Extinction of Conditioned Fear

Seven weeks after CAL or sham surgery, rats underwent extinction training in the same room as the conditioning trials. In order to test the conditioned responses to the tones (rather than learned responses to the context, i.e., environment) and to assess the rats ability to learn that the CS+ now predicted safety, the rats were exposed to the original conditioning tones without shock in a new context with visual, tactile, and olfactory cues distinct from the conditioning apparatus (Chang et al., 2009). This context consisted of a Plexiglas box (11in x 19in x 17in) with a smooth floor. The floor was spray-painted black, and the walls were painted in a black and white vertical striped pattern. Before and after each session, the box was cleaned with 5% acetic acid to remove olfactory cues from the previous rat and to provide a distinct odor from the conditioning chamber. The same 10-second tones of either 1000 or 5000 Hz were delivered by a Dell speaker mounted at the top of the testing box.

For the extinction trials, rats were first transported in pairs to a room adjacent to the testing room. This room was dimly lit and had radio static for background noise (~60 dB). Both rats remained in the acclimation room in clean cages for an hour before an investigator turned on one rat's telemetry probe and transported that rat to the testing room in its cage. As soon as a stable blood pressure and ECG telemetry signal could be detected, the rat was placed in the extinction box and the extinction procedure was initiated. Tone presentation was

controlled by ADinstruments shoftware (Chart v5.3) while recording of blood pressure, heart rate, and ECG were simultaneously collected using Dataquest software (DSI). Video data were recorded on a Cannon FS20 camera and telemetry data were recorded on DSI Dataquest A.R.T. 3.1 software transmitted from a DSI Physiotel receiver (RPC-1) placed directly underneath the Plexiglas testing box. Exctinction training consisted of 20 CS+ tones and 20 CS- tones over the course of 2 hours.

The first tone began 3 minutes after the rat was placed in the box. As in the conditioning trials, tones were presented in a pseudo-random order (no more than two consecutive tones of one type). The inter-trial interval was variable (120–300 seconds) with a mean of 180 seconds. After the extinction trials, the rat was removed from the box, returned to its cage, and transported back to the adjacent habituation room. This process was repeated for the second rat, and then both rats were transported back to the vivarium. All extinction trials took place between 8:00am and 3:00pm. Freezing behavior was analyzed by a blinded investigator as described for the conditioning trials.

Recall of Extinction

The day after extinction trials, rats were transported from the vivarium to test their recall of the extinction training. The recall testing occurred in a third unique context, which allowed us to test specifically the extinction of the tone-shock association. The testing box consisted of a Plexiglas box (11in x 19in x

17in) coated with textured spray paint in a tan color. Before and between testing sessions, the box was cleaned with a 1% Pinesol solution to eliminate olfactory cues from the previous rat and to provide a distinction odor. Again, rats first spent an hour in a room adjacent to the testing room before the first rat was transported to the testing room with its telemetry probe turned on. Recall testing consisted of 10 CS+ tones and 10 CS- tones (with no shocks) presented in pseudo-random order with variable inter-trial intervals (120–300 seconds, average 180 seconds) over the course of 1 hour (with the first tone presented 3 minutes after the rat was placed in the apparatus). After the recall trials, the rat was removed from the box, returned to its cage, and transported back to the adjacent habituation room. This process was repeated for the second rat, and then both rats were transported back to the vivarium. All recall trials took place between 8:00am and 12:00pm, and rats were subjected to recall testing in the same order as for extinction. Freezing behavior was analyzed by a blinded investigator as described for the conditioning and extinction trials.

Euthanasia and Tissue Processing

Rats were deeply anesthetized with sodium pentobarbital (100 mg/kg, i.p.) and euthanized by decapitation. To assess congestion and remodeling, hearts and lungs were removed and weighed, and left tibias were removed and their length measured with a caliper.

Statistical Analysis

For echocardiography data, two-way ANOVA with repeated measures were used to assess differences in fractional shortening and left ventricular diastolic diameter between MI and sham-ligated rats over time (as in Chapters 3 and 4). Tukey *post hoc* tests were used for further analysis of main effects and interactions. For measures of congestion and remodeling, Student's t-tests were used to assess group differences in the ratios of heart and lung weight to both body weight and tibia length (as in chapters 3 and 4).

For freezing behavior during conditioning trials (prior to MI or sham ligation), 3-way ANOVA were used to examine differences in responses to CS+ and CS- presentations over time. This analysis was also used to determine whether rats assigned to MI or sham ligation surgery after conditioning exhibited similar rates of acquisition of the freezing responses during conditioning trials. Freezing behavior during extinction and recall trials was analyzed using 3-way ANOVA with repeated measures to examine effects of surgical treatment, CS type, and trial number. Tukey *post hoc* tests were used for further comparisons of significant interactions and main effects. Repeated measures ANOVA initially examined responses in all trials. However, when freezing behavior reached a stable minimum in both sham and MI rats after several trials, additional analyses examined responses only until freezing times reached this lower plateau. The following 3-parameter exponential decay function was used to calculate the trial

at which the freezing dropped below a minimal value (2 seconds) for each rat and to determine the rate of decrease in freezing over repeated trials:

$$y = y_0 + a*\exp(b^x)$$

In this equation, *y* represents the lower plateau (constrained as less than 2 seconds), *a* represents the maximum value (constrained as the freezing duration in the first trial), and *b* represents the exponential rate of decrease. Two-way ANOVA with repeated measures were used to assess the effect of MI on the number of trials to reach extinction and on freezing time during the first CS+ and CS- presentation (a measure of the conditioned response).

For heart rate and blood pressure data from extinction and recall testing, data were exported to Chart, and the average heart rate and mean arterial pressure were averaged over consecutive 0.2-second periods during the 10-second tone presentation, as well as 10 seconds before and after the tone. Data were plotted for each trial to examine overall responses. Based on the overall patterns of blood pressure and heart rate responses, three-way ANOVA with repeated measures were used to assess the effect of surgical treatment and CS type on maximal change in blood pressure (difference in BP between 1.8 seconds after start of tone and pre-tone baseline) over successive CS presentations. Three-way ANOVA with repeated measures also examined the effect of surgical treatment and CS type on the change in heart rate (difference in HR between last 0.5 seconds of tone and pre-tone baseline) over successive CS presentations.

Results

Echocardiography Measurements and Terminal Measures of Congestion

As in previous experiments, MI rats exhibited lower fractional shortening than sham-ligated rats. In contrast, there was a tendency for an increase in fractional shortening over time in sham-ligated rats, but a decrease over time in MI rats. In MI rats, left ventricular diastolic diameter was increased compared to sham-ligated rats. Diastolic diameter increased over time in both MI and sham-ligated rats, but this increase in diameter over time was greater in MI rats (Figure 22). Thirteen weeks after surgery, sham-ligated rats weighted an average of 438 ± 8 grams, and MI rats weighed an average of 438 ± 7 grams. As shown in Figure 23, MI rats exhibited a tendency for elevated heart weight (P=0.09 normalized to tibia length, P=0.10 normalized to body weight) and lung weight (P=0.33 normalized to tibia length, P=0.33 normalized to body weight), though no significant group differences were observed.

Freezing Behavior During Fear Conditioning Trials

As shown in Figure 24, all rats displayed very little freezing behavior during initial tone presentation prior to tone-shock pairings. Once presented with tone-shock pairings, rats exhibit a dramatic increase in freezing time during presentation of either the tone paired with foot shock (CS+ tone) or the tone never paired with footshock (CS- tone). During the first 6 trials of tone-shock pairings, rats later

subjected to MI (pre-MI) displayed freezing times similar to rats that were later subjected to sham ligation surgery (pre-sham). Additionally, both pre-MI and pre-sham-ligated rats displayed a tendency for greater freezing during CS+ tones than CS- tones during these first 6 trials. After the first 6 trials, however, apparent freezing times decreased in both the MI and sham-ligated rats during both tones. Although sham-ligated rats froze less than MI rats during these intermediate trials, freezing was similar in pre-MI and pre-sham rats by the final trials. During trials in which the group mean reflected decreased freezing, some rats continued to freeze, while some rats exhibited other defensive behaviors, including vigilant scanning (side-to-side head movements) and assuming standing postures that minimized contact with the electrified floor bars.

Freezing Behavior During of Extinction of Conditioned Fear

During presentations of tones previously paired (CS+) or unpaired (CS-) with footshock (7 weeks prior), MI rats spent more time freezing than sham-ligated rats in early trials. While sham-ligated rats consistently froze less during CS- than CS+ presentation, MI rats exhibited similar freezing to both tones for several trials before the duration of freezing during the CS- declined. While freezing to the CS- in sham-ligated rats reached the 2-second extinction criterion (Morgan and LeDoux, 1995) in fewer trials than it did for the CS+, MI rats took a similar number of trials to reach the extinction criterion for the CS+ and CS-. MI rats took a greater number of trials to reach extinction compared to sham-ligated

rats. Three-parameter exponential decay functions fit to freezing durations over successive trials did not reveal significant effects of surgical treatment or CS type on the slope or lower plateau value of freezing (Figure 25).

Blood Pressure and Heart Rate During Extinction of Conditioned Fear

As shown in Figures 26 and 27, both the CS+ and CS- tones evoked a pressor response that became attenuated over successive trials. As shown in Figures 28 and 29, both the CS+ and CS- tones also evoked an overall bradycardic response that lessened over successive trials. MI rats had lower baseline MAP than sham-ligated rats (122±3 vs. 136±4 mmHg at the beginning of the first CS+ trial) and also had a lower baseline heart rate (364±14 vs. 407±10 bpm at the beginning of the first CS+ trial). In most trials, the pressor response was biphasic, consisting of a transient larger rise that was maximal about 1.8 seconds after the the start of the tone and dissipated over a variable length of time depending on the trial. This initial rise was usually followed by a smaller, more gradual increase in MAP with variable timing. As shown in Figure 27, maximal changes in MAP were greater in sham-ligated than MI rats. The magnitude of the pressor response significantly decreased over successive trials in sham-ligated rats, but not MI rats.

Freezing Behavior During Recall Testing of Extinction Learning

The day following extinction training, MI rats exhibited greater freezing than sham-ligated rats during initial CS+ presentations, and MI rats exhibited greater freezing during initial CS+ than CS- presentations, as shown in Figure 30. Freezing during initial CS+ presentations was greater than freezing during later CS+ presentations in MI rats. In contrast, sham-ligated rats displayed great variability in freezing time during both initial and later trials. After the first 5 trials, MI and sham-ligated rats both displayed variability in freezing time. Apparent increases in freezing behavior, especially during later trials, appeared to be related to resting, rather than defensive freezing. However, our criteria for scoring freezing behavior prevented from discriminating between these two behaviors.

Blood Pressure and Heart Rate During Recall of Extinction Recall

In extinction recall testing, both the CS+ and CS- tones evoked a pressor response and a bradycardic response, both of which lessened over successive trials, as shown in Figures 31–34. As in extinction trials, baseline MAP was lower in MI rats than sham-ligated rats (119±3 vs. 134±3 mmHg at the start of the 1st CS+ presentation), and MI and sham-ligated rats had similar baseline heart rate (413±17 bpm for sham-ligated rats and 413±13 bpm for MI rats). As shown in Figure 32, maximal pressor responses were slightly attenuated over successive trials in both sham-ligated rats and MI rats, with sham-ligated rats

exhibiting a somewhat erratic pattern of response. As shown in Figure 33 and 34, MI rats exhibited profound bradycardic responses during CS presentation, which were attenuated over successive trials. In contrast, the magnitude of the bradycardic response exhibited by sham-ligated rats was inconsistent over successive trials.

Defecation Responses to Conditioned Stimuli

The number of fecal boli emitted by MI and sham rats during fear extinction training and extinction recall testing sessions is shown in Figure 35. Although MI rats exhibited a greater average number of fecal boli compared to sham-ligated rats during both the extinction and extinction recall sessions, variability precluded a statistically significant effect of MI.

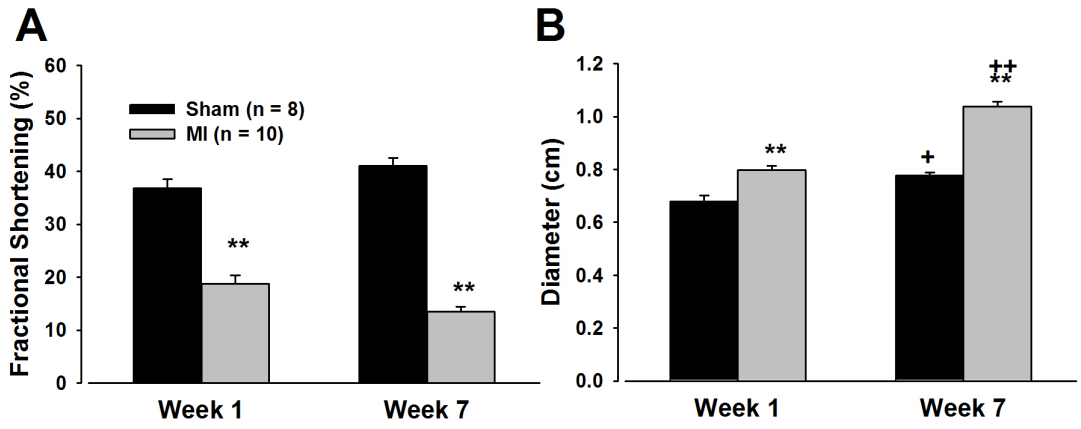

Figure 22. Left ventricular function (Specific Aim 3). Left ventricular fractional shortening (FS) and left ventricular diastolic diameter (LVDD) measured 1 and 7 weeks after MI or sham ligation surgery. Data are group means ±SEM. A two-way ANOVA with repeated measures used to assess the effect of surgery on fractional shortening over time revealed a surgery x time interaction [$F(1,18) = 21.69$, $P<0.01$] due to a tendency for FS to decrease over time in MI rats, but to increase over time in sham-operated rats. A main effect of surgery [$F(1,18) = 283.01$, $P<0.01$] was also observed, due to significantly decreased FS in MI rats vs. sham-operated rats. A separate two-way ANOVA with repeated measures examining the effect of MI on left ventricular diastolic diameter over time revealed a surgery x time interaction [$F(1,18) = 7.11$, $P<0.05$] due to a greater increase in diastolic diameter over time in MI rats than sham-operated rats. The analysis also revealed a main effect of surgery [$F(1,18) = 126.78$, $P<0.01$] due to increased diastolic diameter in MI rats vs. sham-operated rats. A main effect of time [$F(1, 18) = 31.09$, $P<0.01$] was also observed.

Between- and within-group comparisons were made with Tukey's *post hoc* tests.

**P<0.01 vs. sham, $^{++}$P<0.01 vs. week 1, $^{+}$P<0.05 vs. week 1.

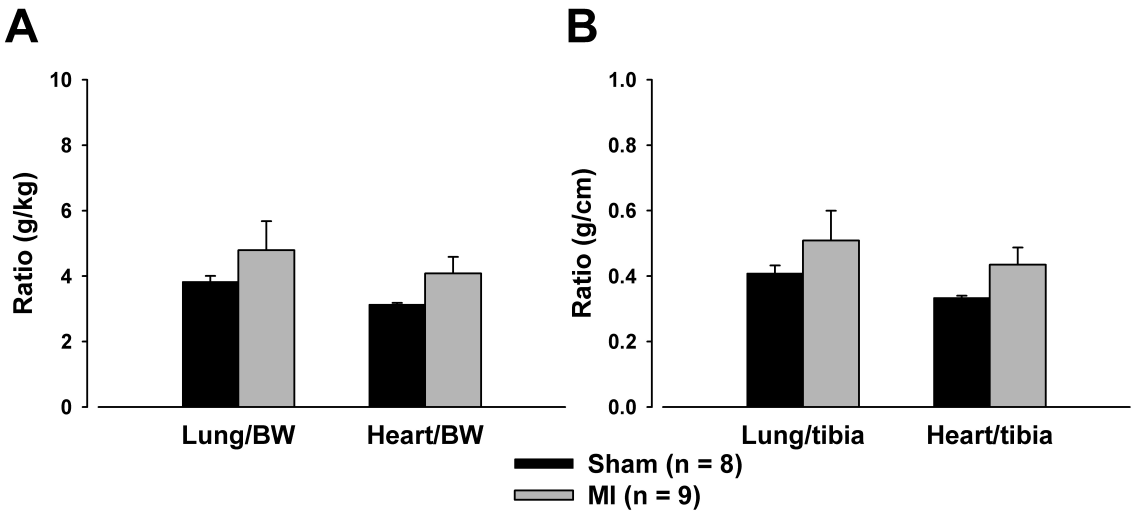

Figure 23. Terminal measures of congestion and remodeling (Specific Aim 3). Ratios of lung and heart weight to body weight (A) and to tibia length (B), measured 13 weeks after MI or sham ligation surgery. Values are group mean ± SEM. Student's t-test revealed no significant effect of either lung weight when normalized to body weight (P=0.33) or tibia length (P=0.33) or heart weight when normalized to either body weight (P=0.10) or tibia length (P=0.09).

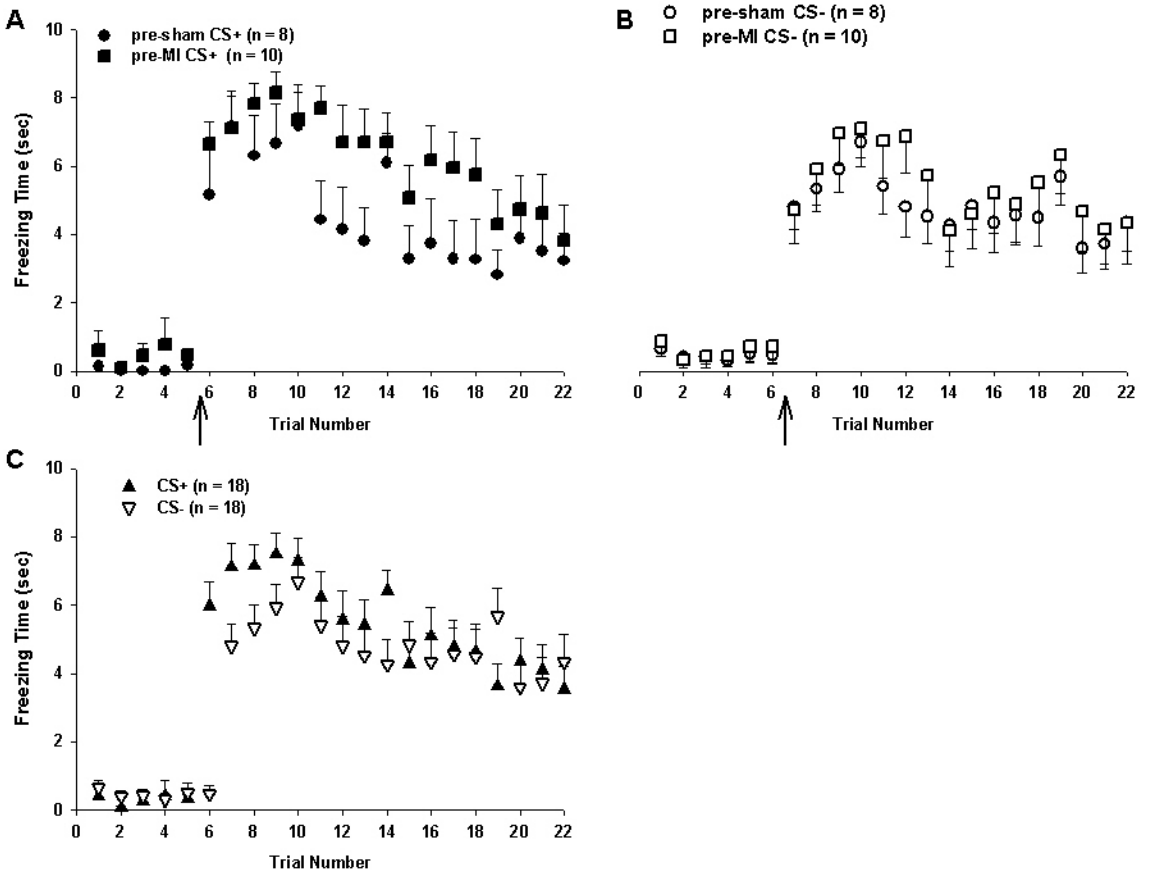

Figure 24. Freezing responses during fear conditioning. Values are displayed as group mean ±SEM. Arrow represents first trial block containing tone-shock pairings. Freezing during CS+ presentations is shown in A, and freezing during CS- presentations is shown in B. Freezing during CS+ or CS- (with surgical groups pooled) is shown in C. A 3-way ANOVA with repeated measures examined the effect of future surgical treatment, CS type, and trial block on freezing during tone presentation. Analysis revealed a significant interaction of MI and trial number [$F(21,336) = 2.70$, $P<0.01$] due to decreased freezing during intermediate trials in rats assigned to receive MI surgery (pre-MI). A significant interaction of CS type and trial number was also observed

[F(21,336) = 31.06, P<0.01] due to greater freezing during CS+ than CS- in the initial tone-shock pairings. Analysis revealed main effects of CS type [F(1,16) = 39.12, P<0.01] due to greater freezing during CS+ tones, as well as a main effect of time [F(21,336) = 43.35, P<0.01] due to a dramatic increase in freezing once tone-shock pairings were initiated.

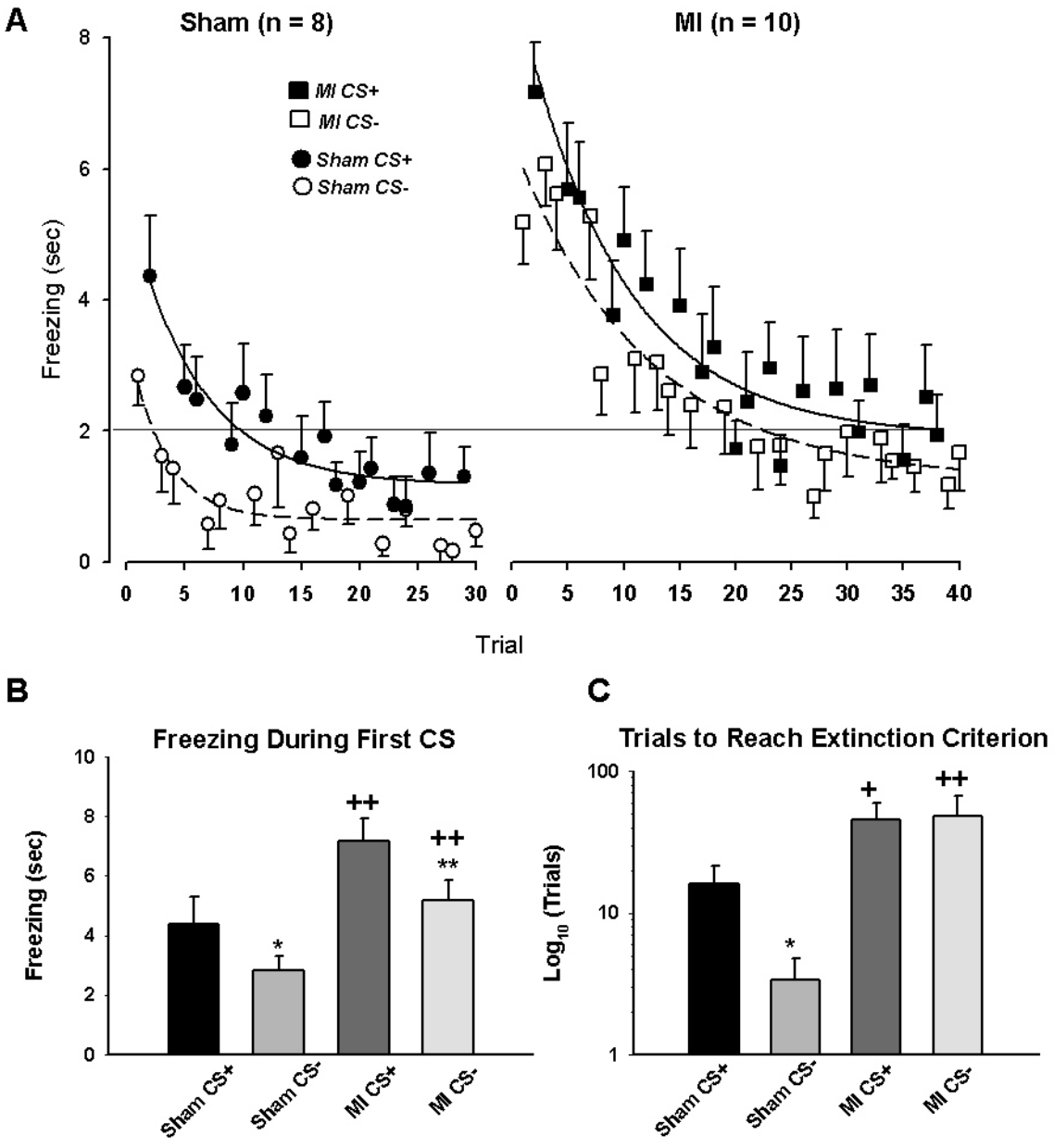

Figure 25. Freezing responses during fear extinction. Values are displayed as group means ±SEM. Freezing times during CS+ and CS- (in the order of presentation) are shown in A. Curves in each plot represent 3-parameter exponential decay functions, fit to each data set with the start value fixed at the first-trial value. Two-way ANOVA with repeated measures to assess the effects

of surgical treatment and CS type on the lower plateau and exponential slope in the exponential decay function did not reveal significant main effects or interactions. Sham-ligated rats reached a lower plateau of 0.78±0.31 seconds and 0.56±0.16 seconds during CS+ and CS- trials, respectively, and MI rats reached a lower pleateau of 0.89±0.27 seconds and 1.23+0.21 during CS+ and CS- trials, respectivity. Sham-ligated rats displayed an exponential slope of 0.16±0.5 and 0.37±0.9 during CS+ and CS- trials, respectively, and MI rats displayed an exponential slop of 0.9 ±0.02 and 0.1±0.02 during CS+ and CS- trials, respectively.

3-way ANOVA with repeated measures to assess the effects of surgical treatment and CS type on freezing during successive tone presentations revealed a significant interaction of surgery and trial number [$F(9,144) = 3.35$, $P<0.01$], due to a decrease in freezing over time that was greater in MI rats compared to shams. Analysis also revealed a CS type x time interaction [$F(9,144) = 2.02$, $P<0.05$], since freezing was greater during CS+ than CS- in initial tones, but not later tones. A significant main effect of surgery [$F(1,16) = 5.81$, $P<0.05$] was observed due to greater freezing times in MI rats compared to shams. A significant main effect of trial number [$F(9,144) = 34.50$, $P<0.01$] was also observed, since freezing decreased over successive trials.

Freezing time during the very first tone is shown in B. Two-way ANOVA with repeated measures revealed a main effect of surgery [$F(1,16) = 7.36$, $P<0.05$] due to increased increased freezing in MI rats vs. sham-ligated rats and a main effect of CS type [$F(1,16) = 22.4$, $P<0.01$] due to increased freezing during CS+ vs. CS- in both MI and sham-ligated rats. The number of CS+ and CS- trials to reach the extinction criterion (2 seconds) is shown in C. Two-way ANOVA (log-transformed data to achieve homogeneity of variance) with repeated measures revealed a main effect of surgery [$F(1,16) = 4.82$, $P<0.05$) due to a greater number of trials to reach extinction in MI rats vs. sham-ligated rats. **$P<0.01$ vs. CS+, *$P<0.05$ vs. CS+, $^{++}P<0.01$ vs. sham, $^{+}P<0.01$ vs. sham.

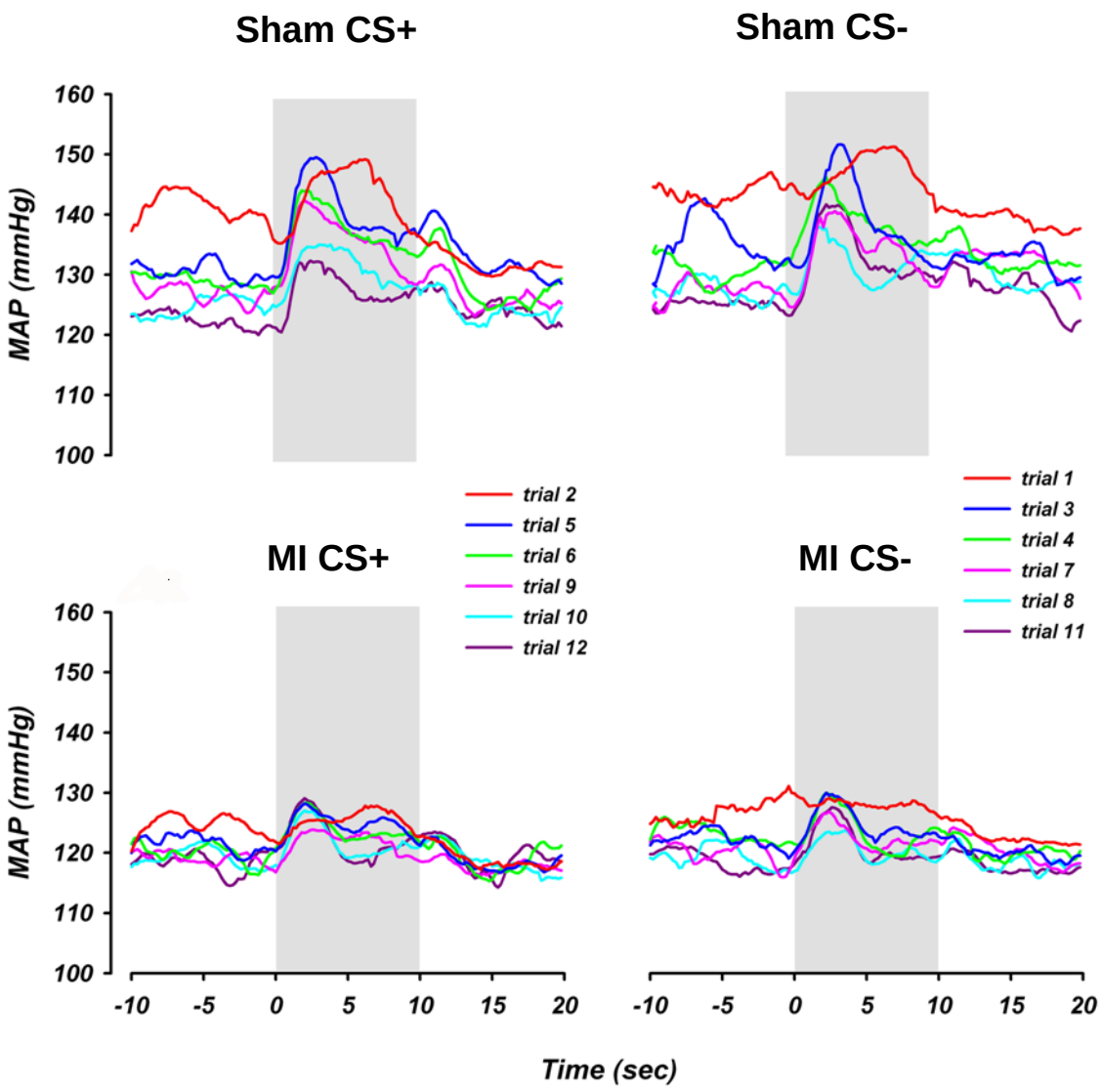

Figure 26. Blood pressure responses during extinction. Mean arterial pressure (MAP) averaged over 0.2-second intervals 10 seconds before, during, and after tone presentation. Gray box indicates time of tone presentation. Plots are group means.

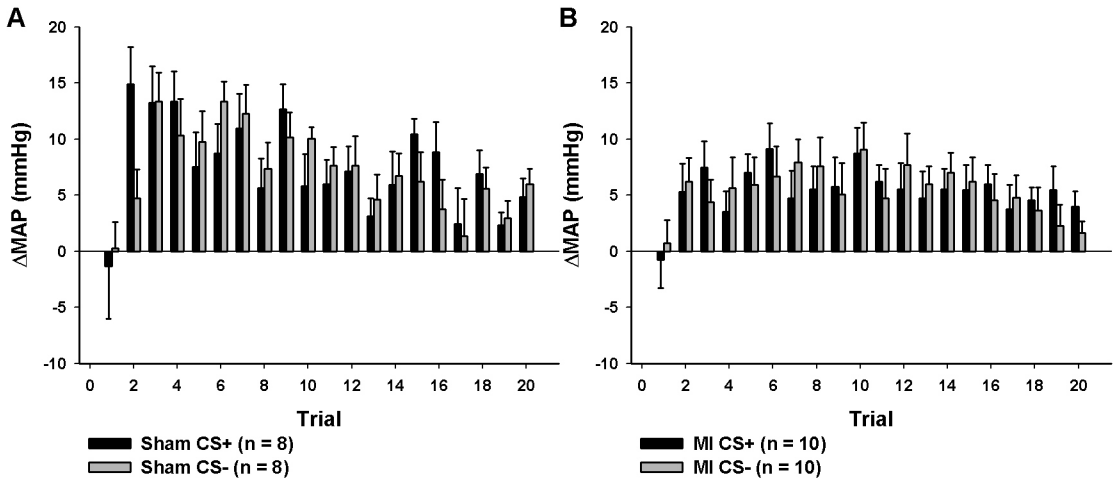

Figure 27. Change in blood pressure in extinction. Change in mean arterial pressure (MAP) at time of maximal pressor response (1.8 sec into tone) vs. baseline during successive CS presentations in sham-ligated rats (A) and MI rats (B). Three-way ANOVA with repeated measures examining the effects of surgical treatment and CS type on change in MAP over successive trials revealed a surgery x trial interaction [$F(19,304) = 2.38$, $P<0.01$] due to a greater attenuation of pressor responses over successive trials in sham-ligated rats compared to MI rats. Analysis also revealed a main effect of trial number [$F(19,304) = 7.15$, $P<0.01$].

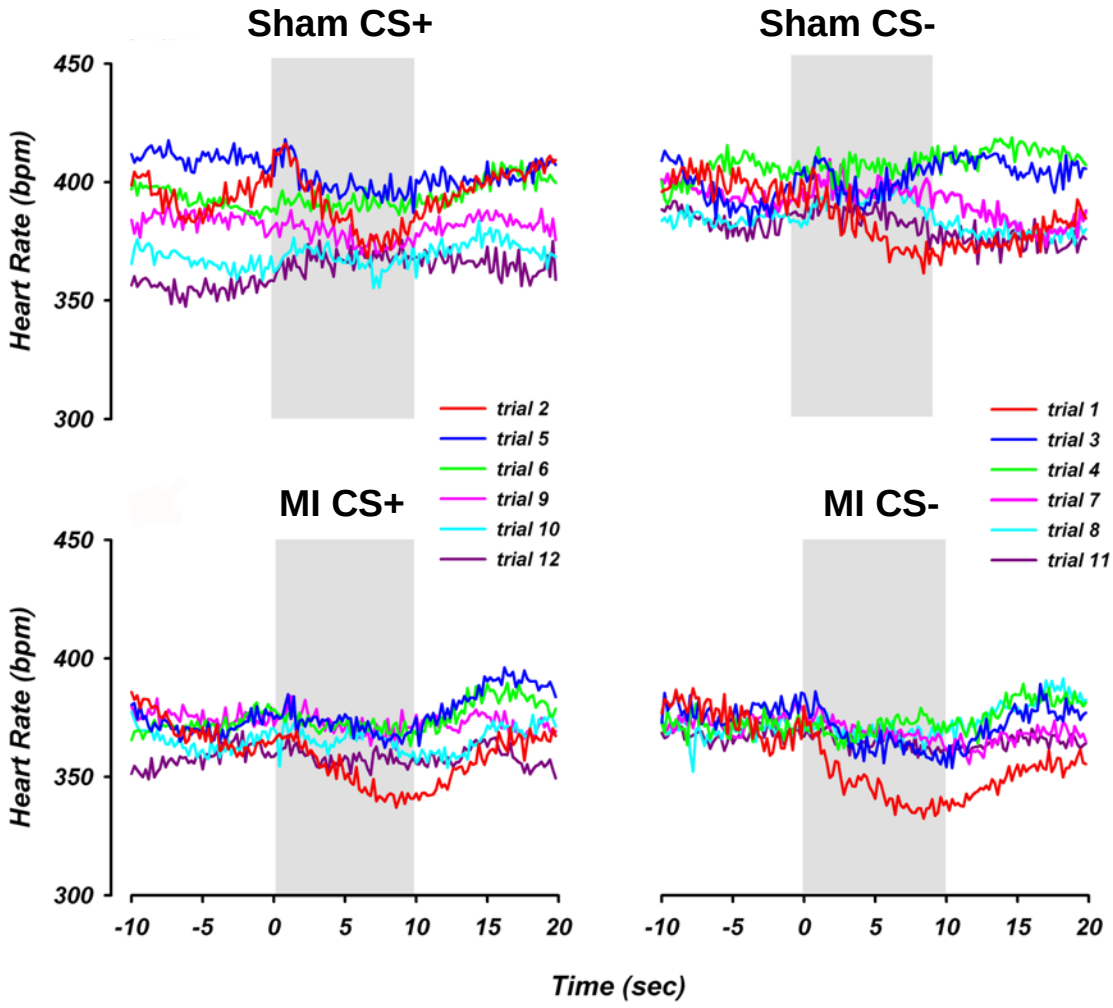

Figure 28. Heart rate responses during extinction. Heart rate (HR) averaged over 0.2-second intervals 10 seconds before, during, and after tone presentation. Gray box indicates time of tone presentation. Plots are group means.

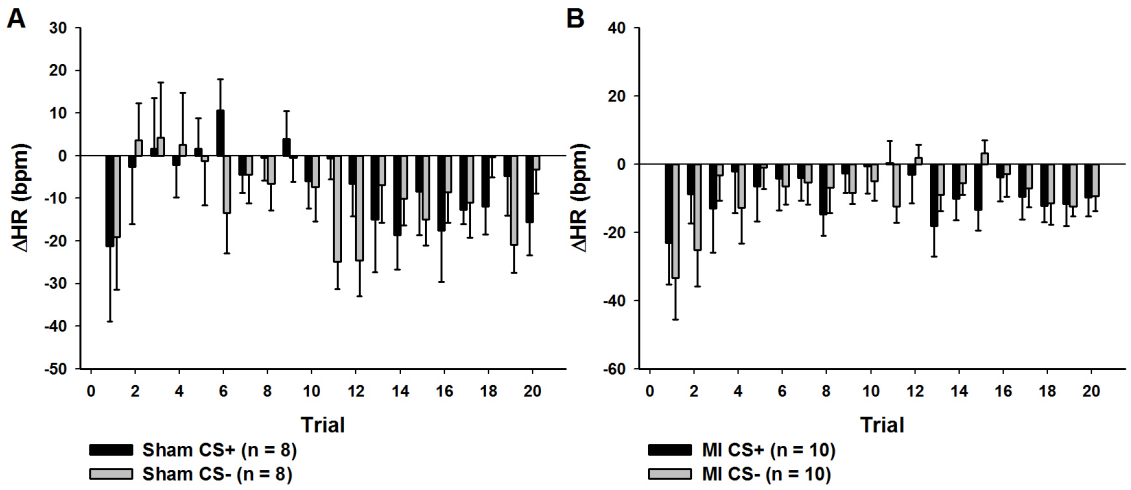

Figure 29. Change in heart rate during extinction. Change in heart rate during tone presentation in sham-ligated rats (left) and MI rats (right). Values are means ± SEM. Three-way ANOVA with repeated measures assessing the effects of surgical treatment and trial type on change in heart rate over successive CS presentations revealed a main effect of trial number [$F(19,304) = 2.69$, $P<0.01$].

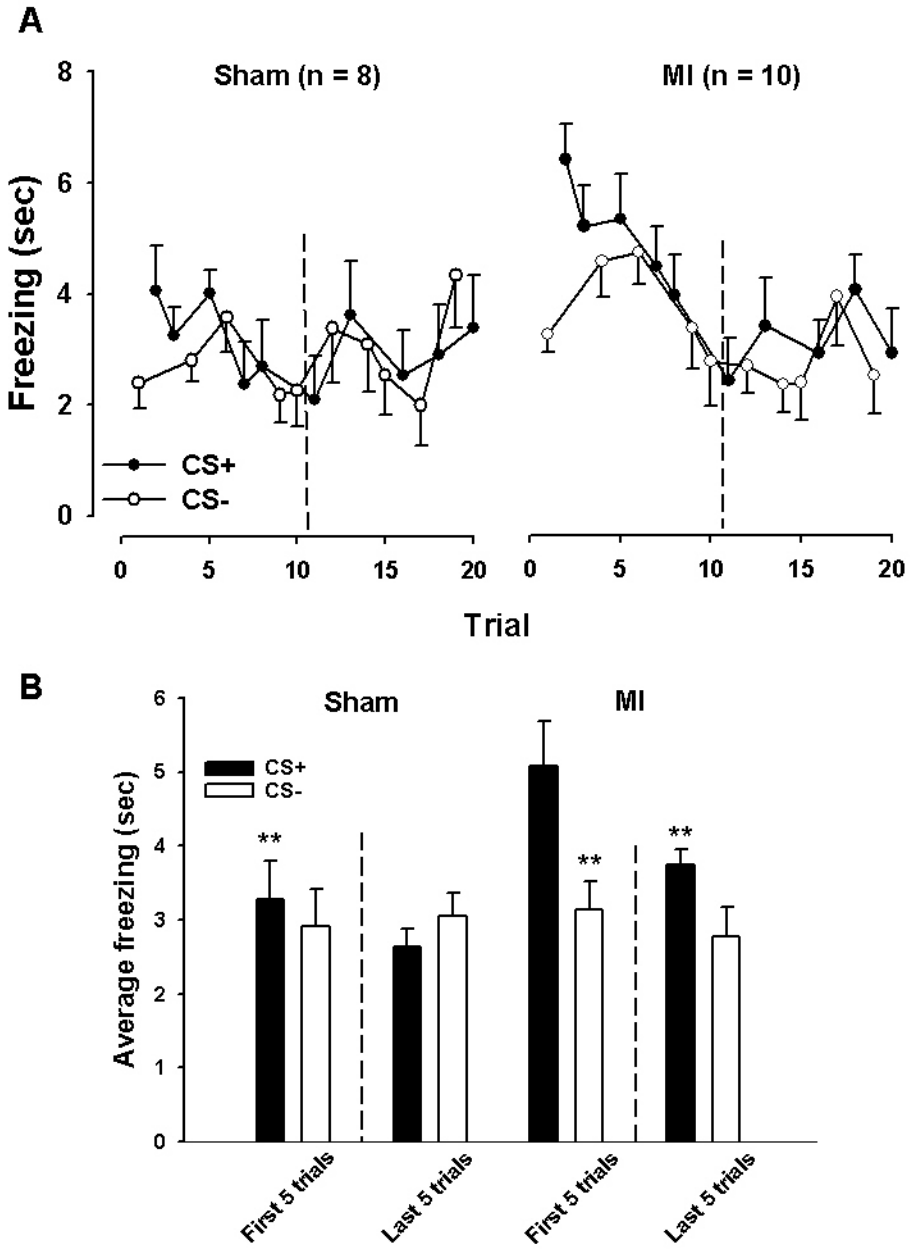

Figure 30. Freezing responses during extinction recall. Values are displayed as group mean ±SEM. Freezing during all trials (in order of presentation) is shown in A. Dashed line is between 5th and 6th trial of each type. Two-way ANOVA with repeated measures assessing the effect of MI and tone type on freezing during the first 5 vs. last 5 trials revealed a surgery x CS type interaction

[F(1,16) = 5.37, P<0.05] due to increased freezing during CS+ in MI rats but not sham-ligated rats, as well as CS type by time interaction [(1,16) = 6.55, P<0.05] due to greater freezing to CS+ in early trials, but not later trials. The analysis also revealed main effects of surgery [F(1,16) = 10.13, P<0.05] due to greater freezing in MI rats, as well as a main effect of time [F(1,16) = 5.77, P<0.05] due to greater freezing in early trials vs. later trials. **P<0.01 vs. MI CS+ in 1st 5 trials.

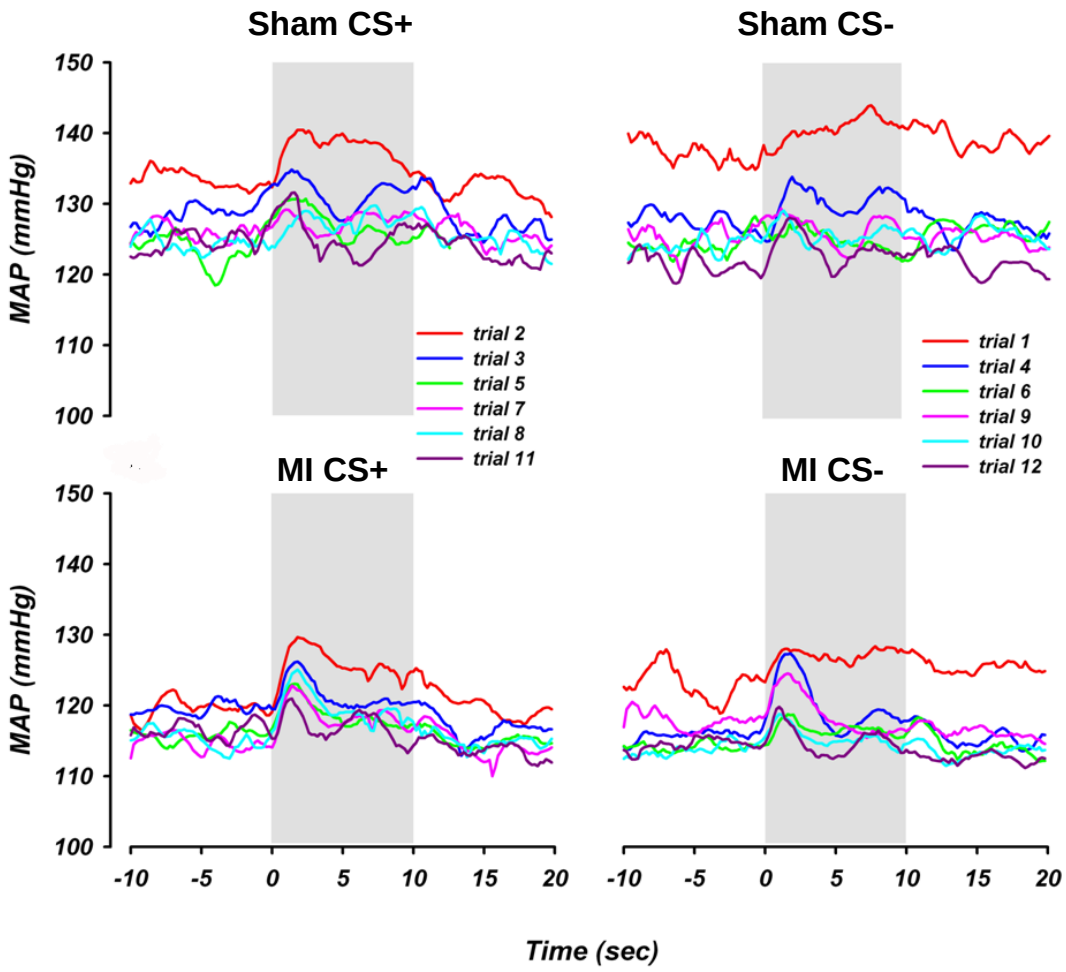

Figure 31. Blood pressure responses during extinction recall. Mean arterial pressure (MAP) averaged over 0.2-second intervals 10 seconds before, during, and after tone presentation. Gray box indicates time of tone presentation. Plots are group means.

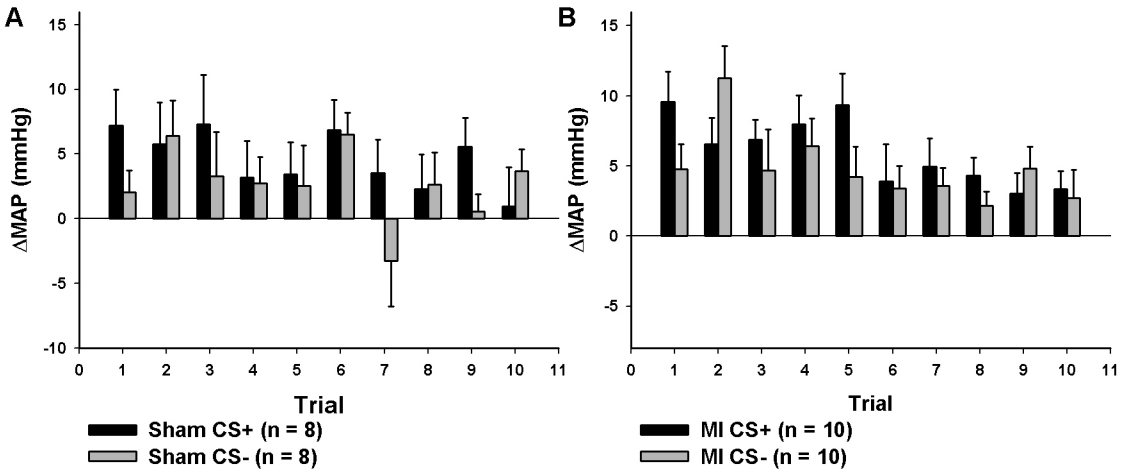

Figure 32. Change in blood pressure in extinction recall. Change in mean arterial pressure (MAP) at time of maximal pressor response (1.8 sec into tone) vs. baseline during successive CS presentations in sham-ligated rats (A) and MI rats (B). Three-way ANOVA examining the effects of surgical treatment and CS type on change in MAP over successive trials revealed a main effect of trial number [$F(9,135) = 3.20$, $P<0.01$] due to attenuation of pressor responses over successive trials. Analysis also revealed a main effect of CS type [$F(9,135) = 8.73$, $P<0.01$]. However, a follow-up 2-way ANOVA examining the effect of CS type on change in MAP over successive trials (with surgical groups pooled) revealed a main effect of trial number without an effect of CS type. .

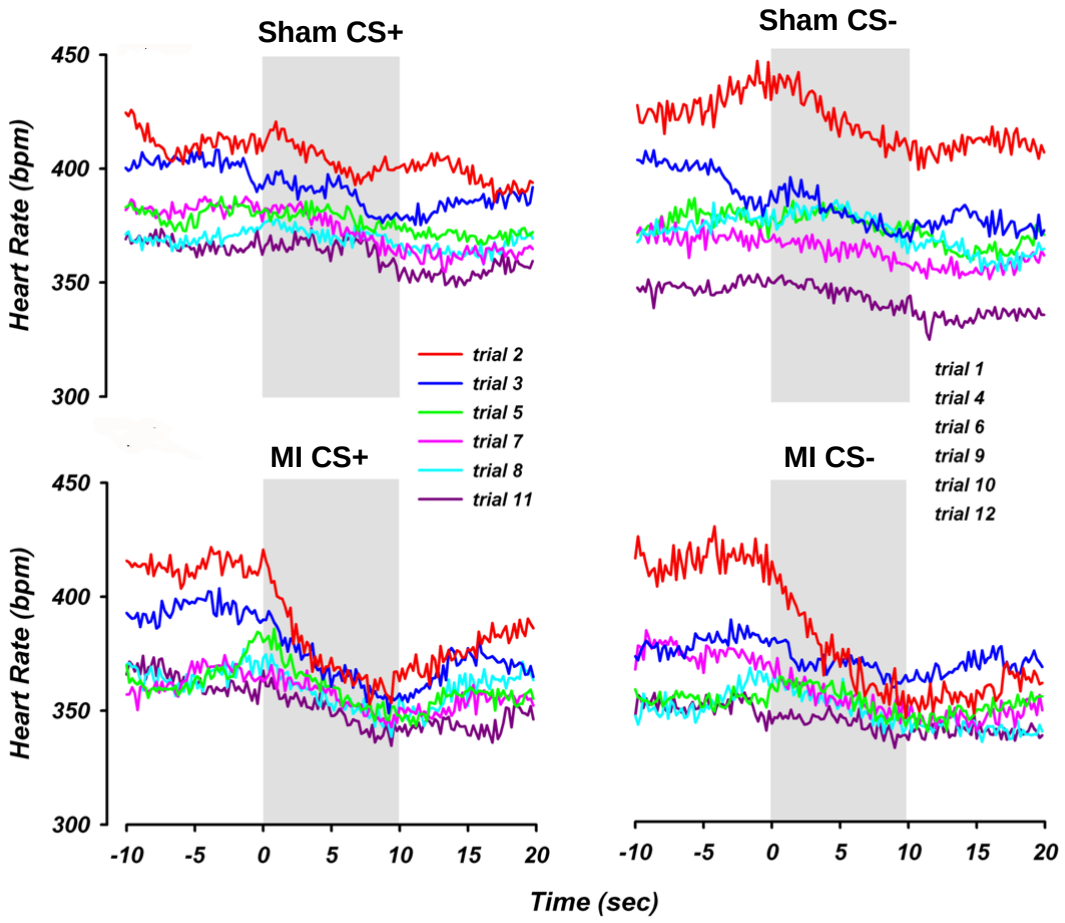

Figure 33. Heart rate responses during extinction recall. Heart rate (HR) averaged over 0.2-second intervals 10 seconds before, during, and after tone presentation. Gray box indicates tone presentation. Plots are group means.

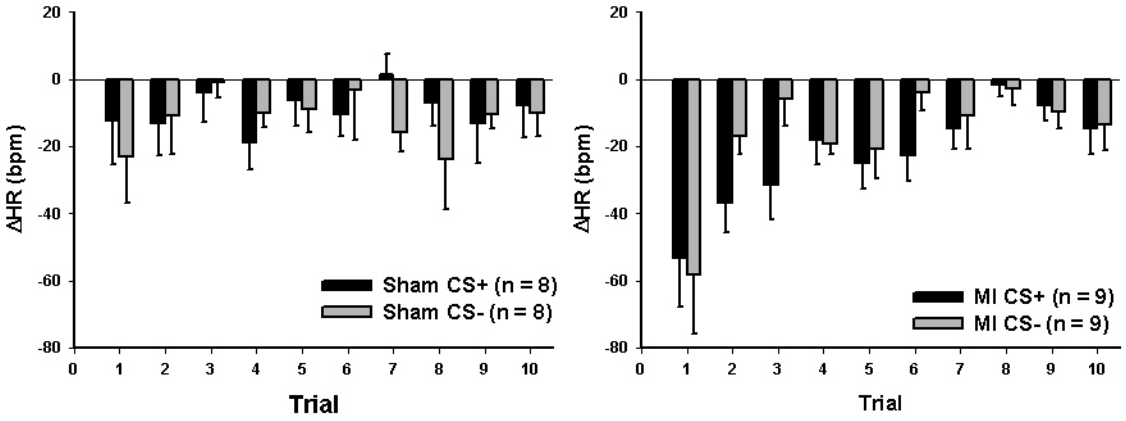

Figure 34. Change in heart rate during extinction recall. Change in heart rate during tone presentation in sham-ligated rats (left) and MI rats (right). Values are means ± SEM. Three-way ANOVA with repeated measures assessing the effects of surgical treatment and trial type on change in heart rate over successive CS presentations revealed a surgery x time interaction [$F(9,135) = 2.42$, $P<0.05$] due to an attenuation in the bradycardic response over successive trials in MI rats, but not sham-ligated rats. Analysis also revealed a main effect of trial number [$F(9,135) = 3.69$, $P<0.01$].

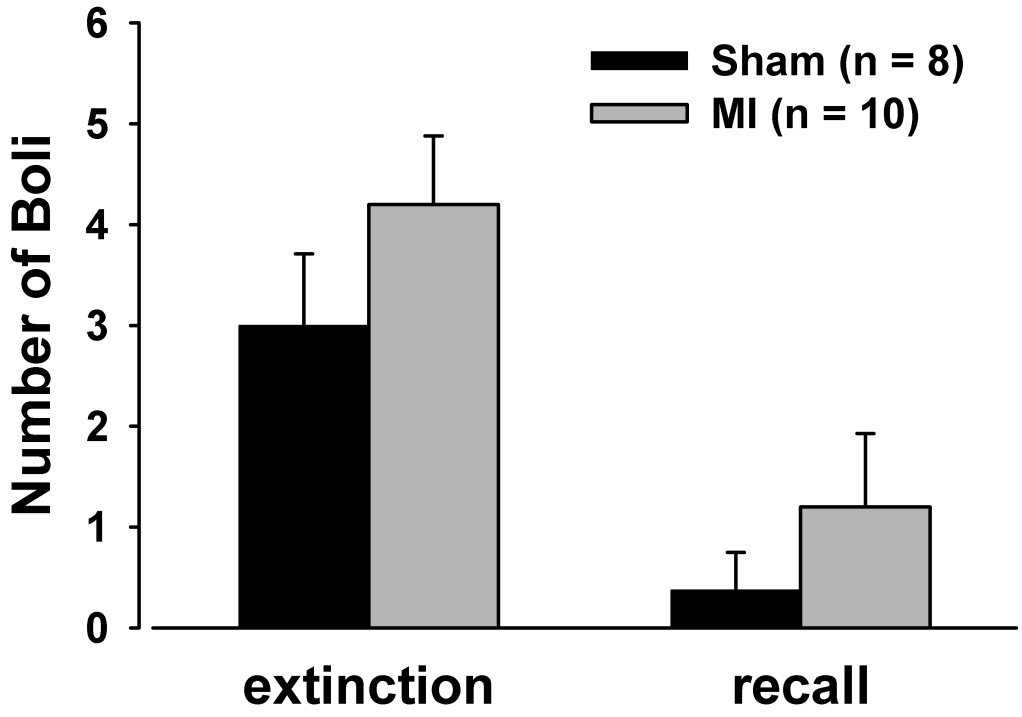

Figure 35. Defecation response during extinction and extinction recall. Student's t-test did not reveal significant differences between MI and sham-ligated rats in either extinction or recall.

Discussion

This study determined the effect of myocardial infarction (MI) on behavioral and cardiovascular assessments of conditioned fear extinction. Prior to MI or sham-ligation surgery, rats acquired freezing responses to tones paired with footshock (CS+) and also exhibited freezing during a different tone that was never paired with footshock (CS-). Seven weeks after MI or sham ligation surgery, rats subjected to MI displayed enhanced freezing responses to initial CS+ and CS- presentations compared to sham-ligated rats. Sham-ligated rats took fewer CS- trials to extinguish freezing responses than CS+ trials, while MI rats took about the same number of CS+ and CS- trials to reach the extinction criterion. MI rats also took more trials to reach extinction than sham-ligated rats, regardless of CS type. The following day, sham-ligated rats displayed a minimal amount of freezing during both CS+ and CS- presentations. In contrast, MI rats displayed greater freezing than sham-ligated rats during intial CS+ presentations, and MI rats also froze more during initial CS+ than CS- presentations. In the second half of the testing session, both MI and sham-ligated rats displayed variability in freezing time. Both MI and sham-ligated rats exhibited a biphasic pressor response and bradycardia during CS+ and CS- presentation in both testing sessions that became attenuated over successive trials.

As in previous studies, echocardiography revealed dramatically decreased fractional shortening and increased left ventricular diastolic diameter in MI rats compared to shams, indicating left ventricular dysfunction. Terminal measures of

congestion and remodeling were made 13 weeks after surgery in this cohort of rats, and MI rats exhibited trends for elevated lung and heart wet weights, but these elevations were not significant compared to sham-ligated rats. This apparent lack of edema and remodeling, respectively, could be due to the different time point of measurement and the fact that some of the most severely infarcted rats were not included in the formal study (to avoid mortality associated with telemetry probe implantation before extinction and recall testing). One severely infarcted MI rat died overnight following the recall testing, thus precluding terminal measurements in this rat.

After the first 6 tone-shock pairings of the conditioning trials, freezing duration began to decline. One explanation for this apparent drop in freezing is that some rats began engaging in vigilant scanning behavior. Vigilant scanning consists of side-to-side head movements without locomotion and is a form of risk assessment (i.e. scanning the environment for threats). While vigilant scanning indicates a defensive response, it is difficult to quantify and cannot be counted as freezing (Choy et al., 2011). Another possible explanation for this drop in freezing is that some rats assumed an unusual posture after a few shock pairings. Specifically, they stood on one foot and leaned against the front wall of the apparatus, presumably in attempt to avoid or minimize the shock. Rats that assumed this position often shifted or wobbled during tone presentation, likely due to muscle fatigue, and thus their behavior could not be counted as freezing, even if it was defensive in nature. Although pre-MI rats exhibited more freezing

than sham-ligated rats during the middle conditioning trials (in response to both CS types), freezing scores in both pre-MI and pre-sham converged by the final trial, suggesting that rats assigned to sham and MI surgery acquired similar CS-US associations.

Our observations of increased freezing in MI rats during initial CS+ presentations suggest rats are more responsive to learned stressors after MI. When freezing was examined during all trials in the order of presentation, MI rats displayed a delay in the attenuation of freezing compared to shams, suggesting a deficit in the acquisition of extinction. Since the IL has been shown to be necessary for both the acquisition and recall of extinction, our results are consistent with dysfunction in the IL cortex. In contrast to the fast decline in freezing among sham-operated rats in initial CS- presentations, MI rats continued to freeze in response to CS- presentations for more trials. Since both tones were presented in the same context (with short inter-trial intervals), MI rats may have developed an association between the CS+ and CS- and a deficit in their ability to discriminate between cues signaling a threat and cues signaling safety. A deficit in accurately assessing stimuli as threatening or safe is a characteristic of human depression and anxiety (Britton et al., 2011).

Both MI and sham-ligated rats displayed overall pressor and bradycardic responses to initial CS+ and CS- presentations in extinction trials, indicating that the rats retained their memory of the conditioning throughout the 2-month post-surgical period. The fact that both blood pressure and heart rate responses

lessened over repeated trials indicates extinction of conditioned autonomic responses. However, MI rats had smaller pressor responses than sham-operated rats, despite evidence of their increased emotional response to the tones. Pressor responses to fear conditioned stimuli have been shown to be dependent on increased cardiac output (Li et al., 1998). Thus, the smaller effect in MI rats was likely due to their inability to generate significant changes in cardiac output in response to stress. Desensitization of cardiac βARs, evidenced by decreased inotropic responses to isoproterenol in rats after MI (Sethi and Dhalla, 1995), may contribute to this blunted response, as may decreased vagal tone (Cohen and Zohar, 2004). If the CS elicits greater sympathetic activation in MI rats, compromised contractility apparently prevents these rats from generating a commensurate blood pressure response.

During extinction recall testing, the increased freezing we observed in MI rats during initial CS presentations suggests a deficit in retention of extinction learning. Given that previous studies have implicated the IL in both the acquisition and retention of extinction learning (Mueller et al., 2008; Sierra-Mercado et al., 2011), our results support the possibility that aberrant signaling in the IL during stress may underlie these deficits in fear extinction. As in extinction trials, both MI and sham-ligated rats displayed a pressor response accompanied by a decrease in heart rate during extinction recall testing. MI rats displayed profound pressor and bradycardic responses that became attenuated over successive trials. In contrast, sham-ligated rats displayed a somewhat random

pattern of pressor and bradycardic responses, especially in later trials. These inconsistent blood pressure and heart rate responses in later trials may reflect a lesser defensive response and more exploration during this session in sham-operated rats, consistent with effective recall of extinction training. Given that MI rats displayed blunted pressor responses to CS presentation (in both sessions) compared to sham-ligated rats, it is surprising that MI rats generated robust and consistent bradycardic responses to CS presentation, especially in the extinction recall session. It has been demonstrated previously that presentation of a CS+ elicits simultaneous activation of both the sympathetic and parasympathetic nervous systems (Frysztak and Neafsey, 1994). Thus, it is possible that the enhanced bradycardia we observed in MI rats may be due to greater desensitization of adrenergic receptors relative to muscarinic receptors.

The number of fecal boli emitted during extinction and recall were counted at the end of each session. Like freezing, defecation is part of the defense response mediated by the midbrain periaqueductal gray (PAG), as electrical stimulation of this region elicits these behaviors (Sudre et al., 1993). MI rats tended to emit more fecal boli than shams in both sessions, but this increase was not statistically significant. However, significant differences could be masked by likely decreases in food intake in MI rats, as heart failure patients often display reduced food intake and cachexia. Angiotensin II is elevated in human and experimental heart failure (McAlpine et al., 1988; Yamagishi et al., 1993), and may contribute to appetite suppression in heart failure, as a recent study

demonstrated that systemic angiotensin II causes a concomitant decrease in food intake and a decrease in expression of orexin and neuropeptide Y (two neuropeptides that positively modulate appetite) in the hypothalamus (Yoshida et al., 2012; Yoshida et al., 2012). Though we did not measure levels of angiotensin II in our rats, it is tempting to speculate that increased angiotensisin II is contributing to a decrease in appetite. This decreasd appetite, in turn, would lead to less defecation in MI rats, potentially masking a significant increase in defecation during extinction and extinction recall.

In many studies of fear extinction, CS trials are presented only until each animal reaches the extinction criterion (e.g. freezing during only 25% of a tone), and thus not all animals undergo the same number of extinction trials (Morgan and LeDoux, 1995). However, since this was the first study to investigate fear extinction after MI, as well as the first fear extinction study in our lab, we utilized a large number of extinction trials (20 of each CS type) to ensure adequate extinction in all rats. It is possible that this large number of trials may have over-extinguished the CS-US association. In the second half of the extinction recall session (and earlier trials for sham-ligated rats), freezing time durations were increased in some trials. Though not easily quantifiable, this later apparent increase in freezing may not necessarily reflect the stereotyped defensive freezing behavior seen in conditioning and in initial extinction trials. Rather, this later immobility may reflect full acclimation to the apparatus and a lack of

response to the CS. Thus, therefore it is possible that this over-training during extinction could be partially masking additional effects of MI on extinction recall.

Taken together, these results indicate that MI rats have exaggerated responses to fear-associated stimuli, that MI rats have deficits in discrimination between cues indicating threat and safety, and that MI rats have deficits in the extinction of these heightened responses. These heightened responses in MI rats are reminiscent of some of the symptoms of post-traumatic stress disorder (PTSD), namely hypervigilance and persistence of anxiety responses to trauma-related cues. Imaging studies of PTSD patients have demonstrated reduced activity in the PFC and concomitant increased activity in the amygdala in response to trauma-related cues (Bremner et al., 1999). Previous studies have also shown that inactivation of the IL cortex results in deficits in the acquisition and recall of fear extinction (Sierra-Mercado et al., 2011). In the studies reported in Chapter 3, we observed an increase in IL metabolic activity at baseline, but a decrease in activity in response to locus coeruleus (LC) stimulation, indicating aberrant responses to cortical NE released during stress. Therefore, decreased IL activity in response to acute stress-induced NE release may contribute to deficits in extinction observed in MI rats in this study.

It is well documented that PTSD patients have hyperresponsive noradrenergic systems, as exaggerated norepinephrine release induced by inhibition of α_2AR autoreceptors with yohimbine has been shown to result in increased anxiety in PTSD patients, as well as decreased blood flow to the PFC,

though it is unclear whether systemic yohimbine is acting primarily on pre-synatpic or post-synatpic α_2ARs (Bremner et al., 1997). Additionally, PTSD patients exhibit elevated levels of NE in the CNS, but have normal levels of plasma NE, in the unstressed state (Geracioti et al., 2001). It has also been shown that lesion of ascending LC projections in rats results in impaired conditioning to auditory cues (Selden et al., 1990), as well as faster extinction of conditioned fear (Tsaltas et al., 1984).

Neurons of the LC have been shown to be activated in response to both a CS+ and CS- presentation (Campeau et al., 1997). It has also been shown that LC neurons fire more when contingencies are switched, as in a reward prediction task (Bouret and Sara, 2004), indicating that the LC is activated by novelty. We observed that MI rats displayed impaired discrimination between CS+ and CS- presentations during initial trials, the trials in which the LC would be most activated. Our studies in Chapter 3 have shown that when the LC is activated by electrical stimulation, mPFC activity is decreased in MI rats. This inhibition of mPFC activity could result in inappropriate salience attribution in MI rats, i.e. increasing the salience of the CS- tone, leading to less discrimination in early trials. Previous studies have shown that pyramidal neurons of the mPFC to be inhibited by NE in an α_2AR-dependent manner (Wang et al., 2010). We observed a decrease in β_1AR density in the IL in MI rats. Thus, this decrease in β_1ARs, as well as a possible (but so far untested) increase in post-synatpic α_2ARs, may mediate, in part, the inhibition of the IL during LC activation. In

conclusion, the changes we observed in fear responses in MI rats support our hypothesis that MI induces plasticity in brain regions governing stress responses, particularly in the noradrenergic system, and these changes likely contribute to the development of anxiety disorders after MI.

CHAPTER 6

GENERAL DISCUSSION

The studies in this dissertation were designed to elucidate the central nervous system changes underlying the development of anxiety and arrhythmia susceptibility after myocardial infarction (MI). The studies presented in this dissertation are the first to examine changes in central noradrenergic responses and receptors after MI, as well as the first to examine changes in the expression and extinction of conditioned fear after MI in the rat. Identification of the discrete brain regions and neurotransmitter systems underlying the development of post-MI anxiety is essential for the development of more targeted therapies to improve and extend the lives of this vulnerable subset of patients.

Here, we demonstrate for the first time that stimulation of the locus coeruleus (LC) in a pattern mimicking a mild stressor induces the generation of cardiac arrhythmias in rats subjected to MI. Given that sudden cardiac death in MI patients is often precipitated by emotional stressors, and that the LC is activated during stress and novelty, this finding provides a potential anatomical substrate for emotionally-induced arrhythmia susceptibility. Increased stimulation of cardiac adrenergic receptors due to sympathetic nervous system activation has been implicated in the generation arrhythmias after MI (Du et al., 1999; Li et al., 2004). Activation of the LC has been shown to increase sympathetic

activation (Drolet and Gauthier, 1985). The mechanism of this sympathetic activation needs clarification since the projection of the LC to the rostral ventrolateral medulla is thought to be inhibitory, but may involve direct projections of the LC to preganglionic neurons of the spinal cord (Proudfit and Clark, 1991). However, norepinephrine (NE) release in the forebrain is also increased after MI (Aggarwal et al., 2002). Thus, it is possbile that the actions of NE on cortical and subcortical loci of cardiovascular and emotional control may also contribute to emotionally-induced arrhythmia susceptibility after MI, given that central β-adrenergic receptor (βAR) blockade has been shown to delay coronary ischemia-induced arrhythmia generation in psychologically stressed pigs (Parker et al., 1990).

The studies presented in this dissertation support the view that chronic LC activation after MI may contribute to changes in the adrenergic receptor profile in the infralimbic (IL) cortex, thereby modulating baseline activity and influencing prefrontal cortical (PFC) metabolic activation in response to LC stimulation. Previous studies have demonstrated chronic increases in metabolic activity of the LC after MI in rats (Patel et al., 1993; Vahid-Ansari and Leenen, 1998). The activation of the LC has been shown to result in increases in forebrain NE (Florin-Lechner et al., 1996; Berridge and Abercrombie, 1999). Chronic increases in synaptic NE (as with chronic desipramine treatment) have been shown to result in decreased βAR density in multiple forebrain regions (Ordway et al., 1988). Here, we observed decreased β_1AR density in the IL cortex, basolateral complex

(BLAc) of the amygdala, and lateral amygdala (LA) of MI rats. This decrease in β_1AR density may be mediated by a chronic increase in forebrain NE in MI rats.

Consequently, this decrease in β_1AR density in MI rats may influence neuronal responses to subsequent LC activation. In the studies presented in Chapter 3, we electrically stimulated the LC in a pattern that mimics a mild stressor and that has been shown to induce NE release in the mPFC (Aston-Jones and Bloom, 1981; Florin-Lechner et al., 1996). We found that LC stimulation had little effect on metabolic activity in the PFC of sham-ligated rats, but resulted in a significant decrease in activity in the infralimbic, prelimbic, and orbitofrontal cortices of MI rats (with the most profound effect in the IL mPFC). These results suggest that LC stimulation-induced NE release has a profound inhibitory effect in the IL after MI, and downregulation of β_1ARs in this region as a result of chronic LC activation may contribute to this inhibition by decreasing the level of β_1AR-mediated excitation of pyramidal neurons. As depicted in Figure 36, long-term changes in the levels of other adrenergic receptors (such as an increase in $\alpha_2$adrenergic receptors, since these receptors are coupled to Gi), may also contribute to the inhibition of PFC activity in response to LC stimulation, though as of yet we have not examined changes in α-adrenergic receptors.

In addition to LC-stimulation induced changes in metabolic activity in the prefrontal cortex, we also observed baseline increases in metabolic activity in the LA and decreases in the BLAc after MI. Previous studies investigating changes in the amygdala after MI have reported apoptosis in whole amygdala

homogenates 2–7 days after MI (Kaloustian et al., 2008; Wann et al., 2007). Other reports have demonstrated gliosis and neuronal degeneration in the BLA of MI rats, but with no change in the number of GABAergic neurons (Lee et al., 2010; Bae et al., 2010). These results suggest that MI may precipitate the death of projection neurons and subsequent inflammatory processes in the BLA that may have contributed to the decreased metabolic activity we observed in the BLA of MI rats.

The studies in this dissertation are the first to report deficits in conditioned fear extinction after MI. These findings are particularly relevant, given that we observed a reduction in LC-stimulation induced metabolic activity and reduced βAR density in the IL mPFC, which has been implicated in the acquisition and retention of conditioned fear extinction (Sierra-Mercado et al., 2011). MI rats exhibited more freezing behavior in response to initial CS presentations than sham-ligated rats, and MI rats took more trials to reach extinction criteria. These results suggest that after MI, rats have an exaggerated response to fear-related stimuli and also exhibit a deficit in extinction of these responses. The following day, MI rats again displayed increased freezing during CS presentation compared to sham-ligated rats, indicating a deficit in retention of extinction learning. These deficits in extinction are consistent with dysfunction in the IL cortex, and are also consistent with deficits in extinction displayed in anxiety disorders. A separate study also indicates that LC neurons are activated in response to both CS+ and CS- tones in awake freely moving rats during in early

extinction trials (Campeau et al., 1997). Taken together with our findings that LC stimulation reduces metabolic activity in the mPFC, it is possibile that LC activation in response to early CS+ and CS- trials during early extinction trials here caused exaggerated inhibition of the mPFC. These results support our hypothesis that MI rats have dysregulated responses to fear-associated stimuli that persist in the absence of the US.

In contrast to the profound anxiety-like behavior displayed by MI rats in our conditioned fear studies, we also reported that MI rats displayed a neophobic response in the open field test. However, this difference was small, and we did not observe any difference in response between MI and sham-ligated rats in other variables assessed in this test. We also failed to observe any differences between MI and sham-ligated rats in a pilot study investigating social behavior in the social interaction test. These results suggest that anxiety associated with MI may precipitate alterations in mechanisms that promote neuroplasticity during learning.

Previous studies have demonstrated that chronic stress leads to changes in fear expression and extinction, with concomitant changes in IL and PrL neuronal activity. Specifically, rats subjected to restraint stress exhibit increased freezing behavior during extinction recall compared to unstressed controls. Accordingly, stressed rats display decreased IL activity (assessed by single unit recordings) during CS presentation the day after extinction while control rats exhibit little change in IL activity (Wilber et al., 2011). These results indicate that

chronic stress results in plasticity in the mPFC (specifically the IL) that influences future neuronal and behavioral responses to conditioned stimuli. Together, our observations of increased baseline and decreased NE-induced metabolic activation in the IL, the reduction in β_1AR density, and the deficits in conditioned fear extinction (and extinction recall) we observed in MI rats suggest that MI, or its biochemical sequelae, induce plasticity in the IL that promotes persistent enhanced responses to fear-related stimuli. Alternatively, the changes we observed may suggest that the biochemical sequelae of MI inhibit the normal plasticity in the IL that is necessary for proper extinction of fear responses.

Potential Mechanisms

Transneuronal labeling studies with pseudorabies virus have demonstrated efferent pathways from multiple forebrain regions to the left ventricular myocardium, including the IL, PrL, and Cg cortices and regions of the hypothalamus (Ter Horst et al., 1996). Additionally, these are activated in response to angina in conscious rats, suggesting these regions are positioned to respond to cardiac changes (Ter Horst, 1999). Shortly after experimental MI (within 72 hours), these regions, especially the mPFC, display endothelial leakage in a pattern similar to that elicited by systemic TNFα injection (Worrall et al., 1997). Previous studies have shown elevated levels of TNFα after MI, and reduction in circulating TNFα attenuates the anhedonia exhibited by MI rats (Grippo et al., 2003a). Furthermore, central blockade of mineralcorticoid receptor

results in decreased circulating TNFα and decreased sympathetic drive after MI (Francis et al., 2003; Francis et al., 2001b). Thus, increased blood-brain barrier permeability soon after MI may allow for the infiltration of inflammatory mediators that initiate long-term structural and functional plasticity we observed that could contribute to the development of anxiety and arrhythmia susceptibility after MI.

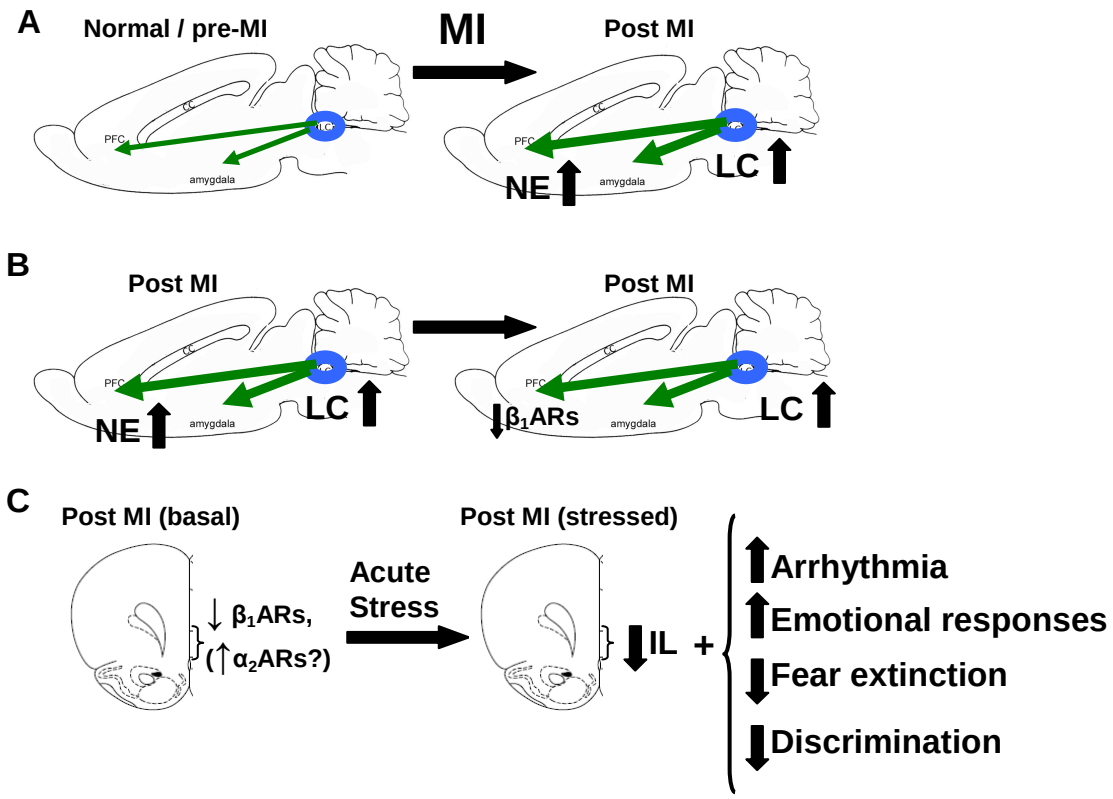

Figure 36. Conclusions and model. Based on the results of these studies, we propose the following model: MI induces chronic increases activity of the locus coeruleus (LC), resulting in an increase in norepinephrine (NE) release throughout the forebrain, including the prefrontal cortex and amygdala (A). In turn, this chronic increase in forebrain NE results in downregulation of β_1ARs in the infralimbic (IL) cortex and basolateral amygdala, as reported in Chapter 4 (B). This reduction in β_1ARs in the IL (possibly combined with an increase in α_2ARs) may contribute to inhibition of IL activity in response to acute stress, such as cue associated with an aversive stimulus. Inhibtion of the IL during stress is accompanied by, and may contribute to enhanced emotional responses,

impaired fear extinction, impaired discrimination between safety and danger cues, and stress-induced arrhythmia after MI (C).

REFERENCE LIST

Effects of enalapril on mortality in severe congestive heart failure. results of the cooperative north scandinavian enalapril survival study (CONSENSUS). the CONSENSUS trial study group. (1987) N Engl J Med (UNITED STATES) 316:1429-1435.

Abercrombie ED, Jacobs BL (1987) Single-unit response of noradrenergic neurons in the locus coeruleus of freely moving cats. I. acutely presented stressful and nonstressful stimuli. J Neurosci (UNITED STATES) 7:2837-2843.

Ader JP, Room P, Postema F, Korf J (1980) Bilaterally diverging axon collaterals and contralateral projections from rat locus coeruleus neurons, demonstrated by fluorescent retrograde double labeling and norepinephrine metabolism. J Neural Transm (AUSTRIA) 49:207-208.

Aggarwal A, Esler MD, Lambert GW, Hastings J, Johnston L, Kaye DM (2002) Norepinephrine turnover is increased in suprabulbar subcortical brain regions and is related to whole-body sympathetic activity in human heart failure. Circulation (United States) 105:1031-1033.

Albert CM, Chae CU, Rexrode KM, Manson JE, Kawachi I (2005) Phobic anxiety and risk of coronary heart disease and sudden cardiac death among women. Circulation (United States) 111:480-487.

Amano T, Unal CT, Pare D (2010) Synaptic correlates of fear extinction in the amygdala. Nat Neurosci (United States) 13:489-494.

Amano T, Duvarci S, Popa D, Pare D (2011) The fear circuit revisited: Contributions of the basal amygdala nuclei to conditioned fear. J Neurosci (United States) 31:15481-15489.

Andrade R, Aghajanian GK (1985) Opiate- and alpha 2-adrenoceptor-induced hyperpolarizations of locus ceruleus neurons in brain slices: Reversal by cyclic adenosine 3':5'-monophosphate analogues. J Neurosci (UNITED STATES) 5:2359-2364.

Anglada-Figueroa D, Quirk GJ (2005) Lesions of the basal amygdala block expression of conditioned fear but not extinction. J Neurosci (United States) 25:9680-9685.

Angrini M, Leslie JC, Shephard RA (1998) Effects of propranolol, buspirone, pCPA, reserpine, and chlordiazepoxide on open-field behavior. Pharmacol Biochem Behav (UNITED STATES) 59:387-397.

Aoki C, Venkatesan C, Kurose H (1998) Noradrenergic modulation of the prefrontal cortex as revealed by electron microscopic immunocytochemistry. Adv Pharmacol (UNITED STATES) 42:777-780.

Appel NM, Mitchell WM, Garlick RK, Glennon RA, Teitler M, De Souza EB (1990) Autoradiographic characterization of (+-)-1-(2,5-dimethoxy-4-[125I] iodophenyl)-2-aminopropane ([125I]DOI) binding to 5-HT2 and 5-HT1c receptors in rat brain. J Pharmacol Exp Ther (UNITED STATES) 255:843-857.

Arango V, Ernsberger P, Reis DJ, Mann JJ (1990) Demonstration of high- and low-affinity beta-adrenergic receptors in slide-mounted sections of rat and human brain. Brain Res (NETHERLANDS) 516:113-121.

Aston-Jones G, Bloom FE (1981) Norepinephrine-containing locus coeruleus neurons in behaving rats exhibit pronounced responses to non-noxious environmental stimuli. J Neurosci (UNITED STATES) 1:887-900.

Aston-Jones G, Chiang C, Alexinsky T (1991) Discharge of noradrenergic locus coeruleus neurons in behaving rats and monkeys suggests a role in vigilance. Prog Brain Res (NETHERLANDS) 88:501-520.

Bae E, Hwang IK, Yoo KY, Han TH, Lee CH, Choi JH, Yi SS, Lee SY, Ryu PD, Yoon YS, Won MH (2010) Gliosis in the amygdala following myocardial infarction in the rat. J Vet Med Sci (Japan) 72:1041-1045.

Baker JG (2005) The selectivity of beta-adrenoceptor antagonists at the human beta1, beta2 and beta3 adrenoceptors. Br J Pharmacol (England) 144:317-322.

Barefoot JC, Helms MJ, Mark DB, Blumenthal JA, Califf RM, Haney TL, O'Connor CM, Siegler IC, Williams RB (1996) Depression and long-term mortality risk in patients with coronary artery disease. Am J Cardiol (UNITED STATES) 78:613-617.

Barretto AC, Santos AC, Munhoz R, Rondon MU, Franco FG, Trombetta IC, Roveda F, de Matos LN, Braga AM, Middlekauff HR, Negrao CE (2009) Increased muscle sympathetic nerve activity predicts mortality in heart failure patients. Int J Cardiol (Netherlands) 135:302-307.

Beck KD, Luine VN (2002) Sex differences in behavioral and neurochemical profiles after chronic stress: Role of housing conditions. Physiol Behav (United States) 75:661-673.

Becker LC, Pepine CJ, Bonsall R, Cohen JD, Goldberg AD, Coghlan C, Stone PH, Forman S, Knatterud G, Sheps DS, Kaufmann PG (1996) Left ventricular, peripheral vascular, and neurohumoral responses to mental stress in normal middle-aged men and women. reference group for the psychophysiological investigations of myocardial ischemia (PIMI) study. Circulation (UNITED STATES) 94:2768-2777.

Benovic JL, Kuhn H, Weyand I, Codina J, Caron MG, Lefkowitz RJ (1987) Functional desensitization of the isolated beta-adrenergic receptor by the beta-adrenergic receptor kinase: Potential role of an analog of the retinal protein arrestin (48-kDa protein). Proc Natl Acad Sci U S A (UNITED STATES) 84:8879-8882.

Berecek KH, Mitchum TN (1986) Role of vasopressin in the cardiovascular response to stimulation of the locus coeruleus. Endocrinology (UNITED STATES) 118:1829-1834.

Berne RM, Levy NL (2001) Cardiovascular physiolology. St. Louis, MO: Mosby.

Berretta S, Pantazopoulos H, Caldera M, Pantazopoulos P, Pare D (2005) Infralimbic cortex activation increases c-fos expression in intercalated neurons of the amygdala. Neuroscience (United States) 132:943-953.

Berridge CW, Abercrombie ED (1999) Relationship between locus coeruleus discharge rates and rates of norepinephrine release within neocortex as assessed by in vivo microdialysis. Neuroscience (UNITED STATES) 93:1263-1270.

Berridge CW, Foote SL (1991) Effects of locus coeruleus activation on electroencephalographic activity in neocortex and hippocampus. J Neurosci (UNITED STATES) 11:3135-3145.

Bhatnagar S, Dallman M (1998) Neuroanatomical basis for facilitation of hypothalamic-pituitary-adrenal responses to a novel stressor after chronic stress. Neuroscience (UNITED STATES) 84:1025-1039.

Bissiere S, Plachta N, Hoyer D, McAllister KH, Olpe HR, Grace AA, Cryan JF (2008) The rostral anterior cingulate cortex modulates the efficiency of amygdala-dependent fear learning. Biol Psychiatry (United States) 63:821-831.

Boulpaep EL (2005) The heart as a pump (chapter 21). In: Medical physiology (Boron WF, Boulpaep EL, eds), pp508. Philadelphia, PA: Elsevier.

Bouret S, Sara SJ (2004) Reward expectation, orientation of attention and locus coeruleus-medial frontal cortex interplay during learning. Eur J Neurosci (France) 20:791-802.

Bremner JD, Staib LH, Kaloupek D, Southwick SM, Soufer R, Charney DS (1999) Neural correlates of exposure to traumatic pictures and sound in vietnam combat veterans with and without posttraumatic stress disorder: A positron emission tomography study. Biol Psychiatry (UNITED STATES) 45:806-816.

Bremner JD, Innis RB, Ng CK, Staib LH, Salomon RM, Bronen RA, Duncan J, Southwick SM, Krystal JH, Rich D, Zubal G, Dey H, Soufer R, Charney DS (1997) Positron emission tomography measurement of cerebral metabolic correlates of yohimbine administration in combat-related posttraumatic stress disorder. Arch Gen Psychiatry (UNITED STATES) 54:246-254.

Britton JC, Lissek S, Grillon C, Norcross MA, Pine DS (2011) Development of anxiety: The role of threat appraisal and fear learning. Depress Anxiety (United States) 28:5-17.

Brockway BP, Mills PA, Azar SH (1991) A new method for continuous chronic measurement and recording of blood pressure, heart rate and activity in the rat via radio-telemetry. Clin Exp Hypertens A (UNITED STATES) 13:885-895.

Brodsky MA, Sato DA, Iseri LT, Wolff LJ, Allen BJ (1987) Ventricular tachyarrhythmia associated with psychological stress. the role of the sympathetic nervous system. JAMA (UNITED STATES) 257:2064-2067.

Brunet A, Orr SP, Tremblay J, Robertson K, Nader K, Pitman RK (2008) Effect of post-retrieval propranolol on psychophysiologic responding during subsequent script-driven traumatic imagery in post-traumatic stress disorder. J Psychiatr Res (England) 42:503-506.

Brunzell DH, Kim JJ (2001) Fear conditioning to tone, but not to context, is attenuated by lesions of the insular cortex and posterior extension of the intralaminar complex in rats. Behav Neurosci (United States) 115:365-375.

Buckman SG, Hodgson SR, Hofford RS, Eitan S (2009) Increased elevated plus maze open-arm time in mice during spontaneous morphine withdrawal. Behav Brain Res (Netherlands) 197:454-456.

Buffalari DM, Grace AA (2009) Chronic cold stress increases excitatory effects of norepinephrine on spontaneous and evoked activity of basolateral amygdala neurons. Int J Neuropsychopharmacol (England) 12:95-107.

Buffalari DM, Grace AA (2007) Noradrenergic modulation of basolateral amygdala neuronal activity: Opposing influences of alpha-2 and beta receptor activation. J Neurosci (United States) 27:12358-12366.

Campeau S, Falls WA, Cullinan WE, Helmreich DL, Davis M, Watson SJ (1997) Elicitation and reduction of fear: Behavioural and neuroendocrine indices and brain induction of the immediate-early gene c-fos. Neuroscience (UNITED STATES) 78:1087-1104.

Cao JM, Chen LS, KenKnight BH, Ohara T, Lee MH, Tsai J, Lai WW, Karagueuzian HS, Wolf PL, Fishbein MC, Chen PS (2000a) Nerve sprouting and sudden cardiac death. Circ Res (UNITED STATES) 86:816-821.

Cao JM, Fishbein MC, Han JB, Lai WW, Lai AC, Wu TJ, Czer L, Wolf PL, Denton TA, Shintaku IP, Chen PS, Chen LS (2000b) Relationship between regional cardiac hyperinnervation and ventricular arrhythmia. Circulation (UNITED STATES) 101:1960-1969.

Carpeggiani C, Landisman C, Montaron MF, Skinner JE (1992) Cryoblockade in limbic brain (amygdala) prevents or delays ventricular fibrillation after coronary artery occlusion in psychologically stressed pigs. Circ Res (UNITED STATES) 70:600-606.

Cassell MD, Gray TS (1989) The amygdala directly innervates adrenergic (C1) neurons in the ventrolateral medulla in the rat. Neurosci Lett (NETHERLANDS) 97:163-168.

Chang CH, Knapska E, Orsini CA, Rabinak CA, Zimmerman JM, Maren S (2009) Fear extinction in rodents. Curr Protoc Neurosci (United States) Chapter 8:Unit8.23.

Chen FJ, Sara SJ (2007) Locus coeruleus activation by foot shock or electrical stimulation inhibits amygdala neurons. Neuroscience (United States) 144:472-481.

Chen PS, Chen LS, Cao JM, Sharifi B, Karagueuzian HS, Fishbein MC (2001) Sympathetic nerve sprouting, electrical remodeling and the mechanisms of sudden cardiac death. Cardiovasc Res (Netherlands) 50:409-416.

Chen SY, Chai CY (2002) Coexistence of neurons integrating urinary bladder activity and pelvic nerve activity in the same cardiovascular areas of the pontomedulla in cats. Chin J Physiol (China (Republic: 1949-)) 45:41-50.

Choy KH, Yu J, Hawkes D, Mayorov DN (2011) Analysis of vigilant scanning behavior in mice using two-point digital video tracking. Psychopharmacology (Berl) .

Chudasama Y, Robbins TW (2003) Dissociable contributions of the orbitofrontal and infralimbic cortex to pavlovian autoshaping and discrimination reversal learning: Further evidence for the functional heterogeneity of the rodent frontal cortex. J Neurosci (United States) 23:8771-8780.

Cohen H, Zohar J (2004) An animal model of posttraumatic stress disorder: The use of cut-off behavioral criteria. Ann N Y Acad Sci (United States) 1032:167-178.

Crane JW, Ebner K, Day TA (2003) Medial prefrontal cortex suppression of the hypothalamic-pituitary-adrenal axis response to a physical stressor, systemic delivery of interleukin-1beta. Eur J Neurosci (France) 17:1473-1481.

Crawley JN, Maas JW, Roth RH (1980) Evidence against specificity of electrical stimulation of the nucleus locus coeruleus in activating the sympathetic nervous system in the rat. Brain Res (NETHERLANDS) 183:301-311.

Cunningham ET,Jr, Sawchenko PE (1988) Anatomical specificity of noradrenergic inputs to the paraventricular and supraoptic nuclei of the rat hypothalamus. J Comp Neurol (UNITED STATES) 274:60-76.

de Jonge P, van den Brink RH, Spijkerman TA, Ormel J (2006) Only incident depressive episodes after myocardial infarction are associated with new cardiovascular events. J Am Coll Cardiol (United States) 48:2204-2208.

Debiec J, LeDoux JE (2006) Noradrenergic signaling in the amygdala contributes to the reconsolidation of fear memory: Treatment implications for PTSD. Ann N Y Acad Sci (United States) 1071:521-524.

Debiec J, Ledoux JE (2004) Disruption of reconsolidation but not consolidation of auditory fear conditioning by noradrenergic blockade in the amygdala. Neuroscience (United States) 129:267-272.

Dickens C, McGowan L, Percival C, Tomenson B, Cotter L, Heagerty A, Creed F (2008) New onset depression following myocardial infarction predicts cardiac mortality. Psychosom Med (United States) 70:450-455.

Diorio D, Viau V, Meaney MJ (1993) The role of the medial prefrontal cortex (cingulate gyrus) in the regulation of hypothalamic-pituitary-adrenal responses to stress. J Neurosci (UNITED STATES) 13:3839-3847.

Docherty JR (2010) Subtypes of functional alpha1-adrenoceptor. Cell Mol Life Sci (Switzerland) 67:405-417.

Drevets WC (2007) Orbitofrontal cortex function and structure in depression. Ann N Y Acad Sci (United States) 1121:499-527.

Drolet G, Gauthier P (1985) Peripheral and central mechanisms of the pressor response elicited by stimulation of the locus coeruleus in the rat. Can J Physiol Pharmacol (CANADA) 63:599-605.

Du XJ, Cox HS, Dart AM, Esler MD (1999) Sympathetic activation triggers ventricular arrhythmias in rat heart with chronic infarction and failure. Cardiovasc Res (NETHERLANDS) 43:919-929.

Dunlap ME, Bibevski S, Rosenberry TL, Ernsberger P (2003) Mechanisms of altered vagal control in heart failure: Influence of muscarinic receptors and acetylcholinesterase activity. Am J Physiol Heart Circ Physiol (United States) 285:H1632-40.

Edmonds DE, Gallistel CR (1974) Parametric analysis of brain stimulation reward in the rat: III. effect of performance variables on the reward summation function. J Comp Physiol Psychol (UNITED STATES) 87:876-883.

Ehrlich I, Humeau Y, Grenier F, Ciocchi S, Herry C, Luthi A (2009) Amygdala inhibitory circuits and the control of fear memory. Neuron (United States) 62:757-771.

Elfving B, Bjornholm B, Knudsen GM (2003) Interference of anaesthetics with radioligand binding in neuroreceptor studies. Eur J Nucl Med Mol Imaging (Germany) 30:912-915.

El-Wazir YM, Li SG, Williams DT, Sprinkle AG, Brown DR, Randall DC (2005) Differential acquisition of specific components of a classically conditioned arterial blood pressure response in rat. Am J Physiol Regul Integr Comp Physiol (United States) 289:R784-8.

Engelen DJ, Gressin V, Krucoff MW, Theuns DA, Green C, Cheriex EC, Maison-Blanche P, Dassen WR, Wellens HJ, Gorgels AP (2003) Usefulness of frequent arrhythmias after epicardial recanalization in anterior wall acute myocardial infarction as a marker of cellular injury leading to poor recovery of left ventricular function. Am J Cardiol (United States) 92:1143-1149.

Erickson JT, Millhorn DE (1994) Hypoxia and electrical stimulation of the carotid sinus nerve induce fos-like immunoreactivity within catecholaminergic and serotoninergic neurons of the rat brainstem. J Comp Neurol (UNITED STATES) 348:161-182.

Esler M, Alvarenga M, Lambert G, Kaye D, Hastings J, Jennings G, Morris M, Schwarz R, Richards J (2004) Cardiac sympathetic nerve biology and brain monoamine turnover in panic disorder. Ann N Y Acad Sci (United States) 1018:505-514.

Esler M, Eikelis N, Schlaich M, Lambert G, Alvarenga M, Kaye D, El-Osta A, Guo L, Barton D, Pier C, Brenchley C, Dawood T, Jennings G, Lambert E (2008) Human sympathetic nerve biology: Parallel influences of stress and epigenetics in essential hypertension and panic disorder. Ann N Y Acad Sci (United States) 1148:338-348.

Fan J, Kolster R, Ghajar J, Suh M, Knight RT, Sarkar R, McCandliss BD (2007) Response anticipation and response conflict: An event-related potential and functional magnetic resonance imaging study. J Neurosci (United States) 27:2272-2282.

Fantidis P (2010) The role of the stress-related anti-inflammatory hormones ACTH and cortisol in atherosclerosis. Curr Vasc Pharmacol (United Arab Emirates) 8:517-525.

Feenstra MG, Vogel M, Botterblom MH, Joosten RN, de Bruin JP (2001) Dopamine and noradrenaline efflux in the rat prefrontal cortex after classical aversive conditioning to an auditory cue. Eur J Neurosci (France) 13:1051-1054.

File SE, Wardill AG (1975a) The reliability of the hole-board apparatus. Psychopharmacologia (GERMANY, WEST) 44:47-51.

File SE, Wardill AG (1975b) Validity of head-dipping as a measure of exploration in a modified hole-board. Psychopharmacologia (GERMANY, WEST) 44:53-59.

File SE, Lippa AS, Beer B, Lippa MT (2004) Animal tests of anxiety. Curr Protoc Neurosci (United States) Chapter 8:Unit 8.3.

Fillenz M, Lowry JP, Boutelle MG, Fray AE (1999) The role of astrocytes and noradrenaline in neuronal glucose metabolism. Acta Physiol Scand (ENGLAND) 167:275-284.

Fleet R, Lesperance F, Arsenault A, Gregoire J, Lavoie K, Laurin C, Harel F, Burelle D, Lambert J, Beitman B, Frasure-Smith N (2005) Myocardial perfusion study of panic attacks in patients with coronary artery disease. Am J Cardiol (United States) 96:1064-1068.

Florin-Lechner SM, Druhan JP, Aston-Jones G, Valentino RJ (1996) Enhanced norepinephrine release in prefrontal cortex with burst stimulation of the locus coeruleus. Brain Res (NETHERLANDS) 742:89-97.

Flugge G (1996) Alterations in the central nervous alpha 2-adrenoceptor system under chronic psychosocial stress. Neuroscience (UNITED STATES) 75:187-196.

Francis J, Weiss RM, Johnson AK, Felder RB (2003) Central mineralocorticoid receptor blockade decreases plasma TNF-alpha after coronary artery ligation in rats. Am J Physiol Regul Integr Comp Physiol (United States) 284:R328-35.

Francis J, Weiss RM, Wei SG, Johnson AK, Felder RB (2001a) Progression of heart failure after myocardial infarction in the rat. Am J Physiol Regul Integr Comp Physiol (United States) 281:R1734-45.

Francis J, Weiss RM, Wei SG, Johnson AK, Beltz TG, Zimmerman K, Felder RB (2001b) Central mineralocorticoid receptor blockade improves volume regulation and reduces sympathetic drive in heart failure. Am J Physiol Heart Circ Physiol (United States) 281:H2241-51.

Franowicz JS, Kessler LE, Borja CM, Kobilka BK, Limbird LE, Arnsten AF (2002) Mutation of the alpha2A-adrenoceptor impairs working memory performance and annuls cognitive enhancement by guanfacine. J Neurosci (United States) 22:8771-8777.

Frasure-Smith N, Lesperance F (2008) Depression and anxiety as predictors of 2-year cardiac events in patients with stable coronary artery disease. Arch Gen Psychiatry (United States) 65:62-71.

Frasure-Smith N, Lesperance F (2003) Depression and other psychological risks following myocardial infarction. Arch Gen Psychiatry (United States) 60:627-636.

Frasure-Smith N, Lesperance F, Talajic M (1993) Depression following myocardial infarction. impact on 6-month survival. JAMA (UNITED STATES) 270:1819-1825.

Friedmann E, Thomas SA, Liu F, Morton PG, Chapa D, Gottlieb SS, Sudden Cardiac Death in Heart Failure Trial Investigators (2006) Relationship of depression, anxiety, and social isolation to chronic heart failure outpatient mortality. Am Heart J (United States) 152:940.e1-940.e8.

Frysztak RJ, Neafsey EJ (1994) The effect of medial frontal cortex lesions on cardiovascular conditioned emotional responses in the rat. Brain Res (NETHERLANDS) 643:181-193.

Fu A, Li X, Zhao B (2008) Role of beta1-adrenoceptor in the basolateral amygdala of rats with anxiety-like behavior. Brain Res (Netherlands) 1211:85-92.

Fu AL, Yan XB, Sui L (2007) Down-regulation of beta1-adrenoceptors gene expression by short interfering RNA impairs the memory retrieval in the basolateral amygdala of rats. Neurosci Lett (Ireland) 428:77-81.

Gabbott PL, Warner TA, Jays PR, Salway P (2005) Prefrontal cortex in the rat: Projections to subcortical autonomic, motor, and limbic centers. 492:145-177.

Gale GD, Anagnostaras SG, Godsil BP, Mitchell S, Nozawa T, Sage JR, Wiltgen B, Fanselow MS (2004) Role of the basolateral amygdala in the storage of fear memories across the adult lifetime of rats. J Neurosci (United States) 24:3810-3815.

Gander ML, von Kanel R (2006) Myocardial infarction and post-traumatic stress disorder: Frequency, outcome, and atherosclerotic mechanisms. Eur J Cardiovasc Prev Rehabil (England) 13:165-172.

Garakani A, Mathew SJ, Charney DS (2006) Neurobiology of anxiety disorders and implications for treatment. Mt Sinai J Med (United States) 73:941-949.

Garnier V, Zini R, Tillement JP (1999) A GppNHp-insensitivity factor modulates the activation of beta-adrenoceptor-coupled gs protein in rat cortex and cerebellum. Fundam Clin Pharmacol (FRANCE) 13:169-179.

Garnier V, Zini R, Sapena R, Tillement JP (1997) A match between binding to beta-adrenoceptors and stimulation of adenylyl cyclase parameters of (-)isoproterenol and salbutamol on rat brain. Pharmacol Res (ENGLAND) 35:303-312.

Geracioti TD,Jr, Baker DG, Ekhator NN, West SA, Hill KK, Bruce AB, Schmidt D, Rounds-Kugler B, Yehuda R, Keck PE,Jr, Kasckow JW (2001) CSF norepinephrine concentrations in posttraumatic stress disorder. Am J Psychiatry (United States) 158:1227-1230.

Ginovart N, Hassoun W, Le Cavorsin M, Veyre L, Le Bars D, Leviel V (2002) Effects of amphetamine and evoked dopamine release on [11C]raclopride binding in anesthetized cats. Neuropsychopharmacology (United States) 27:72-84.

Gourine A, Bondar SI, Spyer KM, Gourine AV (2008) Beneficial effect of the central nervous system beta-adrenoceptor blockade on the failing heart. Circ Res (United States) 102:633-636.

Grimm LJ, Blendy JA, Kellar KJ, Perry DC (1992) Chronic reserpine administration selectively up-regulates beta 1- and alpha 1b-adrenergic receptors in rat brain: An autoradiographic study. Neuroscience (ENGLAND) 47:77-86.

Grippo AJ, Beltz TG, Johnson AK (2003a) Behavioral and cardiovascular changes in the chronic mild stress model of depression. Physiol Behav (United States) 78:703-710.

Grippo AJ, Francis J, Weiss RM, Felder RB, Johnson AK (2003b) Cytokine mediation of experimental heart failure-induced anhedonia. Am J Physiol Regul Integr Comp Physiol (United States) 284:R666-73.

Grippo AJ, Santos CM, Johnson RF, Beltz TG, Martins JB, Felder RB, Johnson AK (2004) Increased susceptibility to ventricular arrhythmias in a rodent model of experimental depression. Am J Physiol Heart Circ Physiol (United States) 286:H619-26.

Hansson E, Ronnback L (1991) Receptor regulation of the glutamate, GABA and taurine high-affinity uptake into astrocytes in primary culture. Brain Res (NETHERLANDS) 548:215-221.

Hasking GJ, Esler MD, Jennings GL, Burton D, Johns JA, Korner PI (1986) Norepinephrine spillover to plasma in patients with congestive heart failure: Evidence of increased overall and cardiorenal sympathetic nervous activity. Circulation (UNITED STATES) 73:615-621.

Hayar A, Guyenet PG (1999) Alpha2-adrenoceptor-mediated presynaptic inhibition in bulbospinal neurons of rostral ventrolateral medulla. Am J Physiol (UNITED STATES) 277:H1069-80.

Heaton LJ, McNeil DW, Milgrom P (2010) Propranolol and D-cycloserine as adjunctive medications in reducing dental fear in sedation practice. SAAD Dig (England) 26:27-35.

Heidenreich PA et al (2011) Forecasting the future of cardiovascular disease in the united states: A policy statement from the american heart association. Circulation (United States) 123:933-944.

Henze M, Hart D, Samarel A, Barakat J, Eckert L, Scrogin K (2008) Persistent alterations in heart rate variability, baroreflex sensitivity, and anxiety-like behaviors during development of heart failure in the rat. Am J Physiol Heart Circ Physiol (United States) 295:H29-38.

Hepler JR, Gilman AG (1992) G proteins. Trends Biochem Sci (ENGLAND) 17:383-387.

Hipolide DC, Tufik S, Raymond R, Nobrega JN (1998) Heterogeneous effects of rapid eye movement sleep deprivation on binding to alpha- and beta-adrenergic receptor subtypes in rat brain. Neuroscience (UNITED STATES) 86:977-987.

Hopkins DA, Holstege G (1978) Amygdaloid projections to the mesencephalon, pons and medulla oblongata in the cat. Exp Brain Res (GERMANY, WEST) 32:529-547.

Hu H, Su L, Xu YQ, Zhang H, Wang LW (2010) Behavioral and [F-18] fluorodeoxyglucose micro positron emission tomography imaging study in a rat chronic mild stress model of depression. Neuroscience (United States) 169:171-181.

Huffman JC, Smith FA, Blais MA, Januzzi JL, Fricchione GL (2008) Anxiety, independent of depressive symptoms, is associated with in-hospital cardiac complications after acute myocardial infarction. J Psychosom Res (England) 65:557-563.

Hurley KM, Herbert H, Moga MM, Saper CB (1991) Efferent projections of the infralimbic cortex of the rat. J Comp Neurol (UNITED STATES) 308:249-276.

Jardine DL, Charles CJ, Ashton RK, Bennett SI, Whitehead M, Frampton CM, Nicholls MG (2005) Increased cardiac sympathetic nerve activity following acute myocardial infarction in a sheep model. J Physiol (England) 565:325-333.

Jasmin L, Burkey AR, Granato A, Ohara PT (2004) Rostral agranular insular cortex and pain areas of the central nervous system: A tract-tracing study in the rat. J Comp Neurol (United States) 468:425-440.

Johnson LR, Hou M, Prager EM, Ledoux JE (2011) Regulation of the fear network by mediators of stress: Norepinephrine alters the balance between cortical and subcortical afferent excitation of the lateral amygdala. Front Behav Neurosci (Switzerland) 5:23.

Kaloustian S, Wann BP, Bah TM, Girard SA, Apostolakis A, Ishak S, Mathieu S, Ryvlin P, Godbout R, Rousseau G (2008) Apoptosis time course in the limbic system after myocardial infarction in the rat. Brain Res (Netherlands) 1216:87-91.

Kalynchuk LE, Pinel JP, Treit D, Kippin TE (1997) Changes in emotional behavior produced by long-term amygdala kindling in rats. Biol Psychiatry (UNITED STATES) 41:438-451.

Kent RS, De Lean A, Lefkowitz RJ (1980) A quantitative analysis of beta-adrenergic receptor interactions: Resolution of high and low affinity states of the receptor by computer modeling of ligand binding data. Mol Pharmacol (UNITED STATES) 17:14-23.

Kilgore L Lon kilgore, PhD: Selected T-shirt graphics. 2012:.

Koenigs M, Grafman J (2009) Posttraumatic stress disorder: The role of medial prefrontal cortex and amygdala. Neuroscientist (United States) 15:540-548.

Kompa AR, Gu XH, Evans BA, Summers RJ (1999) Desensitization of cardiac beta-adrenoceptor signaling with heart failure produced by myocardial infarction in the rat. evidence for the role of gi but not gs or phosphorylating proteins. J Mol Cell Cardiol (ENGLAND) 31:1185-1201.

Kouvelas D, Singewald N, Kaehler ST, Philippu A (2006) Sinoaortic denervation abolishes blood pressure-induced GABA release in the locus coeruleus of conscious rats. Neurosci Lett (Ireland) 393:194-199.

Krantz DS, Helmers KF, Bairey CN, Nebel LE, Hedges SM, Rozanski A (1991) Cardiovascular reactivity and mental stress-induced myocardial ischemia in patients with coronary artery disease. Psychosom Med (UNITED STATES) 53:1-12.

Krause EG, de Kloet AD, Scott KA, Flak JN, Jones K, Smeltzer MD, Ulrich-Lai YM, Woods SC, Wilson SP, Reagan LP, Herman JP, Sakai RR (2011) Blood-borne angiotensin II acts in the brain to influence behavioral and endocrine responses to psychogenic stress. J Neurosci (United States) 31:15009-15015.

Kreiner G, Zelek-Molik A, Kowalska M, Bielawski A, Antkiewicz-Michaluk L, Nalepa I (2011) Effects of the noradrenergic neurotoxin DSP-4 on the expression of alpha1-adrenoceptor subtypes after antidepressant treatment. Pharmacol Rep (Poland) 63:1349-1358.

Krettek JE, Price JL (1977) The cortical projections of the mediodorsal nucleus and adjacent thalamic nuclei in the rat. J Comp Neurol (UNITED STATES) 171:157-191.

Lampert R, Joska T, Burg MM, Batsford WP, McPherson CA, Jain D (2002) Emotional and physical precipitants of ventricular arrhythmia. Circulation (United States) 106:1800-1805.

Lampert R, Shusterman V, Burg M, McPherson C, Batsford W, Goldberg A, Soufer R (2009) Anger-induced T-wave alternans predicts future ventricular arrhythmias in patients with implantable cardioverter-defibrillators. J Am Coll Cardiol (United States) 53:774-778.

Lands AM, Arnold A, McAuliff JP, Luduena FP, Brown TG,Jr (1967) Differentiation of receptor systems activated by sympathomimetic amines. Nature (ENGLAND) 214:597-598.

Lederer WJ (2005) Cardiac electrophysiology and the electrocardiogram (chapter 20). In: Medical physiology (Boron WF, Boulpaep EL, eds), pp483. Philadelphia, PA: Elsevier.

LeDoux JE, Iwata J, Cicchetti P, Reis DJ (1988) Different projections of the central amygdaloid nucleus mediate autonomic and behavioral correlates of conditioned fear. J Neurosci (UNITED STATES) 8:2517-2529.

Lee CH, Hwang IK, Choi JH, Yoo KY, Han TH, Park OK, Lee SY, Ryu PD, Won MH (2010) Calcium binding proteins immunoreactivity in the rat basolateral amygdala following myocardial infarction. Cell Mol Neurobiol (United States) 30:333-338.

Leenen FH (2007) Brain mechanisms contributing to sympathetic hyperactivity and heart failure. Circ Res (United States) 101:221-223.

Lefkowitz RJ, Mullikin D, Caron MG (1976) Regulation of beta-adrenergic receptors by guanyl-5'-yl imidodiphosphate and other purine nucleotides. J Biol Chem (UNITED STATES) 251:4686-4692.

Li Q, Battaglia G, Van de Kar LD (1997) Autoradiographic evidence for differential G-protein coupling of 5-HT1A receptors in rat brain: Lack of effect of repeated injections of fluoxetine. Brain Res (NETHERLANDS) 769:141-151.

Li SG, Randall DC, Brown DR (1998) Roles of cardiac output and peripheral resistance in mediating blood pressure response to stress in rats. Am J Physiol (UNITED STATES) 274:R1065-9.

Li W, Knowlton D, Van Winkle DM, Habecker BA (2004) Infarction alters both the distribution and noradrenergic properties of cardiac sympathetic neurons. Am J Physiol Heart Circ Physiol (United States) 286:H2229-36.

Likhtik E, Pelletier JG, Paz R, Pare D (2005) Prefrontal control of the amygdala. J Neurosci (United States) 25:7429-7437.

Likhtik E, Popa D, Apergis-Schoute J, Fidacaro GA, Pare D (2008) Amygdala intercalated neurons are required for expression of fear extinction. Nature (England) 454:642-645.

Ma S, Mifflin SW, Cunningham JT, Morilak DA (2008) Chronic intermittent hypoxia sensitizes acute hypothalamic-pituitary-adrenal stress reactivity and fos induction in the rat locus coeruleus in response to subsequent immobilization stress. Neuroscience (United States) 154:1639-1647.

Macey PM, Wu P, Kumar R, Ogren JA, Richardson HL, Woo MA, Harper RM (2012) Differential responses of the insular cortex gyri to autonomic challenges. Auton Neurosci .

Mattinson CE, Burmeister JJ, Quintero JE, Pomerleau F, Huettl P, Gerhardt GA (2011) Tonic and phasic release of glutamate and acetylcholine neurotransmission in sub-regions of the rat prefrontal cortex using enzyme-based microelectrode arrays. J Neurosci Methods (Netherlands) 202:199-208.

McAlpine HM, Morton JJ, Leckie B, Rumley A, Gillen G, Dargie HJ (1988) Neuroendocrine activation after acute myocardial infarction. Br Heart J (ENGLAND) 60:117-124.

McAuley JD, Stewart AL, Webber ES, Cromwell HC, Servatius RJ, Pang KC (2009) Wistar-kyoto rats as an animal model of anxiety vulnerability: Support for a hypervigilance hypothesis. Behav Brain Res (Netherlands) 204:162-168.

McDonald AJ (1998) Cortical pathways to the mammalian amygdala. Prog Neurobiol (ENGLAND) 55:257-332.

Mcdonald AJ, Mascagni F, Guo L (1996) Projections of the medial and lateral prefrontal cortices to the amygdala: A phaseolus vulgaris leucoagglutinin study in the rat. Neuroscience (UNITED STATES) 71:55-75.

Milstein JA, Lehmann O, Theobald DE, Dalley JW, Robbins TW (2007) Selective depletion of cortical noradrenaline by anti-dopamine beta-hydroxylase-saporin impairs attentional function and enhances the effects of guanfacine in the rat. Psychopharmacology (Berl) (Germany) 190:51-63.

Morgan MA, LeDoux JE (1995) Differential contribution of dorsal and ventral medial prefrontal cortex to the acquisition and extinction of conditioned fear in rats. Behav Neurosci (UNITED STATES) 109:681-688.

Moser DK, Riegel B, McKinley S, Doering LV, An K, Sheahan S (2007a) Impact of anxiety and perceived control on in-hospital complications after acute myocardial infarction. Psychosom Med (United States) 69:10-16.

Moser DK, Riegel B, McKinley S, Doering LV, An K, Sheahan S (2007b) Impact of anxiety and perceived control on in-hospital complications after acute myocardial infarction. Psychosom Med (United States) 69:10-16.

Movahed MR, Saito Y, Ahmadi-Kashani M, Kasravi B (2006) Relation of pericardial effusion to degree of fractional shortening. Am J Cardiol (United States) 97:910-911.

Mueller D, Porter JT, Quirk GJ (2008) Noradrenergic signaling in infralimbic cortex increases cell excitability and strengthens memory for fear extinction. J Neurosci (United States) 28:369-375.

Muigg P, Hetzenauer A, Hauer G, Hauschild M, Gaburro S, Frank E, Landgraf R, Singewald N (2008) Impaired extinction of learned fear in rats selectively bred for high anxiety - evidence of altered neuronal processing in prefrontal-amygdala pathways. Eur J Neurosci .

Murase S, Takayama M, Nosaka S (1993) Chemical stimulation of the nucleus locus coeruleus: Cardiovascular responses and baroreflex modification. Neurosci Lett (NETHERLANDS) 153:1-4.

Nakamura E, Kitagawa Y, Ozawa S, Suda K, Ando N, Ueda M, Kitajima M (2006) Role of steroid administration to reduce inflammation after thoracotomy in a rat surgical stress model. J Surg Res (United States) 135:364-369.

Neafsey EJ, Hurley-Gius KM, Arvanitis D (1986) The topographical organization of neurons in the rat medial frontal, insular and olfactory cortex projecting to the solitary nucleus, olfactory bulb, periaqueductal gray and superior colliculus. Brain Res (NETHERLANDS) 377:561-570.

Neve KA, McGonigle P, Molinoff PB (1986) Quantitative analysis of the selectivity of radioligands for subtypes of beta adrenergic receptors. J Pharmacol Exp Ther (UNITED STATES) 238:46-53.

Niclauss N, Michel-Reher MB, Alewijnse AE, Michel MC (2006) Comparison of three radioligands for the labelling of human beta-adrenoceptor subtypes. Naunyn Schmiedebergs Arch Pharmacol (Germany) 374:99-105.

Nomura S, Watanabe M, Ukei N, Nakazawa T (1981) Stress and beta-adrenergic receptor binding in the rat's brain. Brain Res (NETHERLANDS) 224:199-203.

Ohte N, Kurokawa K, Iida A, Narita H, Akita S, Yajima K, Miyabe H, Hayano J, Kimura G (2002) Myocardial oxidative metabolism in remote normal regions in the left ventricles with remodeling after myocardial infarction: Effect of beta-adrenoceptor blockers. J Nucl Med (United States) 43:780-785.

Ordway GA, Gambarana C, Frazer A (1988) Quantitative autoradiography of central beta adrenoceptor subtypes: Comparison of the effects of chronic treatment with desipramine or centrally administered l-isoproterenol. J Pharmacol Exp Ther (UNITED STATES) 247:379-389.

Ordway GA, Gambarana C, Tejani-Butt SM, Areso P, Hauptmann M, Frazer A (1991) Preferential reduction of binding of 125I-iodopindolol to beta-1 adrenoceptors in the amygdala of rat after antidepressant treatments. J Pharmacol Exp Ther (UNITED STATES) 257:681-690.

Paine TA, Slipp LE, Carlezon WA,Jr (2011) Schizophrenia-like attentional deficits following blockade of prefrontal cortex GABAA receptors. Neuropsychopharmacology (England) 36:1703-1713.

Papp M, Nalepa I, Vetulani J (1994) Reversal by imipramine of beta-adrenoceptor up-regulation induced in a chronic mild stress model of depression. Eur J Pharmacol (NETHERLANDS) 261:141-147.

Parker GW, Michael LH, Hartley CJ, Skinner JE, Entman ML (1990) Central beta-adrenergic mechanisms may modulate ischemic ventricular fibrillation in pigs. Circ Res (UNITED STATES) 66:259-270.

Passerin AM, Cano G, Rabin BS, Delano BA, Napier JL, Sved AF (2000) Role of locus coeruleus in foot shock-evoked fos expression in rat brain. Neuroscience (UNITED STATES) 101:1071-1082.

Patel KP, Zhang PL, Krukoff TL (1993) Alterations in brain hexokinase activity associated with heart failure in rats. Am J Physiol (UNITED STATES) 265:R923-8.

Paxinos G, Watson C (2004) The rat brain in stereotaxic coordinates, 5th edition. New York, NY: Academic Press.

Pedarzani P, Storm JF (1993) PKA mediates the effects of monoamine transmitters on the K+ current underlying the slow spike frequency adaptation in hippocampal neurons. Neuron (UNITED STATES) 11:1023-1035.

Pellow S, Chopin P, File SE, Briley M (1985) Validation of open:Closed arm entries in an elevated plus-maze as a measure of anxiety in the rat. J Neurosci Methods (NETHERLANDS) 14:149-167.

Pfeffer MA, Braunwald E (1990) Ventricular remodeling after myocardial infarction. experimental observations and clinical implications. Circulation (UNITED STATES) 81:1161-1172.

Pfeifer PC, Musch TI, McAllister RM (2001) Skeletal muscle oxidative capacity and exercise tolerance in rats with heart failure. Med Sci Sports Exerc (United States) 33:542-548.

Phillips RG, LeDoux JE (1992) Differential contribution of amygdala and hippocampus to cued and contextual fear conditioning. Behav Neurosci (UNITED STATES) 106:274-285.

Pinard CR, Mascagni F, McDonald AJ (2012) Medial prefrontal cortical innervation of the intercalated nuclear region of the amygdala. Neuroscience .

Pitkanen A, Savander V, LeDoux JE (1997) Organization of intra-amygdaloid circuitries in the rat: An emerging framework for understanding functions of the amygdala. Trends Neurosci (ENGLAND) 20:517-523.

Pitman RK, Sanders KM, Zusman RM, Healy AR, Cheema F, Lasko NB, Cahill L, Orr SP (2002) Pilot study of secondary prevention of posttraumatic stress disorder with propranolol. Biol Psychiatry (United States) 51:189-192.

Pohl J, Olmstead MC, Wynne-Edwards KE, Harkness K, Menard JL (2007) Repeated exposure to stress across the childhood-adolescent period alters rats' anxiety- and depression-like behaviors in adulthood: The importance of stressor type and gender. Behav Neurosci (United States) 121:462-474.

Porsolt RD, Anton G, Blavet N, Jalfre M (1978) Behavioural despair in rats: A new model sensitive to antidepressant treatments. Eur J Pharmacol (NETHERLANDS) 47:379-391.

Price JL (2007) Definition of the orbital cortex in relation to specific connections with limbic and visceral structures and other cortical regions. Ann N Y Acad Sci (United States) 1121:54-71.

Prickaerts J, Raaijmakers W, Blokland A (1996) Effects of myocardial infarction and captopril therapy on anxiety-related behaviors in the rat. Physiol Behav (UNITED STATES) 60:43-50.

Proudfit HK, Clark FM (1991) The projections of locus coeruleus neurons to the spinal cord. Prog Brain Res (NETHERLANDS) 88:123-141.

Qin D, Zhang ZH, Caref EB, Boutjdir M, Jain P, el-Sherif N (1996) Cellular and ionic basis of arrhythmias in postinfarction remodeled ventricular myocardium. Circ Res (UNITED STATES) 79:461-473.

Quirk GJ, Likhtik E, Pelletier JG, Pare D (2003) Stimulation of medial prefrontal cortex decreases the responsiveness of central amygdala output neurons. J Neurosci (United States) 23:8800-8807.

Quirk MC, Sosulski DL, Feierstein CE, Uchida N, Mainen ZF (2009) A defined network of fast-spiking interneurons in orbitofrontal cortex: Responses to behavioral contingencies and ketamine administration. Front Syst Neurosci (Switzerland) 3:13.

Rada EM, Tharakan EC, Flood P (2003) Volatile anesthetics reduce agonist affinity at nicotinic acetylcholine receptors in the brain. Anesth Analg (United States) 96:108-11, table of contents.

Radley JJ, Williams B, Sawchenko PE (2008) Noradrenergic innervation of the dorsal medial prefrontal cortex modulates hypothalamo-pituitary-adrenal responses to acute emotional stress. J Neurosci (United States) 28:5806-5816.

Radley JJ, Arias CM, Sawchenko PE (2006) Regional differentiation of the medial prefrontal cortex in regulating adaptive responses to acute emotional stress. J Neurosci (United States) 26:12967-12976.

Rainbow TC, Parsons B, Wolfe BB (1984) Quantitative autoradiography of beta 1- and beta 2-adrenergic receptors in rat brain. Proc Natl Acad Sci U S A (UNITED STATES) 81:1585-1589.

Rainbow TC, Bleisch WV, Biegon A, McEwen BS (1982) Quantitative densitometry of neurotransmitter receptors. J Neurosci Methods (NETHERLANDS) 5:127-138.

Ramchandra R, Hood SG, Denton DA, Woods RL, McKinley MJ, McAllen RM, May CN (2009) Basis for the preferential activation of cardiac sympathetic nerve activity in heart failure. Proc Natl Acad Sci U S A (United States) 106:924-928.

Ramos BP, Colgan LA, Nou E, Arnsten AF (2008) Beta2 adrenergic agonist, clenbuterol, enhances working memory performance in aging animals. Neurobiol Aging (United States) 29:1060-1069.

Ramos BP, Colgan L, Nou E, Ovadia S, Wilson SR, Arnsten AF (2005) The beta-1 adrenergic antagonist, betaxolol, improves working memory performance in rats and monkeys. Biol Psychiatry (United States) 58:894-900.

Randall DC, Brown DR, Brown LV, Kilgore JM (1994) Sympathetic nervous activity and arterial blood pressure control in conscious rat during rest and behavioral stress. Am J Physiol (UNITED STATES) 267:R1241-9.

Reiner S, Ambrosio M, Hoffmann C, Lohse MJ (2010) Differential signaling of the endogenous agonists at the beta2-adrenergic receptor. J Biol Chem (United States) 285:36188-36198.

Richerson GB (2005) The autonomic nervous system (chapter 15). In: Medical physiology (Boron WF, Boulpaep EL, eds), pp378. Philadelphia, PA: Elsevier.

Romanski LM, Clugnet MC, Bordi F, LeDoux JE (1993) Somatosensory and auditory convergence in the lateral nucleus of the amygdala. Behav Neurosci (UNITED STATES) 107:444-450.

Rosenkranz JA, Grace AA (2001) Dopamine attenuates prefrontal cortical suppression of sensory inputs to the basolateral amygdala of rats. J Neurosci (United States) 21:4090-4103.

Rosenkranz JA, Moore H, Grace AA (2003) The prefrontal cortex regulates lateral amygdala neuronal plasticity and responses to previously conditioned stimuli. J Neurosci (United States) 23:11054-11064.

Royer S, Martina M, Pare D (1999) An inhibitory interface gates impulse traffic between the input and output stations of the amygdala. J Neurosci (UNITED STATES) 19:10575-10583.

Rubia K, Smith AB, Brammer MJ, Taylor E (2003) Right inferior prefrontal cortex mediates response inhibition while mesial prefrontal cortex is responsible for error detection. Neuroimage (United States) 20:351-358.

Rygula R, Walker SC, Clarke HF, Robbins TW, Roberts AC (2010) Differential contributions of the primate ventrolateral prefrontal and orbitofrontal cortex to serial reversal learning. J Neurosci (United States) 30:14552-14559.

Salome N, Ngampramuan S, Nalivaiko E (2007) Intra-amygdala injection of GABAA agonist, muscimol, reduces tachycardia and modifies cardiac sympatho-vagal balance during restraint stress in rats. Neuroscience (United States) 148:335-341.

Savander V, Go CG, LeDoux JE, Pitkanen A (1995) Intrinsic connections of the rat amygdaloid complex: Projections originating in the basal nucleus. J Comp Neurol (UNITED STATES) 361:345-368.

Saxon LA (2005) Sudden cardiac death: Epidemiology and temporal trends. Rev Cardiovasc Med (United States) 6 Suppl 2:S12-20.

Schultz W, Tremblay L, Hollerman JR (2000) Reward processing in primate orbitofrontal cortex and basal ganglia. Cereb Cortex (UNITED STATES) 10:272-284.

Schutsky K, Ouyang M, Castelino CB, Zhang L, Thomas SA (2011) Stress and glucocorticoids impair memory retrieval via beta2-adrenergic, Gi/o-coupled suppression of cAMP signaling. J Neurosci (United States) 31:14172-14181.

Segal SS (2005) Special circulations (chapter 23). In: Medical physiology (Boron WF, Boulpaep EL, eds), pp558. Philadelphia, PA: Elsevier.

Selden NR, Robbins TW, Everitt BJ (1990) Enhanced behavioral conditioning to context and impaired behavioral and neuroendocrine responses to conditioned stimuli following ceruleocortical noradrenergic lesions: Support for an attentional hypothesis of central noradrenergic function. J Neurosci (UNITED STATES) 10:531-539.

Sethi R, Dhalla NS (1995) Inotropic responses to isoproterenol in congestive heart failure subsequent to myocardial infarction in rats. J Card Fail (United States) 1:391-399.

Shemesh E, Koren-Michowitz M, Yehuda R, Milo-Cotter O, Murdock E, Vered Z, Shneider BL, Gorman JM, Cotter G (2006) Symptoms of posttraumatic stress disorder in patients who have had a myocardial infarction. Psychosomatics (United States) 47:231-239.

Shi C, Davis M (1999) Pain pathways involved in fear conditioning measured with fear-potentiated startle: Lesion studies. J Neurosci (UNITED STATES) 19:420-430.

Shin LM, Orr SP, Carson MA, Rauch SL, Macklin ML, Lasko NB, Peters PM, Metzger LJ, Dougherty DD, Cannistraro PA, Alpert NM, Fischman AJ, Pitman RK (2004) Regional cerebral blood flow in the amygdala and medial prefrontal cortex during traumatic imagery in male and female vietnam veterans with PTSD. Arch Gen Psychiatry (United States) 61:168-176.

Sierra-Mercado D, Padilla-Coreano N, Quirk GJ (2011) Dissociable roles of prelimbic and infralimbic cortices, ventral hippocampus, and basolateral amygdala in the expression and extinction of conditioned fear. Neuropsychopharmacology (United States) 36:529-538.

Silberman Y, Ariwodola OJ, Chappell AM, Yorgason JT, Weiner JL (2010) Lateral paracapsular GABAergic synapses in the basolateral amygdala contribute to the anxiolytic effects of beta 3 adrenoceptor activation. Neuropsychopharmacology (United States) 35:1886-1896.

Singewald N, Zhou GY, Schneider C (1995) Release of excitatory and inhibitory amino acids from the locus coeruleus of conscious rats by cardiovascular stimuli and various forms of acute stress. Brain Res (NETHERLANDS) 704:42-50.

Skinner JE, Reed JC (1981) Blockade of frontocortical-brain stem pathway prevents ventricular fibrillation of ischemic heart. Am J Physiol (UNITED STATES) 240:H156-63.

Smith Y, Pare JF, Pare D (2000) Differential innervation of parvalbumin-immunoreactive interneurons of the basolateral amygdaloid complex by cortical and intrinsic inputs. J Comp Neurol (UNITED STATES) 416:496-508.

Sole MJ, Hussain MN, Versteeg DH, de Kloet ER, Adams D, Lixfeld W (1982) The identification of specific brain nuclei in which catecholamine turnover is increased by left ventricular receptors during acute myocardial infarction in the rat. Brain Res (NETHERLANDS) 235:315-325.

Spencer SJ, Buller KM, Day TA (2005) Medial prefrontal cortex control of the paraventricular hypothalamic nucleus response to psychological stress: Possible role of the bed nucleus of the stria terminalis. J Comp Neurol (United States) 481:363-376.

Sudre EC, de Barros MR, Sudre GN, Schenberg LC (1993) Thresholds of electrically induced defence reaction of the rat: Short- and long-term adaptation mechanisms. Behav Brain Res (NETHERLANDS) 58:141-154.

Sukhanov S, Semprun-Prieto L, Yoshida T, Michael Tabony A, Higashi Y, Galvez S, Delafontaine P (2011) Angiotensin II, oxidative stress and skeletal muscle wasting. Am J Med Sci (United States) 342:143-147.

Sved AF, Felsten G (1987) Stimulation of the locus coeruleus decreases arterial pressure. Brain Res (NETHERLANDS) 414:119-132.

Swanson LW (2003) Maps: Structure of the rat brain, 3rd edition. Los Angeles, CA: Academic Press.

Swanson LW, Sawchenko PE (1980) Paraventricular nucleus: A site for the integration of neuroendocrine and autonomic mechanisms. Neuroendocrinology (SWITZERLAND) 31:410-417.

Swedberg K, Eneroth P, Kjekshus J, Wilhelmsen L (1990) Hormones regulating cardiovascular function in patients with severe congestive heart failure and their relation to mortality. CONSENSUS trial study group. Circulation (UNITED STATES) 82:1730-1736.

Takahashi LK, Kalin NH, Vanden Burgt JA, Sherman JE (1989) Corticotropin-releasing factor modulates defensive-withdrawal and exploratory behavior in rats. Behav Neurosci (UNITED STATES) 103:648-654.

Ter Horst GJ (1999) Central autonomic control of the heart, angina, and pathogenic mechanisms of post-myocardial infarction depression. Eur J Morphol (NETHERLANDS) 37:257-266.

Ter Horst GJ, Hautvast RW, De Jongste MJ, Korf J (1996) Neuroanatomy of cardiac activity-regulating circuitry: A transneuronal retrograde viral labelling study in the rat. Eur J Neurosci (ENGLAND) 8:2029-2041.

Tiong AH, Richardson JS (1990a) The characterization of beta adrenoceptor subtypes in the rat amygdala and hippocampus. Int J Neurosci (ENGLAND) 54:231-244.

Tiong AH, Richardson JS (1990b) Differential effects of olfactory bulbectomy on beta-adrenoceptors in rat amygdala, hippocampus and cerebral cortex. Brain Res (NETHERLANDS) 531:269-275.

Trendelenburg AU, Meyer A, Wess J, Starke K (2005) Distinct mixtures of muscarinic receptor subtypes mediate inhibition of noradrenaline release in different mouse peripheral tissues, as studied with receptor knockout mice. Br J Pharmacol (England) 145:1153-1159.

Tsaltas E, Gray JA, Fillenz M (1984) Alleviation of response suppression to conditioned aversive stimuli by lesions of the dorsal noradrenergic bundle. Behav Brain Res (NETHERLANDS) 13:115-127.

Tseng KY, Amin F, Lewis BL, O'Donnell P (2006) Altered prefrontal cortical metabolic response to mesocortical activation in adult animals with a neonatal ventral hippocampal lesion. Biol Psychiatry (United States) 60:585-590.

Tsumori T, Yokota S, Kishi T, Qin Y, Oka T, Yasui Y (2006) Insular cortical and amygdaloid fibers are in contact with posterolateral hypothalamic neurons projecting to the nucleus of the solitary tract in the rat. Brain Res (Netherlands) 1070:139-144.

Vahid-Ansari F, Leenen FH (1998) Pattern of neuronal activation in rats with CHF after myocardial infarction. Am J Physiol (UNITED STATES) 275:H2140-6.

Van Bockstaele EJ, Pieribone VA, Aston-Jones G (1989) Diverse afferents converge on the nucleus paragigantocellularis in the rat ventrolateral medulla: Retrograde and anterograde tracing studies. J Comp Neurol (UNITED STATES) 290:561-584.

Van de Kar LD, Piechowski RA, Rittenhouse PA, Gray TS (1991) Amygdaloid lesions: Differential effect on conditioned stress and immobilization-induced increases in corticosterone and renin secretion. Neuroendocrinology (SWITZERLAND) 54:89-95.

Vandecasteele G, Eschenhagen T, Scholz H, Stein B, Verde I, Fischmeister R (1999) Muscarinic and beta-adrenergic regulation of heart rate, force of contraction and calcium current is preserved in mice lacking endothelial nitric oxide synthase. Nat Med (UNITED STATES) 5:331-334.

Ventura R, Latagliata EC, Morrone C, La Mela I, Puglisi-Allegra S (2008) Prefrontal norepinephrine determines attribution of "high" motivational salience. PLoS One (United States) 3:e3044.

Vickroy TW, Yamamura HI, Roeske WR (1983) Differential regulation of high-affinity agonist binding to muscarinic sites in the rat heart, cerebellum, and cerebral cortex. Biochem Biophys Res Commun (UNITED STATES) 116:284-290.

Vlastelica M (2008) Emotional stress as a trigger in sudden cardiac death. Psychiatr Danub (Croatia) 20:411-414.

Volman V, Behrens MM, Sejnowski TJ (2011) Downregulation of parvalbumin at cortical GABA synapses reduces network gamma oscillatory activity. J Neurosci (United States) 31:18137-18148.

Walker MJ, Curtis MJ, Hearse DJ, Campbell RW, Janse MJ, Yellon DM, Cobbe SM, Coker SJ, Harness JB, Harron DW (1988) The lambeth conventions: Guidelines for the study of arrhythmias in ischaemia infarction, and reperfusion. Cardiovasc Res (ENGLAND) 22:447-455.

Wallace DM, Magnuson DJ, Gray TS (1992) Organization of amygdaloid projections to brainstem dopaminergic, noradrenergic, and adrenergic cell groups in the rat. Brain Res Bull (UNITED STATES) 28:447-454.

Wang H, Huang BS, Ganten D, Leenen FH (2004) Prevention of sympathetic and cardiac dysfunction after myocardial infarction in transgenic rats deficient in brain angiotensinogen. Circ Res (United States) 94:843.

Wang Y, Zhang QJ, Liu J, Ali U, Gui ZH, Hui YP, Wang T, Chen L, Li Q (2010) Noradrenergic lesion of the locus coeruleus increases the firing activity of the medial prefrontal cortex pyramidal neurons and the role of alpha2-adrenoceptors in normal and medial forebrain bundle lesioned rats. Brain Res (Netherlands) 1324:64-74.

Wann BP, Bah TM, Boucher M, Courtemanche J, Le Marec N, Rousseau G, Godbout R (2007) Vulnerability for apoptosis in the limbic system after myocardial infarction in rats: A possible model for human postinfarct major depression. J Psychiatry Neurosci (Canada) 32:11-16.

Watkins LL, Blumenthal JA, Davidson JR, Babyak MA, McCants CB,Jr, Sketch MH,Jr (2006) Phobic anxiety, depression, and risk of ventricular arrhythmias in patients with coronary heart disease. Psychosom Med (United States) 68:651-656.

Wen H, Jiang H, Lu Z, Hu X, He B, Tang Q, Huang C (2010) Carvedilol ameliorates sympathetic nerve sprouting and electrical remodeling after myocardial infarction in rats. Biomed Pharmacother (France) 64:446-450.

Wessels MR, Mullikin D, Lefkowitz RJ (1978) Differences between agonist and antagonist binding following beta-adrenergic receptor desensitization. J Biol Chem (UNITED STATES) 253:3371-3373.

Whitehead DL, Perkins-Porras L, Strike PC, Steptoe A (2006) Post-traumatic stress disorder in patients with cardiac disease: Predicting vulnerability from emotional responses during admission for acute coronary syndromes. Heart (England) 92:1225-1229.

Wiedemar L, Schmid JP, Muller J, Wittmann L, Schnyder U, Saner H, von Kanel R (2008) Prevalence and predictors of posttraumatic stress disorder in patients with acute myocardial infarction. Heart Lung (United States) 37:113-121.

Wikman A, Bhattacharyya M, Perkins-Porras L, Steptoe A (2008) Persistence of posttraumatic stress symptoms 12 and 36 months after acute coronary syndrome. Psychosom Med (United States) 70:764-772.

Wilber AA, Walker AG, Southwood CJ, Farrell MR, Lin GL, Rebec GV, Wellman CL (2011) Chronic stress alters neural activity in medial prefrontal cortex during retrieval of extinction. Neuroscience (United States) 174:115-131.

Wilkins AJ, Shallice T, McCarthy R (1987) Frontal lesions and sustained attention. Neuropsychologia (ENGLAND) 25:359-365.

Wittstein IS, Thiemann DR, Lima JA, Baughman KL, Schulman SP, Gerstenblith G, Wu KC, Rade JJ, Bivalacqua TJ, Champion HC (2005) Neurohumoral features of myocardial stunning due to sudden emotional stress. N Engl J Med (United States) 352:539-548.

Wong-Riley M (1979) Changes in the visual system of monocularly sutured or enucleated cats demonstrable with cytochrome oxidase histochemistry. Brain Res (NETHERLANDS) 171:11-28.

Wong-Riley MT (1989) Cytochrome oxidase: An endogenous metabolic marker for neuronal activity. Trends Neurosci (ENGLAND) 12:94-101.

Wongwitdecha N, Marsden CA (1996) Social isolation increases aggressive behaviour and alters the effects of diazepam in the rat social interaction test. Behav Brain Res (NETHERLANDS) 75:27-32.

Woo MA, Kumar R, Macey PM, Fonarow GC, Harper RM (2009) Brain injury in autonomic, emotional, and cognitive regulatory areas in patients with heart failure. J Card Fail (United States) 15:214-223.

Worrall NK, Chang K, LeJeune WS, Misko TP, Sullivan PM, Ferguson TB,Jr, Williamson JR (1997) TNF-alpha causes reversible in vivo systemic vascular barrier dysfunction via NO-dependent and -independent mechanisms. Am J Physiol (UNITED STATES) 273:H2565-74.

Yamagishi H, Kim S, Nishikimi T, Takeuchi K, Takeda T (1993) Contribution of cardiac renin-angiotensin system to ventricular remodelling in myocardial-infarcted rats. J Mol Cell Cardiol (ENGLAND) 25:1369-1380.

Yamaguchi S, Knight RT (1990) Gating of somatosensory input by human prefrontal cortex. Brain Res (NETHERLANDS) 521:281-288.

Yasui Y, Breder CD, Saper CB, Cechetto DF (1991) Autonomic responses and efferent pathways from the insular cortex in the rat. J Comp Neurol (UNITED STATES) 303:355-374.

Yoshida T, Semprun-Prieto L, Wainford RD, Sukhanov S, Kapusta DR, Delafontaine P (2012) Angiotensin II reduces food intake by altering orexigenic neuropeptide expression in the mouse hypothalamus. Endocrinology (United States) 153:1411-1420.

Zardetto-Smith AM, Gray TS (1990) Organization of peptidergic and catecholaminergic efferents from the nucleus of the solitary tract to the rat amygdala. Brain Res Bull (UNITED STATES) 25:875-887.

Ziegelstein RC (2007) Acute emotional stress and cardiac arrhythmias. JAMA (United States) 298:324-329.

Zipes DP, Wellens HJ (1998) Sudden cardiac death. Circulation (UNITED STATES) 98:2334-2351.

VITA

The author, Jaimee Elizabeth Glasgow, was born on December 31, 1982 in Corning, NY, to Peggy and Bob Glasgow. Jaimee grew up in eastern Pennsylvania and completed her secondary education at Wyomissing Area High School. From 2001 to 2005, Jaimee attended St. Olaf College in Northfield, MN, where she graduated with honors with a BA in Biology and Psychology. She was also a member of the St. Olaf Choir.

Jaimee entered the Cell Biology, Neurobiology, and Anatomy PhD program in August 2006 and joined the lab of Dr. Karie Scrogin in the summer of 2007. Her dissertation research focused on anxiety and changes in the central noradrenergic system following myocardial infarction. She was awarded a pre-doctoral fellowship from the American Heart Association, Mid-West Affiliate, to pursue her dissertation project. In addition, Jaimee was the recipient of a dissertation fellowship from the Schmitt Foundation. Jaimee has accepted a medical writer position at a medical communications agency in Chicago.